

**MODELLING OF THERMAL AND WATER MANAGEMENT IN  
AUTOMOTIVE POLYMER ELECTROLYTE MEMBRANE  
FUEL CELL SYSTEMS**

**OTOMOTİV POLİMER MEMBRAN ELEKTROLİT YAKIT  
HÜCRESİ SİSTEMLERİNİN ISIL VE SU YÖNETİMİNİN  
MODELENMESİ**

**ABDULRAZZAK AKROOT**

**Dr. ÖZGÜR EKİCİ**  
**Supervisor**

Submitted to Institute of Science of Hacettepe University  
as a Partial Fulfillment to the Requirement  
for the Award of the Degree of Master of Science  
in Mechanical Engineering

January 2014

This work named “**Modelling of Thermal and Water Management in Automotive Polymer Electrolyte Membrane Fuel Cell Systems**” by **ABDULRAZZAK AKROOT** has been approved as a thesis for the degree of **MASTER OF SCIENCE IN MECHANICAL ENGINEERING** by the below mentioned Examining Committee Members.

Prof. Dr. Aynur ERAY

Head

.....

Dr. Özgür EKİCİ

Supervisor

.....

Assoc. Prof. Dr. Şule ERGUN

Member

.....

Assoc. Prof. Dr. Murat KÖKSAL

Member

.....

Dr. Bilsay SÜMER

Member

.....

This thesis has been approved as a thesis for the degree of **MASTER OF SCIENCE IN MECHANICAL ENGINEERING** by a board of Director of the Institute for Graduate Studies in Science and Engineering.

Prof. Dr. Fatma SEVİN DÜZ

Director of the Institute of  
Graduate Studies in Science

## ETHICS

In this thesis study, prepared in accordance with the spelling rules of Institute of Graduate Studies of Hacettepe University,

I declare that

- all the information and documents have been obtained in the base of the academic rules.
- all audio-visual and written information and results have been presented according to the rules of scientific ethics.
- in case of using others works, related studies have been cited in accordance with the scientific standards.
- all cited studies have been fully referenced.
- i did not any distortion in the data set.
- and any part of this thesis has not been presented as another thesis study at this or any other university.

16/01/2014

ABDULRAZZAK AKROOT

## ÖZET

# OTOMOTİV POLİMER MEMBRAN ELEKTROLİT YAKIT HÜCRESİ SİSTEMLERİNİN ISIL VE SU YÖNETİMİNİN MODELENMESİ

**Abdulrazzak AKROOT**

**Yüksek Lisans, Makina Mühendisliği Bölümü**

**Tez Danışmanı: Dr. Özgür EKİCİ**

**Ocak 2014**

Polimer membran elektrolit (PEM) yakıt hücreleri yüksek güç yoğunlukları, düşük çalışma sıcaklıkları (60°C - 80°C arası) ve düşük çevresel kirlilikleri nedeniyle otomotiv uygulamaları için umut verici güç kaynaklarıdır. Membranı nemli tutarak yüksek proton iletkenliğini sağlamak, polimer membran elektrolit yakıt hücresi malzemelerinin dayanıklılığı ve yakıt hücresinin çalışma sıcaklığının kabul edilir sınırlar altında kalması için uygun su ve termal yönetim gerekmektedir.

Sistemin güç çıktısı, üretilen su ve ısı miktarı ve sistem verimliliği ile ilgili olarak bilgi sağlamak; ve böylece en iyi su ve termal yönetim koşullarına ulaşmak amacıyla genel bir hesaplama yöntemi geliştirilmiştir.

Bu tezde araç hızı, çalışma basıncı gibi değişkenlerin sistem bileşenlerinin boyutları, ısı ve su oluşumu, yakıt tüketimi ve verimlilik üzerindeki etkilerini anlamak üzere 90 kW PEM yakıt hücreli bir otomotiv sistemi için sistem düzeyinde, sıfır-boyutlu bir termodinamik model geliştirilmiştir. Ek olarak, güç çıkışı ve sistemin güç kayıpları 1.5 atm ve 3 atm olarak iki farklı çalışma basıncında incelenmiştir. Yakıt hücresi

sisteminin modellenmesi MATLAB'da gerçekleştirilmiştir. Sonuçlar, 10km/saat ile 140 km/saat hız aralığında, 1.5 atm ve 3 atm çalışma basınçları için farklı sistem yapılandırmalarının gerekli olduğunu göstermektedir. Sonuçların açıkça gösterdiği üzere katodun çıkışındaki su miktarı çalışma basıncı ve hava stokiometri oranından etkilenmektedir. Yüksek çalışma basıncı nemlendirme için ihtiyaç duyulan su miktarında azalmaya neden olmaktadır. Buna karşılık, düşük çalışma basıncında, katot çıkışındaki su miktarı tepkiyenleri nemlendirmek için yetersiz kalmakta ve gerekli sıvı suyu sağlamak üzere egzozdaki su buharını yoğuşturmak için katot çıkışında bir kondensatör gerekmektedir. Sonuçlar ayrıca göstermiştir ki, yüksek çalışma basıncı radyatörde daha yüksek miktarda atık ısıya neden olmakta ve dolayısıyla radyatör boyutu büyümektedir.

**Anahtar Kelimeler:** Polimer membran elektrolit yakıt hücresi, ısıl analiz, su yönetimi.

# **ABSTRACT**

## **MODELLING OF THERMAL AND WATER MANAGEMENT IN AUTOMOTIVE POLYMER ELECTROLYTE MEMBRANE FUEL CELL SYSTEMS**

**Abdulrazzak AKROOT**

**Master of Science in Mechanical Engineering**

**Supervisor: Dr. Özgür EKİCİ**

**January 2014**

Proton electrolyte membrane fuel cells (PEMFC) are promising power sources for automotive applications because of their high power density, low operation temperature (between 60°C - 80°C), and lower environmental pollution. A proper water and thermal management are needed to keep the membrane humidified for high proton conductivity, durability for PEMFC materials, and to ensure the operation temperature of fuel cell stack remains under a tolerable limit.

A general calculation methodology has been developed to provide information regarding the system power output, amount of water and heat products, and system efficiency, thereby assisting to achieve the best water and thermal management conditions

In this thesis, a system level zero-dimensional, steady state thermodynamics model for an automotive 90 kW PEM fuel cell system has been developed to investigate the effects of various operating parameters such as vehicle speed, and operating pressure on the size of the system components, heat and water formation, fuel consumption and efficiency. Moreover the power output and power losses of the system are investigated at two different operating pressures: 1.5 atm and 3 atm. The

model of the fuel cell system was implemented in MATLAB. The results show that different system configurations are needed for 1.5 atm and 3 atm operating pressures in a speed range of 10-140 km/hr. It is clear from the results that the amount of water at the exit of cathode is affected by the operating pressure and air stoichiometry ratio. Higher operating pressure causes a decrease in water needed for humidification process. On the other hand, at lower operating pressure the water at the exit of cathode is not enough to humidify the reactants and a condenser at the exit of the cathode is needed to condense the water vapor at the exhaust to supply the required liquid water. The results also show that higher operating pressure causes a large amount of heat rejected in the radiator and therefore increases the size of radiator.

**Keywords:** Polymer electrolyte membrane fuel cell, thermal analysis, water management.

Dedicated to my mother, wife and sons



## **ACKNOWLEDGMENTS**

This thesis would not have been possible without the support of many people. I wish to send my deepest appreciation to my supervisor, Dr. Özgür EKİCİ. This thesis would not be possible without his support and guidance.

I would also like to thank Assoc. Prof. Dr. Murat KÖKSAL who were abundantly helpful and provided me with the optimum guidance, support and motivation. Many thanks also go to other faculty members at the Department of Mechanical Engineering, Hacettepe University.

Lastly, I would like to thank Hacettepe University and especially the Department of Mechanical Engineering for the enormous learning outcome I have gained during the past three years.

# TABLE OF CONTENTS

	<u>Page</u>
ÖZET .....	iv
ABSTRACT .....	vi
ACKNOWLEDGMENTS .....	ix
TABLE OF CONTENTS.....	x
LIST OF FIGURES .....	xiii
LIST OF TABLES .....	xvi
NOMENCLATURE.....	xvii
CHAPTER 1 .....	1
INTRODUCTION AND LITERATURE REVIEW .....	1
1.1 Main Components of a Polymer Electrolyte Membrane Fuel Cell.....	1
1.1.1 Membrane Electrode Assembly (MEA).....	2
1.1.2 Bipolar Plates.....	4
1.2 Principle Operation of a PEM Fuel Cell .....	4
1.3 Water Management in the PEM Fuel Cell.....	6
1.3.1 Membrane Dehydration .....	8
1.3.2 Electrodes Flooding .....	8
1.4 Thermal Management in the PEM Fuel Cell .....	9
1.5 Literature Review .....	10
1-6 Thesis Objectives .....	18
1-7 Thesis Structure .....	19
CHAPTER 2 .....	20
A 0-D STEADY-STATE SYSTEM MODEL FOR A PEM FUEL CELL SYSTEM.....	20
2.1 Fuel Cell Stack Model.....	24

2.1.1 Fuel Cell Voltage Model .....	24
2.1.1.1 Thermodynamics .....	24
2.1.1.2 Nernst Potential .....	26
2.1.1.3 Cell Potential .....	28
2.1.1.3.1 Activation Losses.....	29
2.1.1.3.2 Ohmic Losses.....	30
2.1.1.3.3 Concentration Losses.....	32
2.1.1.4 Fuel Cell Thermal Efficiency .....	33
2.1.2 Anode Flow Model.....	33
2.1.3 Cathode Flow Model.....	36
2.1.4 Membrane Hydration Model .....	40
2.1.5 Heat Transfer Model.....	42
2.2 Fuel Cell System Model.....	45
2-2-1 Compressor Model.....	45
2.2.2 Humidifier Model .....	46
2.2.3 Radiator Model .....	48
2.2.4 Pump Model .....	49
2.2.5 Net System Power and System Thermal Efficiency.....	49
2.3 Vehicle Model.....	50
2.4 Summary .....	51
CHAPTER 3 .....	52
SOLUTION METHODOLOGY .....	52
3-1 PEM fuel cell Stack Model Integration in MATLAB.....	54
3-2 Automotive PEM fuel cell System Integration in MATLAB.....	57

CHAPTER 4 .....	59
RESULTS AND DISCUSSIONS .....	59
4.1 Analysis of PEM Fuel Cell Model.....	59
4-2 Analysis of an Automotive PEM Fuel Cell System Model.....	63
4.2.1 Power Output.....	63
4.2.2 Fuel Consumption.....	68
4.2.3 Fuel Cell Thermal Efficiency, and System Thermal Efficiency .....	69
4.2.4 Water Management .....	70
4.2.5 Thermal Management.....	75
CHAPTER 5 .....	80
CONCLUSIONS AND RECOMMENDATIONS FOR FUTURE WORK.....	80
Recommendations for Future Work.....	81
REFERENCES .....	83
APPENDIX .....	88
MATLAB CODE .....	88
CURRICULUM VITA.....	99

## LIST OF FIGURES

	<u>Page</u>
Figure 1.1. Construction of a PEM fuel cell stack (Ahn, 2011). .....	2
Figure 1.2. Construction of a membrane electrode assembly .....	3
Figure 1.3. The transport processes for a PEM fuel cell (U.S. DOE, 2011).....	6
Figure 1.4. Mechanism of water transport in PEM fuel cell .....	7
Figure 1.5. Schematic of a direct –hydrogen fuel cell system (Badrinarayanan, 1999) .	12
Figure 1.6. Direct hydrogen fuel cell system (Moore et al, 2005) .....	13
Figure 1.7. Schematic diagrams of the water and thermal management system in a pure-hydrogen PEM fuel cell system (Bao et al, 2006). .....	14
Figure 1.8. Fuel cell system schematic (Wishart et al, 2006) .....	15
Figure 1.9. Schematic view of a fuel cell engine system (Mert et al, 2012) .....	16
Figure 1.10. Schematic view of a fuel cell power system (Hosseini et al., 2012).....	17
Figure 1.11. Schematic diagram of PEM fuel cell system (Elham et al, 2013) .....	18
Figure 2.1. A schematic diagram of an automotive PEM fuel cell system at 1.5 atm operation pressure .....	21
Figure 2.2. A schematic diagram of an automotive PEM fuel cell system at 1.5 atm operation pressure .....	23
Figure 2.3. Schematic diagram of the polarization curve of a PEM fuel cell.....	29
Figure 2.4. Effect of electrolyte thickness on the cell voltage .....	32
Figure 2.5. Anode mass flow balance .....	34
Figure 2.6. Cathode mass flow balance .....	37
Figure 2.7. Mass flow in the membrane flow model .....	40
Figure 2.8. Energy balance of the fuel cell system .....	43
Figure 3.1. Flow Chart of the Automotive PEM Fuel Cell System .....	53
Figure 3.2. PEM fuel cell model overview.....	57
Figure 4.1. Fuel cell voltage and voltage losses as a function of cell’s current density for an operating pressure of 3 atm .....	60

Figure 4.2. Fuel cell output voltages as a function of cell's current density for operating pressures of 1.5 and 3 atm. ....61

Figure 4.3. The power density of fuel cell as a function of cell's current density for different pressures. ....63

Figure 4.4. Power output as a function of vehicle speed for two different operating pressures. ....64

Figure 4.5. Propulsion power required as a function of vehicle speed.....65

Figure 4.6. Auxiliary powers as a function of vehicle speed for two different operating pressures. ....66

Figure 4.7. Auxiliary powers as a function of vehicle speed for 3 atm operating pressure.....67

Figure 4.8. Auxiliary powers as a function of vehicle speed for 1.5 atm operating pressure.....68

Figure 4.9. Hydrogen consumption as a function of vehicle speed for two different operating pressures. ....69

Figure 4.10. Efficiencies as a function of vehicle speed at two different pressures .....70

Figure 4.11. The amount of water at the exit of stack and injected water required for humidification process as a function of vehicle speed for 3 atm operation pressure. ....71

Figure 4.12. The amount of water at the exit of stack and injected water required for humidification process as a function of vehicle's speed for 1.5 atm operation pressure.72

Figure 4.13. The water needed for humidification process as a function of vehicle speed for two different operating pressures. ....73

Figure 4.14. The amount of liquid water at the exit of cathode and injected water required for humidification process at constant vehicle speed at 120 km/hr with variable air stoichiometric ratio at two different operating pressures. ....74

Figure 4.15. Heat balance of fuel cell stack as a function of vehicle speed for two different operating pressures. ....76

Figure 4.16. Heat rejected in radiator as a function of vehicle speed for two different operating pressures. ....77

Figure 4.17. Required heat exchanger areas as a function of vehicle speed at two different operation pressures. ....78

Figure 4.18. The amount of coolant flow rate as a function of vehicle speed for different pressures.....79

## LIST OF TABLES

	<u>Page</u>
Table 3.1. The Fuel Cell Stack Parameters .....	55
Table 3.2. PEMFC Model Constants .....	56
Table 3.3. PEMFC Model Outputs .....	56
Table 3.4. TOYOTA Vehicle Specifications .....	58
Table 3.5. Thermal System Characteristics .....	58
Table 3.6. PEM Fuel Cell System Model Outputs .....	58



## NOMENCLATURE

$a$	vehicle acceleration due to gravity ( $\text{m. sec}^{-2}$ )
$A$	Stack exposed surface area ( $\text{m}^2$ )
$a_w$	Water activity
$A_{\text{cell}}$	Active area of the fuel cell ( $\text{cm}^2$ )
$A_{\text{cond}}$	Cross-sectional area of the conductor ( $\text{cm}^2$ )
$A_{\text{eff}}$	Effective area of radiator
$A_{\text{frontal}}$	Frontal area of vehicle ( $\text{m}^2$ )
$A_{\text{rad}}$	Frontal area of the radiator
$C$	Concentration
$C_{\text{H}_2,\text{an}}$	Concentration of hydrogen at the anode
$C_{\text{O}_2,\text{ca}}$	Concentration of oxygen at the cathode
$C_d$	Aerodynamic drag coefficient
$C_{P,w}$	Specific heat of water at constant pressure ( $\text{kg}^{-1}\text{K}^{-1}$ )
$C_{\text{RR}}$	Rolling resistance coefficient
$C_W^m$	Ionomer water concentration
$D_{\text{AB}}$	Diffusion coefficient ( $\text{cm s}^{-1}$ ) ( $\text{cm. sec}^{-1}$ )
$D_W$	Diffusion coefficient ( $\text{cm. sec}^{-1}$ )
$E$	potential (V)
$E^\circ$	Standard reversible potential (V)
$EW$	Equivalent molecular weight of the ionomer material
$E^\circ_{T,P}$	Equilibrium potential for a give temperature and pressure (V)
$F$	Faraday constant ( $\text{Cmol}^{-1}$ )
$H$	Enthalpy of formation (W)
$h_{\text{air}}$	Natural convection heat transfer coefficient of air ( $\text{W. m}^{-2}. \text{K}^{-1}$ )
$H_{\text{fg}}^0$	Enthalpy of evaporative (W)
$\text{HHV}_{\text{H}_2}$	Higher heating value of hydrogen (W)
$i$	Current density ( $\text{A. m}^2$ )
$i_0$	Exchange current density ( $\text{A. m}^2$ )

$i_L$	Limiting current density ( $A. m^2$ )
$k$	Thermal conductivity of coolant ( $W. m^{-2}$ )
$L$	Thickness of the electrolyte (cm)
$L_{cond}$	Length of the conductor (cm)
$m_{veh}$	Total vehicle mass (kg)
$\dot{m}_w$	Mass flow of water vapor ( $g. sec^{-1}$ )
$M_{H_2}$	Molecular weight of hydrogen ( $kg. kmol^{-1}$ )
$M_{H_2O}$	Molecular weight of water ( $kg. kmol^{-1}$ )
$M_{N_2}$	Molecular weight nitrogen
$M_{O_2}$	Molecular weight of oxygen
$\dot{m}_{O_2,reacted}$	Mass flow rate of oxygen reacted ( $g. sec^{-1}$ )
$\dot{m}_{cool}$	Mass flow rate of the coolant water
$\dot{m}_{H_2,an,in}$	Mass flow rate of hydrogen gas entering the anode ( $g. sec^{-1}$ )
$\dot{m}_{H_2,an,out}$	Mass flow rate of hydrogen gas leaving the anode ( $g. sec^{-1}$ )
$\dot{m}_{H_2,reacted}$	Mass flow rate of hydrogen reacted ( $g. sec^{-1}$ )
$\dot{m}_{H_2,in}$	Mass flow rate of hydrogen ( $g. sec^{-1}$ )
$\dot{m}_{H_2O,an,in}$	Mass flow rate of water vapor entering the anode ( $g. sec^{-1}$ )
$\dot{m}_{H_2O,in,an,out,liquid}$	Mass flow rate of liquid water leaving the anode ( $g. sec^{-1}$ )
$\dot{m}_{H_2O,an,out}$	Mass flow rate of water leaving the anode ( $g. sec^{-1}$ )
$\dot{m}_{H_2O,ca,in}$	Mass flow rate of water vapor leaving the cathode ( $g. sec^{-1}$ )
$\dot{m}_{H_2O,ca,out,liquid}$	Mass flow rate of liquid water leaving the cathode ( $g. sec^{-1}$ )
$\dot{m}_{H_2O,ca,out}$	Mass flow rate of water vapor leaving the cathode ( $g. sec^{-1}$ )
$\dot{m}_{H_2O,gen}$	Mass flow rate of water generated in fuel cell reaction ( $g. sec^{-1}$ )
$\dot{m}_{N_2,ca,in}$	Mass flow rate of nitrogen gas entering the cathode ( $g. sec^{-1}$ )
$\dot{m}_{N_2,ca,out}$	Mass flow rate of nitrogen gas leaving the cathode ( $g. sec^{-1}$ )
$\dot{m}_{O_2,ca,in}$	Mass flow rate of oxygen gas entering the cathode ( $g. sec^{-1}$ )
$\dot{m}_{O_2,ca,out}$	Mass flow rate of oxygen gas leaving the cathode ( $g. sec^{-1}$ )
$\dot{m}_{air,in}$	Mass flow rate of inlet air ( $g. sec^{-1}$ )
$\dot{m}_{diff,mem}$	Mass flow rate of water transfer by back diffusion ( $g. sec^{-1}$ )

$\dot{m}_{osm,mem}$	Mass flow rate of water transfer by electro osmotic drag ( $\text{g. sec}^{-1}$ )
$n$	Number of moles of electrons transferred
$n_{cell}$	Number of cells
$n_d$	Electro-osmotic drag coefficient
$P_{H_2}$	Hydrogen pressure (Pa)
$P_{H_2O}$	Pressure of the water vapor (Pa)
$P_{HO_2}$	Oxygen pressure (Pa)
$P_{N_2}$	Nitrogen partial pressure
$P_{O_2}$	Oxygen partial pressure at the cathode
$p_{an}$	Pressure of anode (Pa)
$P_{aux}$	Parasitic loads by all auxiliary system equipment
$p_{ca}$	Pressure of cathode
$P_{comp}$	Compressor power (w)
$P_{fan}$	Electric power consumption for the fan
$P_{in}$	Theoretical power of incoming fuel
$P_{pump}$	Pump work rate consumption
$P_{road}$	Road load power (w)
$P_{sat}$	Water vapor saturated pressure (Pa)
$P_{v,an}$	Water vapor pressure at anode (Pa)
$P_{v,ca}$	Cathode water vapor pressure
$q$	Air volume flow delivered by the fan ( $\text{m}^3 \cdot \text{sec}^{-1}$ )
$Q$	Charge ( $\text{C. mol}^{-1}$ )
$Q_{i,in}$	Heat of reactant gases (W)
$Q_{i,out}$	Heat of unused and produced by the product reactant gases (W)
$\dot{Q}_{conv}$	Heat loss due to convection (W)
$\dot{Q}_{cool}$	Heat carried from the fuel cell to the coolant (W)
$\dot{Q}_{env}$	Heat dissipated to the environment (W)
$\dot{Q}_{rad}$	Heat loss due to radiation (W)
$\dot{Q}_{radiator}$	Heat transfer dissipated through radiator
$R$	Universal gas constant ( $\text{J. mol}^{-1} \cdot \text{K}^{-1}$ )

$r_{O_2,in}$	Oxygen volume fraction
$R_{elec}$	Electrical resistance ( $\Omega$ )
$R_{ionic}$	Ionic resistance ( $\Omega$ )
$R_{Ohmic}$	Ohmic resistance ( $\Omega$ )
$S$	Entropy
$T$	Absolute temperature (K)
$t_m$	Thickness of the membrane (cm)
$T_{cool}$	Temperature of water which enters the fuel cell (K)
$T_{stack}$	Stack temperature (K)
$U$	Overall heat transfer coefficient
$V$	Average velocity of air ( $m \cdot s^{-1}$ )
$V_{act}$	Voltage loss due to activation polarization (V)
$V_{con}$	Voltage loss due to concentration polarization (V)
$V_{Ohmic}$	Voltage loss due to ohmic polarization (V)
$V_{stack}$	Stack voltage (V)
$V_{cell}$	Cell potential (V)
$v$	Vehicle speed ( $m \cdot s^{-1}$ )
$W_e$	Electrical power output (W)
$W_{elc}$	Electricity generated (W)
$\dot{W}_{com}$	Compressor work done (W)
$y_{H_2,an,in}$	Mole fraction of hydrogen at the inlet flow
$y_{H_2,an,un\ used}$	Mole fraction of hydrogen unused
$y_{N_2,ca,in}$	Mole fraction of nitrogen at the inlet of cathode
$y_{O_2,an,used}$	Mole fraction of unused oxygen
$y_{O_2,anode,in}$	Mole fraction of oxygen at the inlet of cathode
$y_{v,an,in}$	Molar fraction of inlet water vapor
$y_{v,ca,in}$	Molar fraction of inlet water vapor at the inlet of cathode

## Greek Letters

$\phi_{an}$	Relative humidity inside the anode (%)
$\phi_{ca}$	Relative humidity inside the cathode
$\Delta S^{\circ}$	Change in standard-state entropy
$\Delta T_{LM}$	Mean temperature difference
$\Delta P_{ca}$	Pressure drop on the cathode side
$\epsilon_{stack}$	Emissivity of stack surface
$\eta_{comp}$	Compressor efficiency
$\eta_{fc}$	Actual fuel cell efficiency
$\eta_{sys}$	System efficiency
$\eta_{theo}$	Theoretical efficiency of fuel cell
$\lambda_{H_2}$	Stoichiometric ratio of hydrogen ( $g \cdot sec^{-1}$ )
$\lambda_{O_2}$	Stoichiometric ratio of oxygen
$\lambda_m$	Membrane water content
$\rho_{air}$	Ambient air density ( $Kg \cdot m^{-3}$ )
$\rho_{dry}$	Density of dry ionomer ( $Kg \cdot m^{-3}$ )
$\omega$	Humidity ratio at the inlet of humidifier
$\alpha$	Charge transfer coefficient
$\delta$	Thickness (cm)
$\Delta G$	Gibbs free energy (W)
$\Delta p$	Total pressure increase in the fan (Pa)
$\sigma$	Electrical conductivity ( $\Omega^{-1} cm^{-1}$ )
$\sigma$	Stefan-Boltzmann constant ( $W \cdot m^{-2} \cdot K^{-4}$ )



# **CHAPTER 1**

## **INTRODUCTION AND LITERATURE REVIEW**

Fuel cell systems, which recently have been emerged, are one of the most promising power-generation technologies for the future. They convert the chemical energy of the fuel directly to useful electricity at very high efficiencies. Fuel cells were invented in 1839 by Sir. William Grove. Fuel cells offer many advantages which make them best suited to the production of energy. The most important one is the combination of relatively high efficiency and reduction in atmospheric pollution at the same time.

Fuel cells are commonly classified by the type of electrolyte used in the cells: Polymer electrolyte membrane (PEMFC), alkaline (AFC), phosphoric acid (PAFC), molten carbonate (MCFC) and solid oxide (SOFC). PEM Fuel cell appears to be the most attractive option for automotive applications because of its low operating temperature.

### **1.1 Main Components of a Polymer Electrolyte Membrane Fuel Cell**

Polymer electrolyte membrane fuel cell (also known as proton exchange membrane fuel cell) typically consists of the following components as seen in Figure 1.1 These include a membrane electrode assembly (MEA), and two bipolar plates (BPs) at the cathode and anode sides.

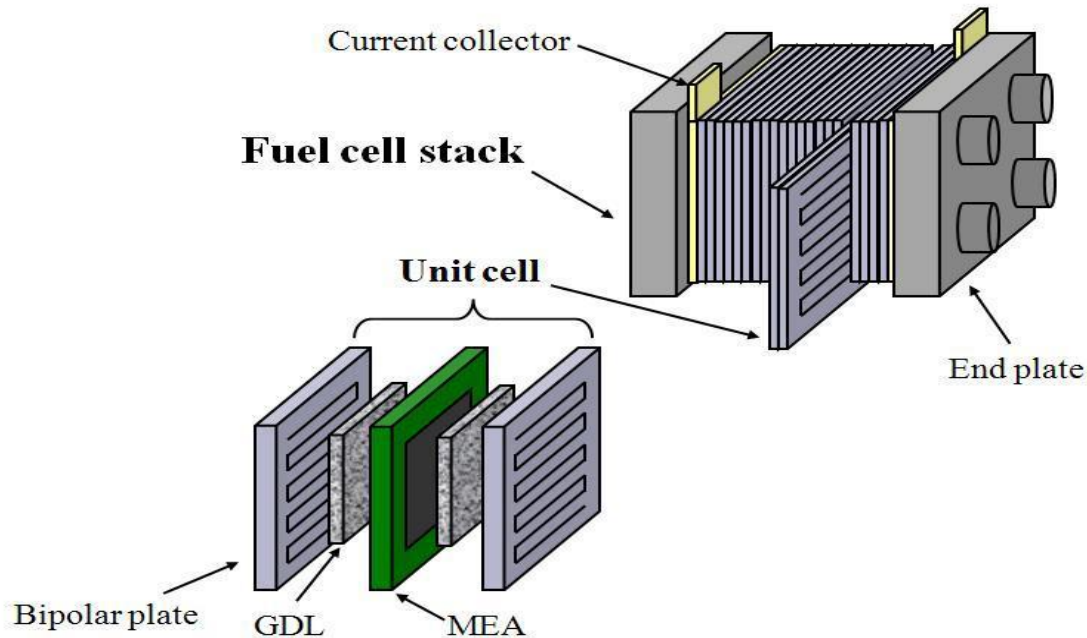


Figure 1.1. Construction of a PEM fuel cell stack (Ahn, 2011).

### 1.1.1 Membrane Electrode Assembly (MEA)

The key part of a PEM fuel cell is a membrane. It is made of a polymer electrolyte membrane sandwiched between the two electrodes doped with catalysts particles. Therefore, a membrane electrode assembly is composed of an electrolyte, two gas diffusion layers (electrodes) and two catalyst layers as seen in Figure 1.2.

The most commonly used type of membrane material is Nafion™, a member of the perfluorosulfonic acid (PFSA) family of polymer membranes. The main functions of the membrane are to conduct the protons from anode side to cathode side while preventing the transport of electrons through it, and to separate the gases in the adjacent cells (Barbir, 2005).

According to Spiegel (2008), a PEM fuel cell electrolyte must meet the following requirements in order for the fuel cell to work properly:

- Must have high ionic conductivity.



- Must present an adequate barrier to the reactants.
- Must be stable chemically and mechanically.
- Must have low electronic conductivity.
- Must have ASE of manufacturability.
- Must have preferably low cost.

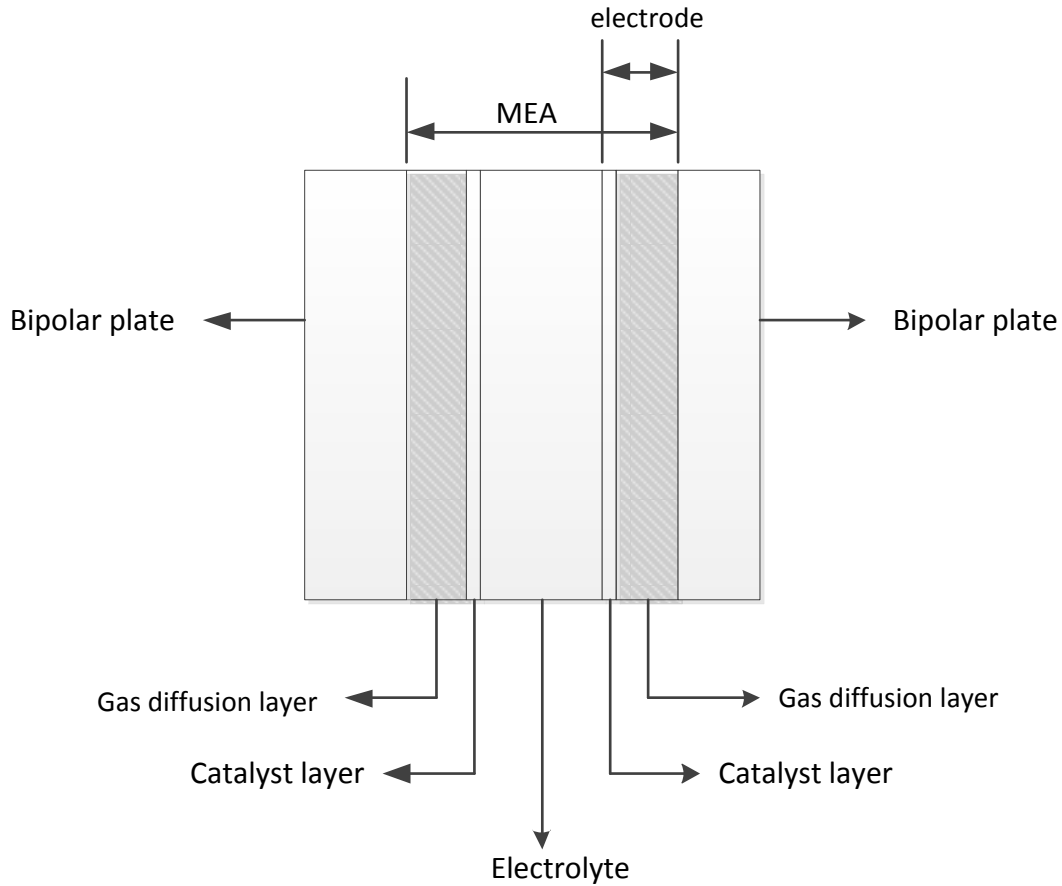


Figure 1.2. Construction of a membrane electrode assembly

The catalyst layer is a complex structure in the PEM fuel cell because it is where the half electrochemical reactions take place for both cathode and anode promoting the half electrochemical reactions. The anode is the negative side of the fuel cell, conducts the electrons that are liberated from the hydrogen oxidation reaction so that they can be used to produce power in an external circuit. The cathode is the positive side of the fuel cell, conducts the electrons back from the external circuit to the

catalyst, where they are consumed and combined with the hydrogen ions and oxygen to produce water (Zhang, 2008). They are usually made of carbon black particles supporting platinum or platinum alloys particles. These layers are porous. The thickness of these layers is in the range of 5 to 30  $\mu\text{m}$  (Mench, 2008).

The gas diffusion layer is the layer between the catalyst layer and bipolar plates. It is made of porous media such as carbon fiber or carbon cloth. It has a thickness in the range of 200 to 400  $\mu\text{m}$  (Mench, 2008). The gas diffusion layer in a PEM fuel cell plays multiple roles: provides electronic connection between the bipolar plate with channel-land structure, provides a pathway for reactant transport and heat/water removal, prevents the membrane electrode assembly (MEA) from sagging into the flow field channels, and protects the catalyst layer from corrosion or erosion caused by flows or other factors (Barbir, 2005).

### **1.1.2 Bipolar Plates**

The bipolar plates in a fuel cell are traditionally made of a highly conductive material such as graphite because of it has good mechanical, electronic and thermal properties. Bipolar plates are a significant part of the PEM fuel cell stack, which account for about 80% of total weight and 45% of stack cost (Hermann, 2005). The bipolar plates have multifunctional character in a PEM fuel cell. They connect and transport electrons from the cell to an external electrical circuit, separate the reactant gas in adjacent cell, conduct heat from active cell to the environment and to the cooling section of a stack, and provide structural support for the stack (Barbir et al, 1999).

## **1.2 Principle Operation of a PEM Fuel Cell**

The basic electrochemical reaction cell consists of an anode and a cathode electrode where on their surfaces the electrochemical reactions occur, electrolyte to conduct ions from one electrode to the other, and the external circuit between electrodes for current flow. During the fuel cell operation, hydrogen is supplied at the anode side of

fuel cell and the reaction in the anode catalyst layer cause the hydrogen to be converted into protons ( $H^+$ ) and electrons ( $e^-$ ). The protons diffuse through the membrane to the cathode side. The electrons flow from the anode side to the cathode side through an external circuit to power the load. Oxygen is supplied as reactant gas at the cathode side of fuel cell. At the cathode, the electrons and protons combine with oxygen molecules to produce water, which flows out of the cell. The transport processes for a PEM fuel cell are shown in Figure 1.3.

The electrochemical reactions that take place within PEM fuel cell are given below.

The reaction occurring at the anode side is:



The reaction occurring at the cathode side is:



The overall cell reaction by combining the anode and cathode reactions is:



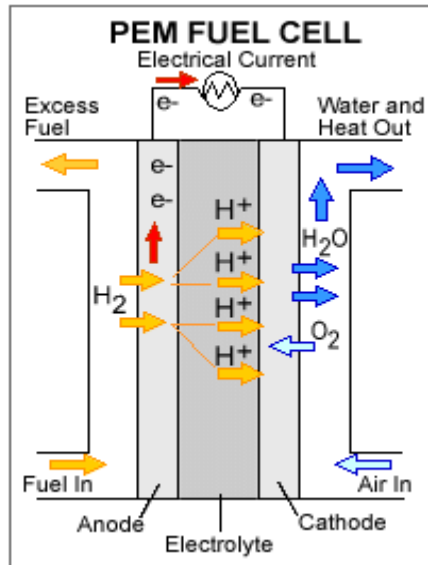


Figure 1.3. The transport processes for a PEM fuel cell (U.S. DOE, 2011)

### 1.3 Water Management in the PEM Fuel Cell

Water management is an important problem in PEM fuel cells. For high ionic conductivity through the electrolyte, membrane must be kept hydrated. However, liquid water formation can restrict the flow channels and degrade the performance (also known as flooding) if the excess water is not removed. A well designed fuel cell system must operate with a well humidified electrolyte without any flooding.

In a PEM fuel cell operation, water is formed due to the oxidation reduction reaction (ORR) at the cathode side (Eq. 1.2). Water is also supplied by an external humidification system to the anode and the cathode since both the fuel and air streams are humidified. Water gets transported through the electrolyte via various mechanisms. Figure 1.4 shows a schematic diagram for the mechanism of water transport in a PEM fuel cell. It can be seen from this figure that the water transported across the the membrane occurs under three different transport mechanisms: the electro-osmotic drag (water transport from anode to cathode) which is related to the transfer of protons through the membrane, back diffusion due to the water concentration gradients from the cathode to the anode, and convective transfer due to pressure

gradients in the fuel cell (Yan et al., 2004). Water may be transferred from one side of the membrane to the other if there is a pressure difference between the cathode and the anode.

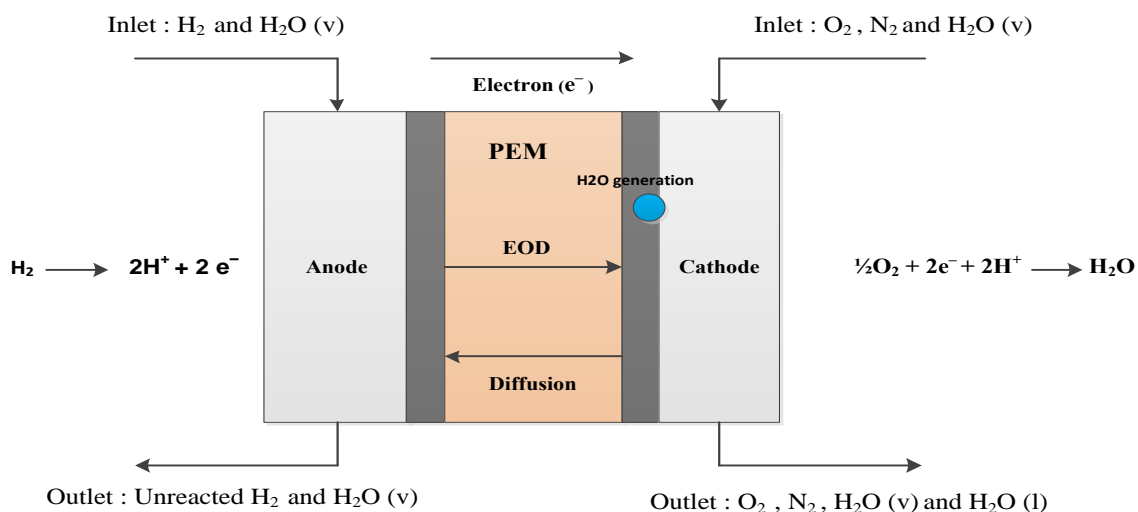


Figure 1.4. Mechanism of water transport in PEM fuel cell

Electro-osmotic drag (EOD) is one of the main water transport forces in the proton exchange membrane. It occurs due to the motion of the protons across the membrane from the anode to cathode carrying water molecules with them. The rate of water transport due to electro-osmotic drag is important because it directly affects the water balance in the PEM fuel cell and it is proportional to current density. It has been suggested that the number of water molecules dragged is relatively dependent on the nature of the polymer and the operating temperature but not on the thickness of membrane. (Zawodzinski et al, 1993). The number of water molecules carried by each proton is normally between 0.5 and 1.5 molecules per proton.

Back diffusion means the transfer of water through the membrane from the cathode to the anode as a result of concentration gradient of water across the membrane. Water transport in the membrane by back diffusion is usually affected by the fuel cell

temperature, the current density, the humidity of the feed gases and the membrane water content (Yan et al, 2004).

In the convective transfer (hydraulic permeation), the water transports in PEM fuel cell between the anode and the cathode due to the pressure gradient. The hydraulic permeation is generally negligible compared to the effects of electro-osmotic drag and the back diffusion, due to very low membrane hydraulic permeability (Dai et al, 2009)

### **1.3.1 Membrane Dehydration**

Insufficient water causes dehydration of membrane that decreases proton conductivity and increases ohmic resistance for proton transport, which leads to a reduction in output power, degraded of fuel cell performance, and the membrane may be permanently exposed to drying conditions (Canut et al., 2006). Membrane dehydration may be caused due to the following reasons: the reactants are fed to the cell with low humidified or dry gas streams; water generation at the cathode alone is not able to compensate the lack of water, especially at higher cell operating temperatures; and electro-osmotic drag can also cause to dehydrated condition at the anode because at high current densities the water replenishment by back-diffusion is not sufficient to keep the anode side of the membrane hydrated (Schmittinger and Vahidi, 2008).

Dehydration can be mitigated by humidifying the reactant gases at a large value to ensure that the membrane remains fully hydrated, by decreasing the flow rates of the reactants or by decreasing the operating temperature of the fuel cell.

### **1.3.2 Electrodes Flooding**

Floods occur in both the anode and the cathode of the membrane due to the accumulation of excess water at high current densities. When the water generated is greater than the water removal, the flooding occurs at the pores of the catalyst layer (CL), the gas diffusion layer (GDL), and the gas flow channels (Li et al, 2008). This

water flooding increases the internal resistance of the cell, prevents the reactants from reaching the catalysts' active sites, and reducing the PEM fuel cell performance dramatically (Jiao & Li, 2011).

Flooding of the cathode is more common than flooding of the anode because of the water generation as a result of oxidation reduction reaction, water transfer across the membrane due to the influence of electro-osmotic drag phenomena, and water supply with oxygen/air and hydrogen flows. Nevertheless, the anode may be exposed to flooding at lower current densities, lower cell temperatures, and water back-diffusion from the cathode together with a low hydration state of the fuel gas stream (Schmittinger&Vahidi, 2008). The flooding of the cathode and the anode can be alleviated by increasing the operating temperature resulting in a higher vapor pressure of water (Ji & Wei, 2009; Jiao & Li, 2011)

#### **1.4 Thermal Management in the PEM Fuel Cell**

In a PEM fuel cell, although the operating temperature is low, there is significant amount of heat dissipated during operation. This energy will lead to an increase in the operating temperature of the fuel cell drying the electrolyte and decreasing the proton transfer across, if it is not adequately removed from the stack. Engineering design and sizing of the stack cooling system is an important issue in a fuel cell system.

At the fuel cell stack, the chemical energy of hydrogen is converted to electricity and heat. The stack is the main source of heat generation in the fuel cell system. The heat generation in a PEM fuel cell stack includes entropic heat due to change of the entropy of the electrochemical reaction, irreversibility's of the electrochemical reactions inside a fuel cell, and ohmic heat that results from both the proton current and the electron current (Kandlikar and Lu, 2009). This heat has to be removed from the cell by the cooling system to avoid overheating.

The performance of the heat management of the fuel cell depends strongly on the temperature. The operating temperature has a significant influence on PEM fuel cell performance. The increase in the operating temperature affects cell performance since it decreases the reversible open circuit voltage (Nernst equation), increases the reaction rate and decreases the activation over potential, and increases the rate of mass transport (Peng and Lee, 2006). However, in a PEM fuel cell, the operating temperature also affects the water management components because the temperature inside the cell affects the water balance through the vapor pressure of water (Zaffou et al, 2006). Moreover, the most critical challenges from the water management point of view are membrane dehydration and cathode flooding which are affected by the operating temperature of a PEM fuel cell (Kandlikar and Lu, 2009).

The PEM fuel cells are usually developed to operate in a temperature range of 60 to 80°C. If the PEM fuel cell is working at a lower temperature, water condensation can be accelerated and water flooding occurs which causes low proton conductivity and low electrochemical reaction rates. On the other hand, if the PEM fuel cell is working at higher temperature, water removal increases from both the cathode and anode. As a result, the membrane may be exposed to dehydration that causes high ohmic resistance of the membrane which leads to low conductivity of protons. Therefore, proper thermal management is necessary in order to ensure that a stack operates within the specific range of temperatures (Ahn, 2011).

## **1.5 Literature Review**

Most of the research efforts for automotive applications focus on PEM fuel cells due to their capability of higher power density and faster start-up compared to other fuel cell types. Water and thermal management for PEM fuel cells has become one of the key technical challenges that must be resolved in order to be used in automotive applications. Proper water and thermal management is important for optimizing the performance of a fuel cell stack.



Water and heat management in automotive fuel cell systems can be categorized and analyzed at cell and systems levels. The cell level studies investigate the effects of parameters such as pressure, flow rate, temperature, humidity, and membrane thickness on the performance of the fuel cell stack (Freire and Gonzalez, 2001; Amirinejad et al, 2006; Yuan et al.,2010; Yu and Jung, 2008; Yan et al, 2008; Guvelioglu and Stenger, 2007).

The system level studies investigate the performance of the overall system including the air and hydrogen supply systems, pumps, compressors, fans and other auxiliary equipments. There are numerous system level studies PEM fuel cell systems. Some of these systems are directly for automotive applications whereas others are more generic.

Badrinarayanan (1999) studied a direct hydrogen fuel cell system model as presented in Figure 1.5. The model investigated the impacts of various parameters on the water and thermal management of the fuel cell system. The results showed that an increase in cathode pressure or decrease in cathode stoichiometry can decrease the water and thermal management parasitic loads. The results also showed that the size of the radiator and condenser should be taken into account in a full optimization of system performance.

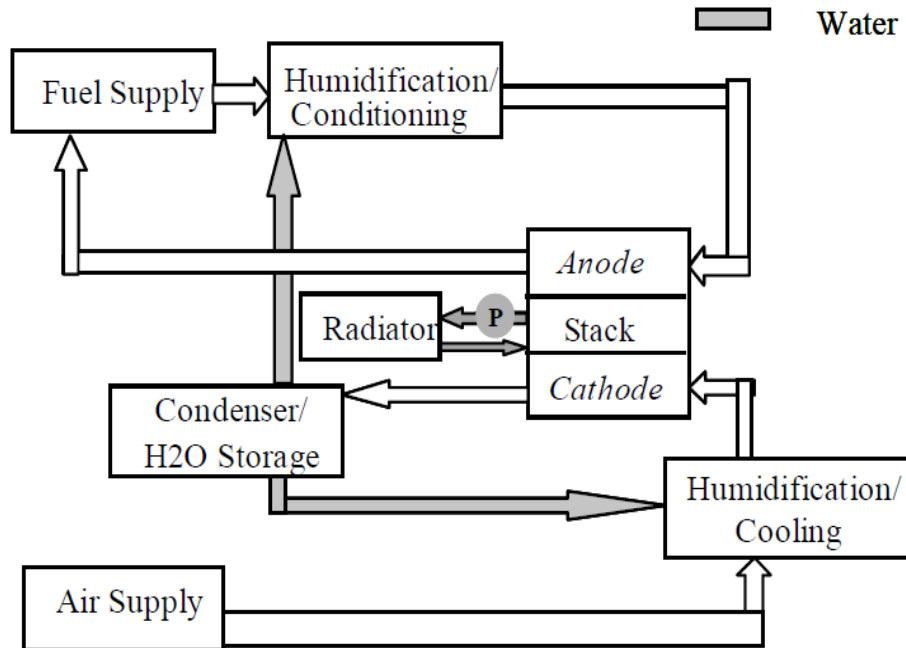


Figure 1.5. Schematic of a direct –hydrogen fuel cell system (Badrinarayanan, 1999)

Maxoulis et al. (2004) studied numerically the effects of various design and operation variables of the fuel cell stack, such as maximum stack power, catalyst activity and water concentration in the channels, in the fuel consumption of a vehicle equipped with a specific stack. The results showed that the cathode reaction kinetic rates have a higher impact on stack temperature and fuel consumption than the kinetics of the anode, and the cathode water concentration significantly affects the fuel consumption, while the anode water concentration has a negligible effect.

Moore et al. (2004) studied a direct hydrogen fuel cell system model as shown in Figure 1.6. There are four major subsystems in this model: fuel cell stack, air supply system, water and thermal management system, and hydrogen supply. The air supply at high pressure is provided by a compressor. In this system no humidifier is included for controlling the air humidity entering the cathode. The water and thermal management (WTM) system includes the primary heat transfer component (radiator) and primary water recovery unit (condenser) within the fuel cell system. The hydrogen

supply subsystem consists of a high-pressure hydrogen tank for the hydrogen storage, and a recirculation loop to add the unused hydrogen in the stack exhaust into the flow of fresh hydrogen from the storage tank. The results showed that the WTM system is strongly affected by the operating parameters (cathode pressure and cathode stoichiometry).

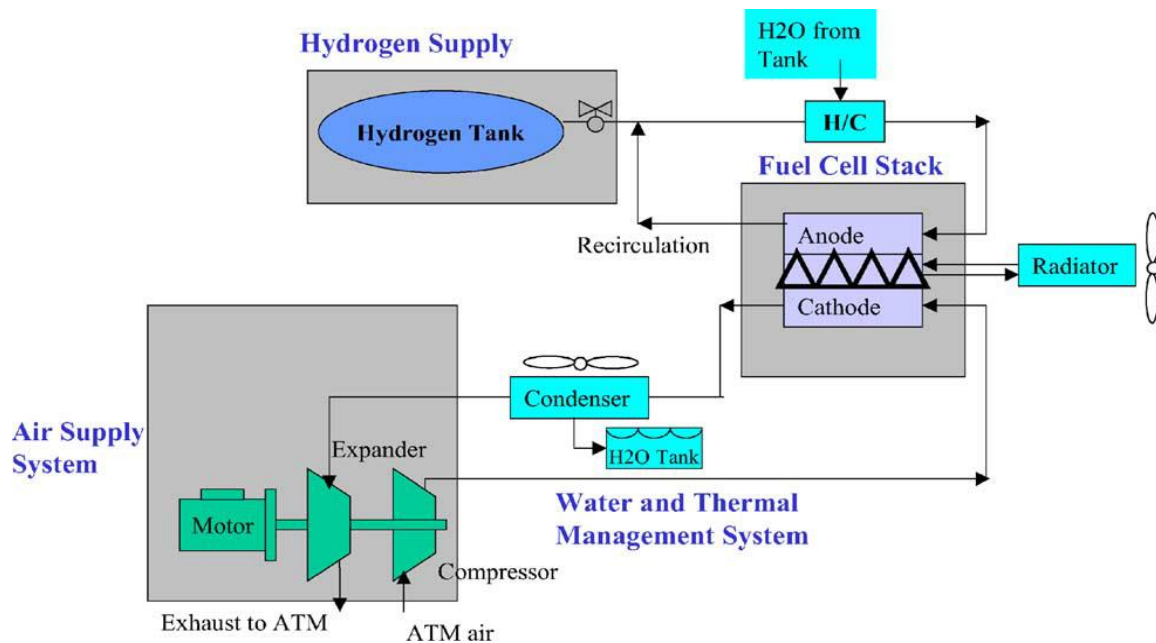


Figure 1.6. Direct hydrogen fuel cell system (Moore et al, 2005)

Bao et al. (2006) simulated a steady-state, one-dimensional, isothermal PEM fuel cell system model as seen in Figure 1.7. The model was developed to investigate the effects of air stoichiometric ratio and the cathode outlet pressure on the thermal loads of different components, including fuel cell stack, radiator, condenser, and membrane humidifier. The decrease of air stoichiometric ratio or the increase of cathode outlet pressure decreases the parasitic load of condenser because the moisture content in the cathode exhaust mixture decreases.

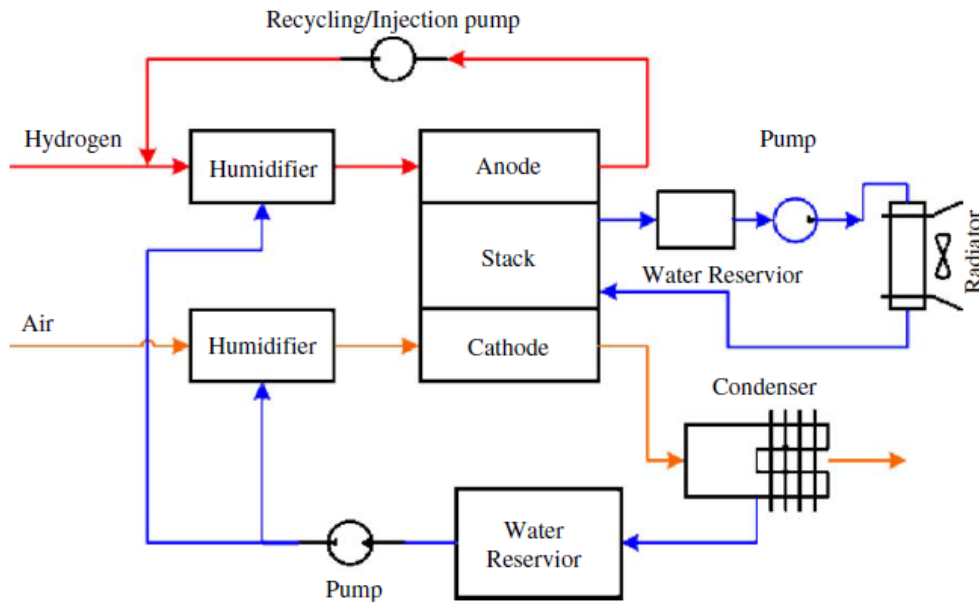


Figure 1.7. Schematic diagrams of the water and thermal management system in a pure-hydrogen PEM fuel cell system (Bao et al, 2006).

Wishart et al. (2008) studied numerically a zero-dimensional, steady-state electrochemical model of fuel cell system as seen in Figure 1.8. The model investigated the optimal operating conditions applied to a fuel cell system designed to operate in automotive and stationary applications. The system model is developed to provide the time-independent polarization curves, power curves and system efficiencies at various operating conditions. The results showed that the reduction in the air stoichiometric ratio and operating pressure causing an increase in net power is due to a decrease in the necessary power of the auxiliary devices (compressor and cooling system). It is also showed that the system efficiency increases with a decrease in operating pressure and stoichiometric ratio.

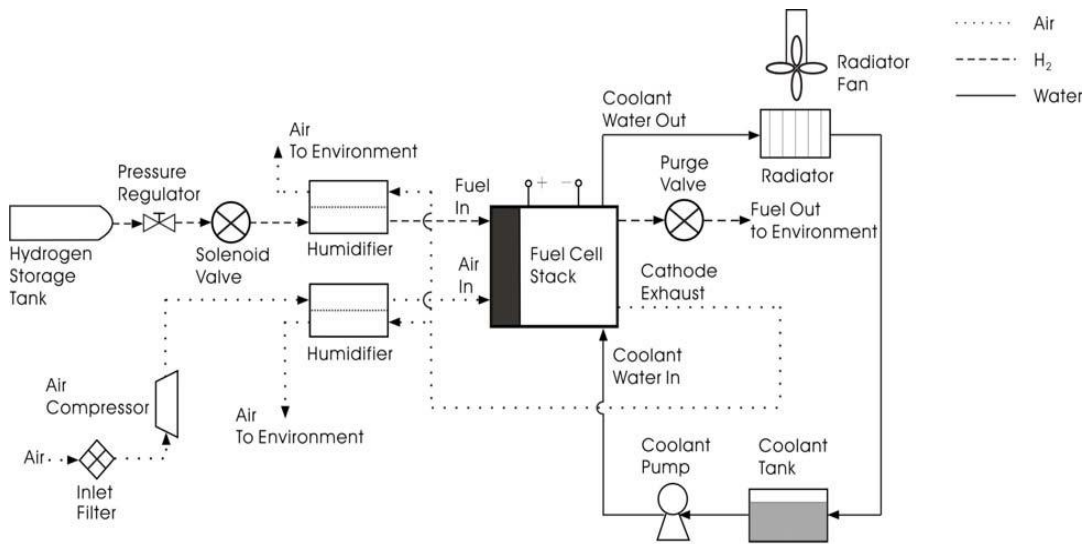


Figure 1.8. Fuel cell system schematic (Wishart et al, 2006)

Mert et al. (2012) analyzed a PEM fuel cell engine system as seen in Figure 1.9 which is used in transportation applications. This system consists of components such as a compressor, humidifiers, pressure regulator, hydrogen storage tank, cooling system, heat exchanger and the fuel cell stack. The system performance was investigated through parametric studies of energy, exergy and work output values by changing operating conditions and system parameters. The results showed that the system efficiency increases with the increase of temperature and pressure and it is also showed that an increase in relative humidity of the system has a positive effect on the efficiency and power production values. In addition, the results showed that the efficiency increases with the decrease of membrane thickness, anode stoichiometry, and cathode stoichiometry.

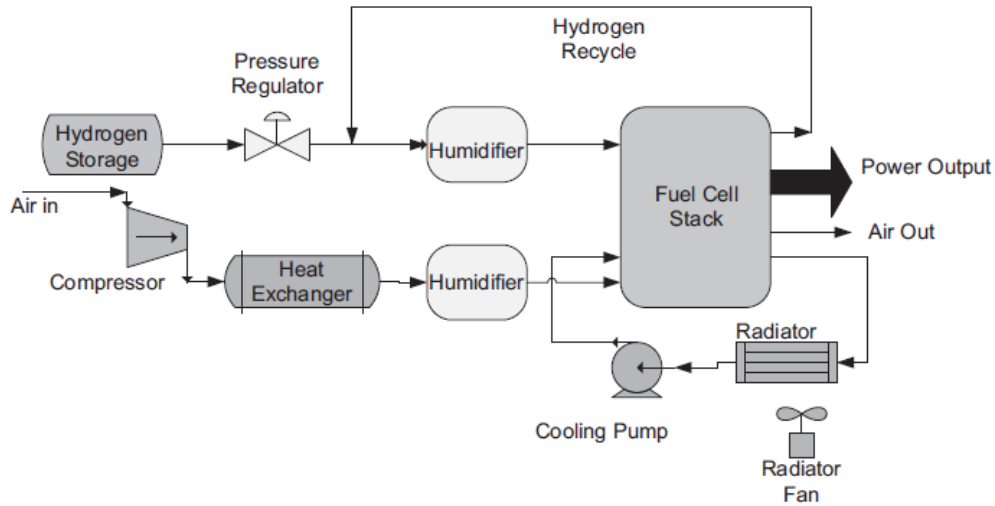


Figure 1.9. Schematic view of a fuel cell engine system (Mert et al, 2012)

Hosseini et al. (2012) simulated a fuel cell power system as seen in Figure 1.10. They studied the effects of current densities, membrane humidity, and pressure difference between anode and cathode on the generated power. It is shown that if the pressure difference between anode and cathode arises, hydrogen ions flow through the membrane is disturbed. This disturbance will decrease the terminal voltage of fuel cell system. The results also showed that the amount of injected water into the flow is a critical parameter of power generated by the system. As the humidity of inlet air increases the terminal stack voltage increases too. They also indicated that the best range for current density to have efficient and powerful system is between 0.6 to 0.9  $A/cm^2$ . At high current densities electrochemical reaction rate increases therefore terminal voltage of the system increases. On the other hand, the fuel cell stack losses increases while the current increases and fuel cell efficiency drops down rapidly due to these losses.

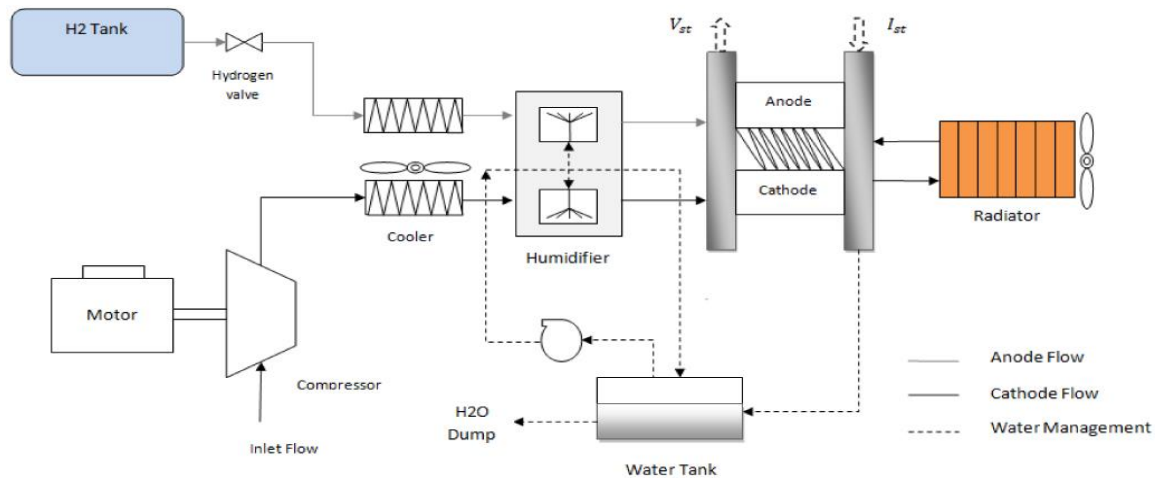


Figure 1.10. Schematic view of a fuel cell power system (Hosseini et al., 2012)

Hosseinzadeh et al. (2013) recently presented a general zero-dimensional PEM fuel cell model for a truck application as seen in Figure 1.11. The model was developed to study the water and thermal management and balance of the fuel cell stack. The results showed that the decrease of air humidity increases the ionic resistance eventually and it causes a significant drop in the voltage. In addition, the air stoichiometric ratio must be greater than one to remove produced water from the stack to prevent cathode from flooding. Furthermore, the operating temperature of the cell significantly affects the fuel cell performance. Higher the temperature increases the need for humidification and water production cannot meet the corresponding demand.

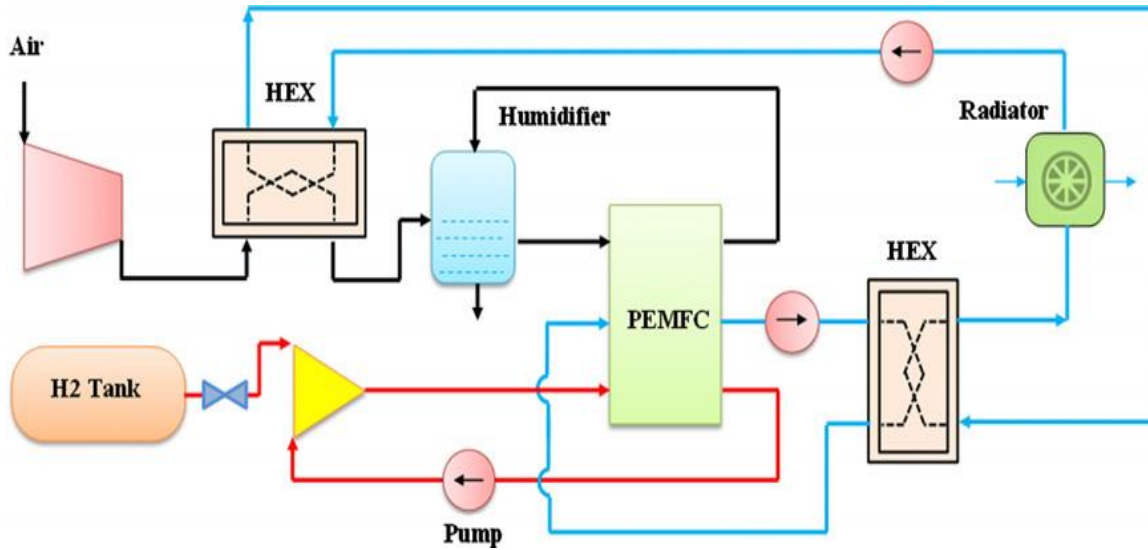


Figure 1.11. Schematic diagram of PEM fuel cell system (Hosseinzadeh et al, 2013)

### 1-6 Thesis Objectives

As can be seen from the literature review of previous system level studies, a PEM fuel cell system model that directly links the performance parameters of a typical passenger car to its fuel cell system is not available in the literature. While designing a sedan size car, it is very important to be able to predict the typical sizes of the fuel cell system components (fuel cell and the radiator), water and heat balance during operation, fuel consumption and efficiency based on the speed of the vehicle.

Therefore, the first objective of this thesis is to develop a system level (0-D) steady-state thermodynamics model for an automotive PEM fuel cell system.

The second objective of this thesis is to investigate the effects of various operating parameters such as vehicle speed, and operating pressure on the size of the system components, heat and water formation, fuel consumption and efficiency.



## **1-7 Thesis Structure**

This work presents an analytical model of an automotive PEM fuel cell system with a maximum power of 90 kW. The first chapter provides an overview of main components and operation principles of PEM fuel cells. A literature review on PEM fuel cell system modeling was included.

The development of a thermodynamic model is explained in Chapter 2. The PEM fuel cell system model is composed of three interacting sub- models, namely fuel cell stack, auxiliary components, and a vehicle model. The fuel cell stack model consists of the following sub- models: fuel cell voltage model, anode flow model, cathode flow model, membrane hydration model, and a heat transfer model. Models of the auxiliary components include the compressor, humidifier, radiator, and pumps.

The solution methodology of the PEM fuel cell system model is presented in Chapter 3. The system was modeled in MATLAB.

Results and discussions are given in Chapter 4. Results are composed of the following parts: the analysis of the PEM fuel cell stack model to obtain the stack gross power and cell voltage and analysis of the system power output, fuel consumption, system efficiency, and water and heat management.

The conclusions and recommendations for future work are given in Chapter 5.

## CHAPTER 2

### A 0-D STEADY-STATE SYSTEM MODEL FOR A PEM FUEL CELL SYSTEM

In this chapter, a general zero-dimensional Proton Exchange Membrane (PEM) fuel cell model is presented for automotive applications. The first step in the development of such a model is design the system layout including the fuel cell stack and all auxiliary equipments. As explained in the forthcoming chapters, as the operation pressure is increased the layout of the system changes due to the cooling requirement of the compressed air. In this thesis, system simulations are carried at two different operating pressures 3 atm and 1.5 atm.

Figure 2.1 shows the schematic diagram of an automotive PEM fuel cell system proposed for 3 atmosphere operating pressure. This diagram is similar to existing commercial PEM fuel cell automotive systems available in the market and consists of components necessary to supply reactants, remove the heat generated, and manage the water produced. The fuel cell stack requires three flow systems that interact with each other: air supply system, hydrogen supply system, and water and thermal management systems.

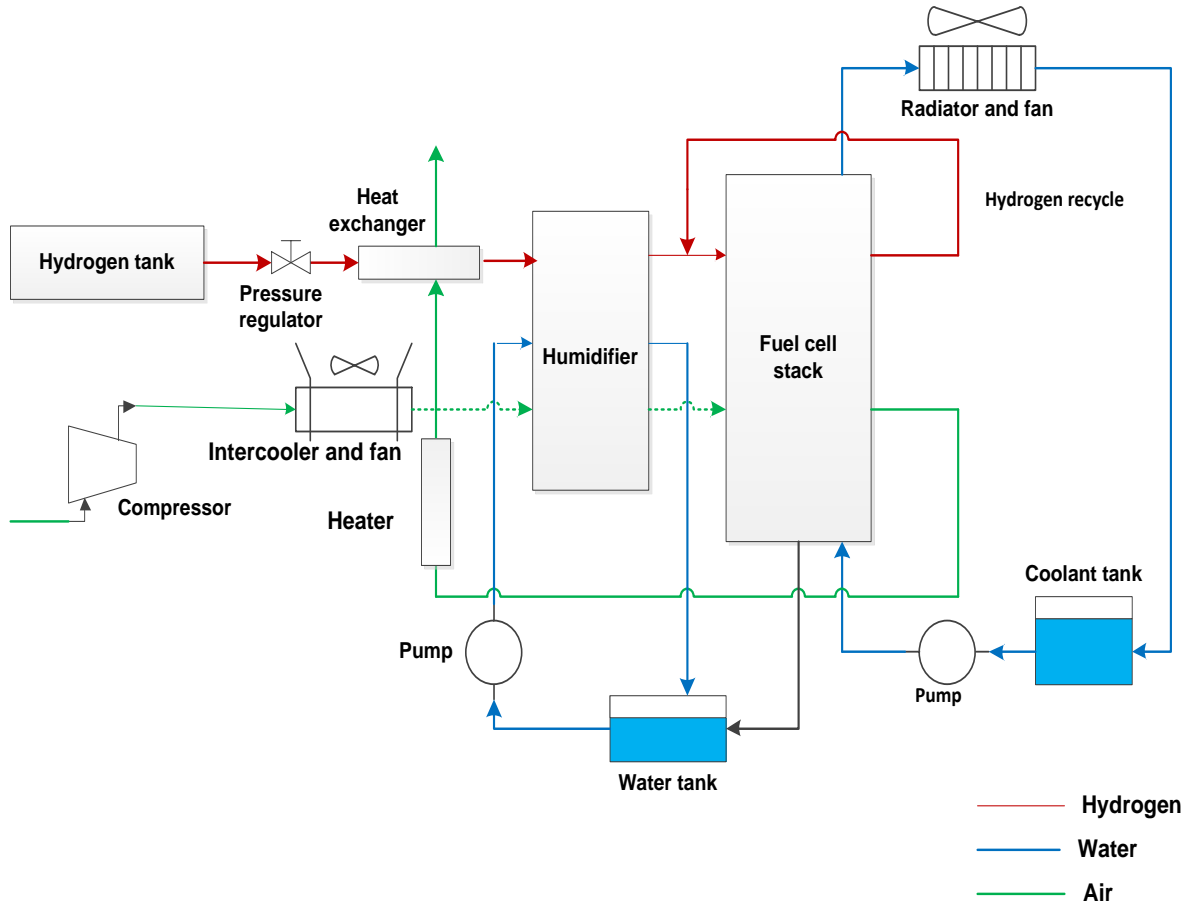


Figure 2.1. A schematic diagram of an automotive PEM fuel cell system at 3 atm operation pressure

The air supply system consists of a compressor, air cooler (intercooler), humidifier, and a heater. The air supply at high pressure is provided by the compressor. The compression process causes a temperature rise in the air supplied. To lower the temperature of the incoming air to the humidifier, the air passes through an intercooler. Air is humidified by the humidifier before entering the cathode side of fuel cell stack to ensure an adequate hydration level of the membrane. The unused air leaving the stack can be heated by the heater and used to increase the hydrogen temperature through a heat exchanger in the hydrogen supply line.

The hydrogen supply system consists of a hydrogen tank, pressure regulator valve, heat exchanger, humidifier, and the unused hydrogen recycle line. The hydrogen is

stored in a tank at high pressure. A pressure regulator valve is used to adjust the flow rate of hydrogen. The heat exchanger helps warm the incoming hydrogen which is then fed to the humidifier. Like air flow, hydrogen is humidified by the humidifier before entering the anode side of fuel cell stack. The recycling system for hydrogen is used to collect the hydrogen that is not reacted inside the stack and sent back to mix with the incoming anode stream after the humidifier.

The water and thermal management systems consist of a radiator, a fan, pumps, and a water tank. The main function of the radiator is to maintain the fuel cell stack at its operating temperature by dissipating heat to the coolant. The fan increases the effectiveness of heat convection at lower vehicle speeds. The pumps recirculate the water and the coolant through the system and the water tank is used to restore and save the generated water. The generated water is used to humidify the reactant gases through the humidifier.

Figure 2.2 shows the schematic diagram of an automotive PEM fuel cell system at 1.5 atmosphere. This figure is different from the previous figure only in the air supply system. The intercooler is replaced by a heater to increase the air temperature before entering the humidifier and a condenser is used at the exhaust of air to condense the water vapor (mixed with air at exit of cathode) to be used in humidification of the reactants. The exhaust temperature after the condenser is expected low, the cathode stream is directly rejected to atmosphere.

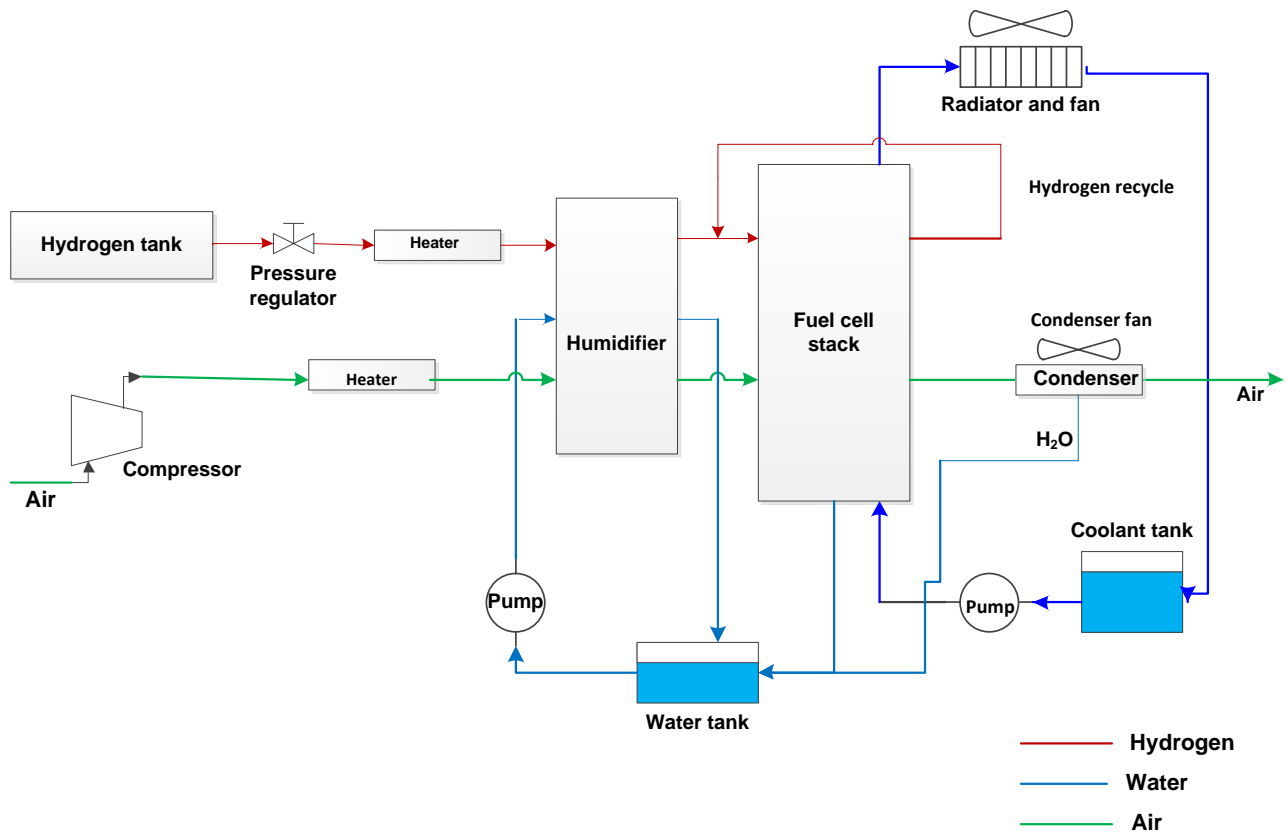


Figure 2.2. A schematic diagram of an automotive PEM fuel cell system at 1.5 atm operation pressure

The stack used throughout this research is chosen to be a 230 cell stack with composite bipolar plates and an active area of 625 cm<sup>2</sup>. The maximum power of the system is 90 kW at 3 atm. This system is typical of those found in automotive applications and is similar to the particular system found in Toyota Motor Corporation FC vehicle. The design of the fuel cell stack is further detailed in the Chapter 4.

## 2.1 Fuel Cell Stack Model

The fuel cell stack model consists of the following sub-models: fuel cell voltage model, anode flow model, cathode flow model, membrane hydration model, and heat transfer model. In the voltage model, an equation (based on Nernst equation) is used to calculate the stack voltage as a function of the operating conditions: pressure, temperature, and membrane humidity. The cathode and anode flow models represent the reactants gas flow behavior inside the stack flow channels. The membrane hydration model represents the water content in the membrane and the rate of mass flow of water across the membrane. The heat transfer model is based on the total thermal power produced by the electrochemical reactions.

### 2.1.1 Fuel Cell Voltage Model

#### 2.1.1.1 Thermodynamics

The fuel cell directly converts chemical energy into electrochemical energy. The chemical energy released from the fuel cell can be calculated from the change in the Gibbs free energy ( $\Delta G$ ). At a given temperature and pressure, the maximum amount of energy that can be used to do electrical work,  $W_e$  is given by the change in Gibbs free energy (Spiegel, 2008):

$$W_e = -\Delta G \quad (2.1)$$

$\Delta G$  which is the difference between the Gibbs free energy of the products and the Gibbs free energy of the inputs or reactants at a given temperature and pressure (Spiegel, 2008):

$$\Delta G = G_{\text{products}} - G_{\text{reactants}} \quad (2.2)$$

where  $G_{\text{products}}$  is the Gibbs free energy of the products and  $G_{\text{reactants}}$  is the Gibbs free energy of the reactants. The Gibbs free energy ( $G$ ) can be defined as the net energy required to create a system and making room for it minus the energy received

from the environment due to heat transfer. The Gibbs free energy of a system is related to the enthalpy and entropy by (Spiegel, 2008):

$$G = H - TS \quad (2.3)$$

where H is the enthalpy for a substance, T is the absolute temperature, and S is the entropy. Thus,  $W_e$ , the maximum electrical power output is given as (Spiegel, 2008):

$$W_e = \Delta G = \Delta H - T \cdot \Delta S \quad (2-4)$$

In general, the electrical work is a product of charge and potential:

$$W_e = Q \cdot E \quad (2.5)$$

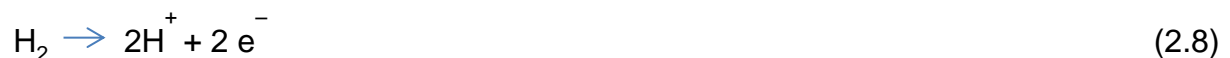
where Q is charge (Coulombs mol<sup>-1</sup>), E is potential (Volts). If the charge is assumed to be carried out by electrons:

$$Q = n \cdot F \quad (2.6)$$

where n is the number of moles of electrons transferred per mole of fuel consumed and F is the Faraday's constant (96,485 coulombs per mole of electrons), one can combine the equations 2.4, 2.5, and 2.6 to give us the maximum reversible voltage (or standard reversible potential) provided by the cell:

$$E^\circ = - \frac{\Delta G}{n F} \quad (2.7)$$

The reaction occurring at the anode side is:



The reaction occurring at the cathode side is:



The Gibbs free energy for the fuel cell reaction at the standard reference temperature and pressure, and the corresponding reversible cell potential can be calculated as follows:

$$\Delta G = \Delta H - T \cdot \Delta S \quad (2.10.a)$$

$$\Delta G = \left[ (h_f)_{\text{H}_2\text{O}(l)} - \left[ (h_f)_{\text{H}_2} + \frac{1}{2} (h_f)_{\text{O}_2} \right] \right] - T * \left[ s_{\text{H}_2\text{O}(l)} - \left[ s_{\text{H}_2} + \frac{1}{2} s_{\text{O}_2} \right] \right] \quad (2.10.b)$$

$$\Delta G = \left[ -285,826 \frac{\text{J}}{\text{mol}_{\text{H}_2\text{O}}} - \left[ 0 + \frac{1}{2} * 0 \right] - T * \left[ 69.92 \frac{\text{J}}{\text{mol}_{\text{H}_2\text{O}}} - \left[ 130.68 \frac{\text{J}}{\text{mol}_{\text{H}_2}} + \frac{1}{2} * 205.14 \frac{\text{J}}{\text{mol}_{\text{O}_2}} \right] \right] \right] \quad (2.10.c)$$

$$\Delta G = \left[ -285,826 \frac{\text{J}}{\text{mol}_{\text{H}_2\text{O}}} - 298\text{K} * -163.25 \frac{\text{J}}{\text{mol K}} \right] = -237.177 \text{ KJ/mole} \quad (2.10.d)$$

$$E^\circ = \frac{-237.177 \text{ KJ/mole}}{2 \text{ mole} * 96,485 \text{ C/mole}} = 1.229 \text{ V} \quad (2.11)$$

At standard temperature and pressure, this is the highest voltage obtainable from a hydrogen–oxygen fuel cell. It also shows that for a hydrogen fuel cell reaction the reversible cell voltage decreases with temperature and increases with pressure.

### 2.1.1.2 Nernst Potential

When the PEM fuel cell is not connected to an external load, there is no current flow outside of the cell and the operating voltage is equal to the open-circuit voltage (OCV). Furthermore, in a practical fuel cell operation, hydrogen and oxygen streams are not pure. Hydrogen is mixed with water vapor for humidification purposes and oxygen is supplied with humidified air. Therefore, the concentrations of the hydrogen and oxygen (or the partial pressures) affect the OCV according to the well-known Nernst potential equation.



The OCV is typically assumed to be the equilibrium Nernst potential for the overall electrochemical reaction (Larminie and Dicks , 2003):

$$E_{\text{Nernst}}(T, P_i) = E^\circ(T, P) + \frac{RT}{2F} \left[ \frac{P_{\text{H}_2} \cdot P_{\text{O}_2}^{1/2}}{P_{\text{H}_2\text{O}}} \right] \quad (2.12)$$

Where  $E^\circ$  the reversible OCV,  $R$  is the universal gas constant,  $P_{\text{H}_2}$  and  $P_{\text{O}_2}$  are the hydrogen and oxygen partial pressures at the surface of the catalyst at the anode and cathode, respectively, and  $P_{\text{H}_2\text{O}}$  is the vapor pressure at the cathode catalyst generated from the electrochemical reaction. In the case of liquid water product, it is a reasonable to assume that  $P_{\text{H}_2\text{O}}=1$ .

The maximum reversible OCV,  $E^\circ_{\text{max}}$ , has a value of 1.229 V at standard temperature and pressure. The reversible OCV will vary with temperature according to (Mench, 2008):

$$E^\circ(T, P) = E^\circ_{\text{max}}(298 \text{ K}, 1 \text{ atm}) - (T - T_0) \left[ \frac{\Delta s^\circ}{nF} \right] \quad (2.13)$$

where  $\Delta s^\circ$  is the change in standard-state entropy, which for the reaction of equation (2.9) can be calculated by (Mench , 2008):

$$\Delta s^\circ = \Delta s^\circ_{\text{H}_2\text{O}} - \frac{1}{2} \Delta s^\circ_{\text{O}_2} - \Delta s^\circ_{\text{H}_2} \quad (2.14)$$

The entropy change for the fuel cell reaction at the standard reference temperature and pressure,  $\Delta s^\circ$ , can be assumed to have a constant value of  $-163.303 \text{ J} \cdot \text{mol}^{-1} \cdot \text{K}^{-1}$  (it will actually change with temperature, but only marginally.) The equation for the reversible OCV is thus:

$$E^\circ(T, P) = 1.229 - 0.83 \cdot 10^{-3} (T - 298.15) \quad (2.15)$$

Combining Eq. 2.12 and 2.15 gives:

$$E^{\circ}_{\text{Nernst}} = 1.229 - 0.83 * 10^{-3} (T - 298.15) + \frac{RT}{2F} \left[ \ln P_{\text{H}_2} + \frac{1}{2} \ln P_{\text{O}_2} \right] \quad (2.16)$$

### 2.1.1.3 Cell Potential

The cell potential  $v_{\text{cell}}$  is obtained by subtracting all potential losses from the equilibrium potential:

$$v_{\text{cell}} = E^{\circ}_{\text{Nernst}} - v_{\text{act}} - v_{\text{Ohmic}} - v_{\text{con}} \quad (2.17)$$

where  $E^{\circ}_{\text{Nernst}}$  is the Nernst potential for a given temperature and pressure calculated from Eq. 2.16,  $v_{\text{act}}$  is the voltage loss due to activation polarization,  $v_{\text{Ohmic}}$  is the voltage loss due to ohmic polarization and  $v_{\text{con}}$  is the voltage loss due to concentration polarization. These losses are shown in the polarization curve as a plot of cell potential versus current density. Figure 2.3 shows a typical polarization curve for a single PEM fuel cell. The polarization curve illustrates the voltage-current relationship based upon operating conditions such as temperature, humidity, applied load, and fuel/oxidant flow rates. The polarization curve can be divided into three regions: the region of the activation polarization is due to the slowness of the reactions taking place on the catalyst surface of the electrode, region of the ohmic polarization is due to the resistance of the transport of charged species in the polymer electrolyte membrane, catalyst and gas diffusion layers and bipolar plates, and region of the concentration polarization is due to mass transport limitations.

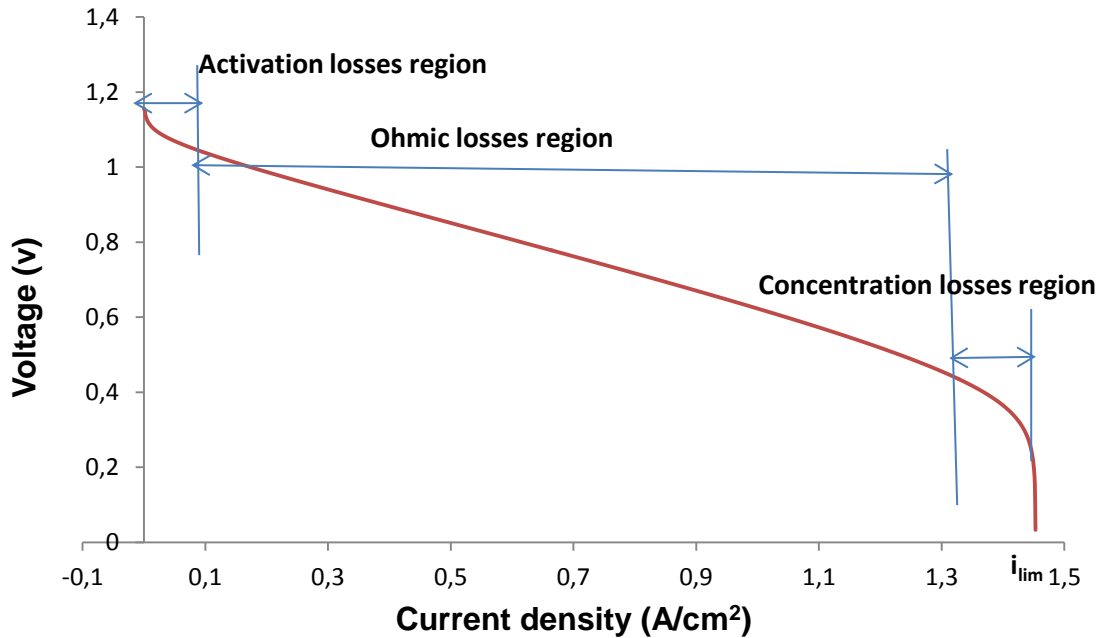


Figure 2.3. Schematic diagram of the polarization curve of a PEM fuel cell

The stack voltage is simply the cell voltage multiplied by the number of cells (Larminie and Dicks, 2003):

$$V_{\text{stack}} = V_{\text{cell}} \cdot n_{\text{cell}} \quad (2.18)$$

The power output of the fuel cell stack (W) is given by (Larminie and Dicks, 2003):

$$P_e = i \cdot v_{\text{cell}} \cdot n_{\text{cell}} = i \cdot E_{\text{stack}} \quad (2.19)$$

### 2.1.1.3.1 Activation Losses

The activation loss is the energy required to initiate the chemical reactions and it is considered one of the characteristic of the fuel cell reaction kinetics. These are caused by the slowness of the reactions taking place on the surface of the electrodes. Activation polarization depends on the type of the electrodes, ionic interactions, ion-solvent interactions and the electrode-electrolyte interface (Shivhare, 2012). The exchange current density  $i_0$  is the critical factor in reducing the activation losses. An increase of exchange current density leads to minimize the activation losses.

Exchange current density can be increased in the following ways: raising the cell temperature; increasing the roughness of the electrodes by increasing electrodes active cell area; using more effective catalysts; increasing reactant concentration; and increasing operation pressure (Larminie and Dicks, 2003).

The activation losses in fuel cell voltage can be calculated using the well-known Butler- Volmer equation (O'Hayre et al, 2006):

$$V_{act} = V_{act,anode} + V_{act,cathode} \quad (2.20 a)$$

$$V_{act} = \frac{RT}{n\alpha_{anode}F} \left[ \ln \frac{i}{i_0} \right]_{anode} + \frac{RT}{n\alpha_{cathode}F} \left[ \ln \frac{i}{i_0} \right]_{cathode} \quad (2.20 b)$$

where  $i$  is the current density, and  $i_0$  is the reaction exchange current density,  $n$  is the number of exchange protons per mole of reactant,  $F$  is Faraday's constant, and  $\alpha$  is the charge transfer coefficient (Barbir, 2005). The exchange current density for the oxygen reduction reaction at the cathode is much smaller than that for the hydrogen oxidation reaction at the anode, which it may be up to  $10^5$  times smaller. Therefore, the activation polarization at the anode is negligible compared to that of the cathode (Larminie and Dicks, 2003).

### 2.1.1.3.2 Ohmic Losses

Ohmic losses are usually dominated by ionic resistance in the electrolyte and the electrical resistance of the electrodes. These losses can be reduced by using electrolytes with high ionic conductivity, electrodes with high electronic conductivity and by reducing /minimizing the electrolyte thickness (Larminie and Dicks, 2003).

The total cell ohmic-resistance can be calculated as the sum of the electrical and ionic resistances (O'Hayre et al, 2006):

$$V_{Ohmic} = i R_{Ohmic} = i (R_{elec} + R_{ionic}) \quad (2.21)$$

where  $v_{\text{Ohmic}}$  represents the Ohmic loss,  $i$  is the current density, and  $R_{\text{Ohmic}}$  represents the effective resistance,  $R_{\text{elec}}$  includes the total electrical resistance of all other conductive components, including the bipolar plates, cell interconnects, and contacts, and  $R_{\text{ionic}}$  represents the ionic resistance of the electrolyte.

Resistance is characteristic of the size, shape and properties of the material, as expressed by the following equation (O'Hayre et al, 2006):

$$R = \frac{L_{\text{cond}}}{\sigma A_{\text{cond}}} \quad (2.22)$$

where  $L_{\text{cond}}$ , is the length or thickness (cm) of the conductor,  $A_{\text{cond}}$  is the cross-sectional area ( $\text{cm}^2$ ) of the conductor, and  $\sigma$  is the electrical conductivity ( $\text{ohm}^{-1} \text{cm}^{-1}$ ). The current density,  $i$ , ( $\text{A}/\text{cm}^2$ ), can be defined as the current (of electrons or ions) per unit area of the surface (O'Hayre et al, 2006):

$$i = \frac{I}{A_{\text{cell}}} \quad (2.23)$$

The total fuel cell ohmic losses can be written as (O'Hayre et al, 2006):

$$E_{\text{Ohmic}} = i A \sum R = i A \left[ \left( \frac{L}{\sigma A} \right)_{\text{anode}} + \left( \frac{L}{\sigma A} \right)_{\text{electrolyte}} + \left( \frac{L}{\sigma A} \right)_{\text{cathode}} \right] \quad (2.24)$$

where  $L$  the thickness of the electrolyte layer, and  $\sigma$  is the conductivity, and  $A$  is the active area of the fuel cell. As can be seen from Equation 2.24 and Figure 2.4, the cell voltage can be reduced by using a thicker electrolyte layer.

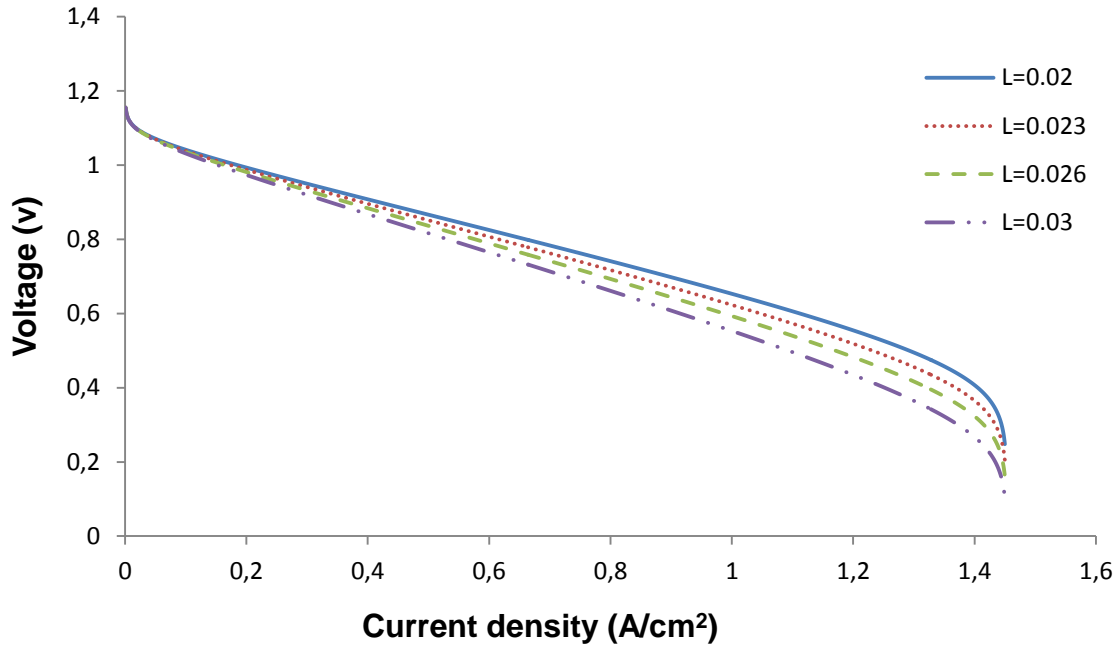


Figure 2.4. Effect of electrolyte thickness on the cell voltage

### 2.1.1.3.3 Concentration Losses

Concentration loss occurs due to a decrease in the concentration of the reactants at the electrode-electrolyte interface. These losses can be minimized by the following: increasing reactant concentration; increasing reactant flow rate and/or pressure; and improving gas diffusion layer structure and optimizing its porosity.

The concentration losses can be calculated using the following equation (Barbir, 2005):

$$V_{\text{con}} = \frac{RT}{nF} \ln \frac{i_L}{i_L - i} \quad (2.25)$$

where  $i_L$  the limiting current density. The limiting current density of the fuel cell is the point where the current density becomes large and the reactant concentration falls to zero so the fuel cell will not be able to produce a higher current density than its limiting current density. The limiting current density ( $i_L$ ) of the fuel cell can be calculated as follows:

$$i_L = \frac{nFD_{AB}(C_1 - C_2)}{\delta} \quad (2.26)$$

where  $D_{AB}$  is the diffusion coefficient of the reacting species,  $C$  is the concentration, and  $\delta$  is the thickness of membrane. The limiting current density can be increased by ensuring that  $D_{AB}$  is large and  $\delta$  is small.

#### 2.1.1.4 Fuel Cell Thermal Efficiency

General the thermodynamic fuel cell efficiency is the relation between the electrical power produced and the total rate of fuel energy entering the fuel cell;

$$\eta_{\text{ther}} = \frac{I \cdot V_{\text{cell}} \cdot n_{\text{cell}}}{\dot{m}_{\text{H}_2, \text{in}} \cdot \text{HHV}_{\text{H}_2}} \quad (2.27)$$

where  $\eta_{\text{ther}}$  is the thermodynamic efficiency of fuel cell,  $\dot{m}_{\text{H}_2, \text{in}}$  is the the mass flow rate of hydrogen gas entering the fuel cell, and HHV is the higher heating value of hydrogen.

#### 2.1.2 Anode Flow Model

In the anode flow model, hydrogen is supplied to the anode of the fuel cell stack by a hydrogen tank at high pressure. The gases inside are assumed to be ideal. The temperature of the flow is equal to the stack temperature, and is therefore assumed constant. Anode mass balance requires that the sum of all mass inputs must be equal to the sum of all mass outputs. The inputs are the flows of hydrogen and the water vapor present in those gases. The outputs are the flows of unused fuel and water vapor, plus any liquid water present in the exhaust. Generally, the anode mass balance can be expressed as:

$$\sum(\dot{m}_i)_{\text{in}} = \sum(\dot{m}_i)_{\text{out}} \quad (2.28)$$

where  $\dot{m}_i$  is the mass flow rate going into and out of the anode, and can be any species, including hydrogen and water vapor. Figure 2.5 illustrates mass flow balance for the anode.

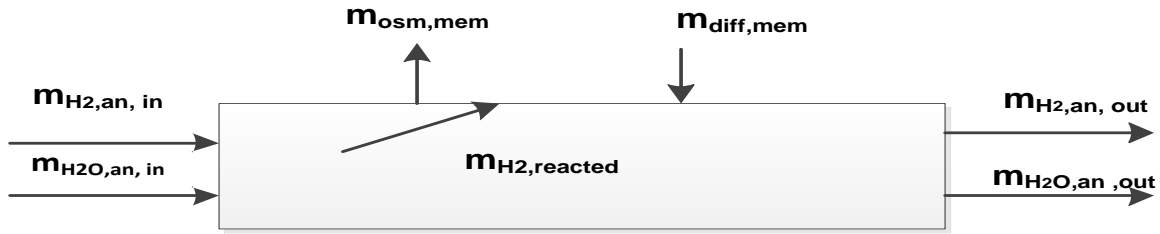


Figure 2.5. Anode mass flow balance

The steady state mass flow rate balance of hydrogen on the anode side can be described as:

$$\dot{m}_{H_2,an,in} = \dot{m}_{H_2,an,out} + \dot{m}_{H_2,reacted} \quad (2.29)$$

where  $\dot{m}_{H_2,an,in}$  is the mass flow rate of hydrogen gas entering the anode,  $\dot{m}_{H_2,an,out}$  is the mass flow rate of hydrogen gas leaving the anode, and  $\dot{m}_{H_2,reacted}$  is the rate of hydrogen reacted. The mass flow rate of hydrogen entering the anode can be calculated from as:

$$\dot{m}_{H_2,an,in} = \frac{\lambda_{H_2} \cdot M_{H_2} \cdot i \cdot A_{cell} \cdot n_{cell}}{2F} \quad (2.30)$$

where  $\lambda_{H_2}$  is the ratio between the actual rate of fuel delivered to anode and the theoretical rate of fuel required (stoichiometric ratio of hydrogen), and  $M_{H_2}$  is the molecular weight of hydrogen. The molar mass of hydrogen is  $2.02 \times 10^{-3} \text{ kg mole}^{-1}$ . The mass flow rate of hydrogen consumed in the electrochemical reaction is a function of stack current:



$$\dot{m}_{H_2,reacted} = M_{H_2} \cdot \frac{i \cdot A_{cell} \cdot n_{cell}}{2F} \quad (2.31)$$

The mass flow rate of water in the anode exhaust is equal to the mass flow rate of water vapor entering the anode minus the net water transport across the membrane. The outlet water vapor mass flow rate is:

$$\dot{m}_{H_2O,an,out} = \dot{m}_{H_2O,an,in} - \dot{m}_{osm,mem} + \dot{m}_{diff,mem} \quad (2.32)$$

where  $\dot{m}_{H_2O,an,out}$  is the mass flow rate of water leaving the anode,  $\dot{m}_{H_2O,an,in}$  is the mass flow rate of water vapor entering the anode,  $\dot{m}_{osm,mem}$  is the mass flow rate of water transfer to the membrane by electro osmotic drag force, and  $\dot{m}_{diff,mem}$  is the mass flow rate of water transfer from the membrane by back diffusion. The mass flow rate of water vapor entering the anode is the amount of water injected to fully humidify the hydrogen and will be explained at the humidifier model.

Relative humidity is defined as the ratio between the water vapor partial pressure,  $P_{v,an}$ , and saturation water vapor pressure,  $P_{sat}$ :

$$\phi_{an} = \frac{P_{v,an}}{P_{sat}(T_{an})} \quad (2.33)$$

where  $\phi_{an}$  is the relative humidity inside the anode. The water vapor saturation pressure is a function of temperature and has been calculated from this equation:

$$P_{sat}(T) = -2846.4 + 411.24(T) - 10.554(T)^2 + 0.16636(T)^3 \quad (2.34)$$

Water at anode exhaust may be present as vapor only, or liquid water may be present with water vapor depending on the hydrogen flow rate, stoichiometry, and temperature and pressure at the outlet. The water vapor content at the anode outlet is the smaller of the total water flux (Barbir, 2005):

$$\dot{m}_{\text{H}_2\text{O,an,out,v}} = \min \left[ \lambda_{\text{H}_2} \frac{M_{\text{H}_2\text{O}}}{2F} \frac{P_{\text{sat}}(T_{\text{an}})}{p_{\text{an}} - \Delta P_{\text{an}} - P_{\text{sat}}(T_{\text{an}})} i \cdot A_{\text{cell}} \cdot n_{\text{cell}}, \dot{m}_{\text{H}_2\text{O,an,out}} \right] \quad (2.35)$$

where  $\Delta P_{\text{an}}$  is the pressure drop on the anode side, that is, the difference in pressure between the inlet and outlet.

The amount of liquid water is the difference between the total water present at the exhaust of anode and water vapor content at the anode outlet (Barbir, 2005):

$$\dot{m}_{\text{H}_2\text{O,an,out,liquid}} = \dot{m}_{\text{H}_2\text{O,an,out}} - \dot{m}_{\text{H}_2\text{O,an,out,v}} \quad (2.36)$$

The mass flow rate of water liquid transfer across fuel cell membrane will be explained at the membrane hydration model and the amount of water injected to fully humidify the hydrogen will be explained at the humidifier model section.

### 2.1.3 Cathode Flow Model

In the cathode flow model, air is supplied to the cathode of the fuel cell stack by a compressor. The gases inside are assumed to be ideal. The temperature of the flow is equal to the stack temperature, and is therefore assumed constant. Cathode mass balance requires that the sum of all mass inputs must be equal to the sum of all mass outputs. The inputs are the flows of air and water vapor. The outputs are the flows of unused air and water vapor present in those gases, plus any liquid water present in the exhaust. Figure 2.6 illustrates mass flow balance in the cathode model.

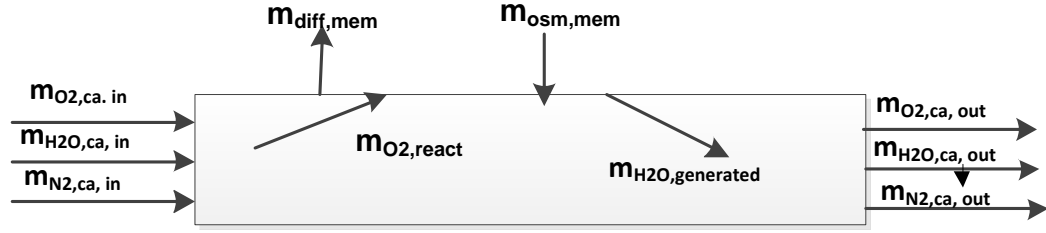


Figure 2.6. Cathode mass flow balance

The cathode mass flow model represents the air flow behavior inside the cathode of the fuel cell stack. The steady state mass flow rate of oxygen on the cathode side can be described as:

$$\dot{m}_{O_2,ca,in} = \dot{m}_{O_2,ca,out} + \dot{m}_{O_2,reacted} \quad (2.37)$$

where  $\dot{m}_{O_2,ca,in}$  is the mass flow rate of oxygen gas entering the cathode,  $\dot{m}_{O_2,ca,out}$  is the mass flow rate of oxygen gas leaving the cathode, and  $\dot{m}_{O_2,reacted}$  is the rate of oxygen reacted. The mass flow rates of oxygen entering the cathode can be calculated as (Barbir, 2005):

$$\dot{m}_{O_2,ca,in} = \lambda_{O_2} \frac{M_{O_2}}{4F} I \cdot n_{cell} \quad (2.38)$$

where  $M_{O_2}$  is the molecular weight of oxygen, and  $\lambda_{O_2}$  is the ratio between the actual rate of oxidizer delivered to cathode and theoretical rate of oxidizer required (air stoichiometric ratio) of oxygen. The molar mass of oxygen is  $32 \times 10^{-3} \text{ kg mole}^{-1}$ . The mass flow rate of oxygen consumed in the electrochemical reaction is a function of stack current (Barbir, 2005):

$$\dot{m}_{O_2,reacted} = M_{O_2} \cdot \frac{i \cdot A_{cell} \cdot n_{cell}}{4F} \quad (2.39)$$

The outlet oxygen and nitrogen can be calculated by the following equations:

$$\dot{m}_{O_2,ca,out} = (\lambda_{O_2} - 1) \frac{M_{O_2}}{4F} i \cdot A_{cell} \cdot n_{cell} \quad (2.40)$$

The steady state mass flow rate of nitrogen on the anode side can be described as:

$$\dot{m}_{N_2,ca,in} = \dot{m}_{N_2,ca,out} \quad (2.41)$$

where  $\dot{m}_{N_2,ca,in}$  is the mass flow rate of nitrogen gas entering the cathode, and  $\dot{m}_{N_2,ca,out}$  is the mass flow rate of nitrogen gas leaving the cathode. The mass flow rates of nitrogen entering the cathode can be calculated as:

$$\dot{m}_{N_2,ca,in} = \lambda_{O_2} \frac{M_{N_2}}{4F} \frac{1 - r_{O_2,in}}{r_{O_2,in}} i \cdot A_{cell} \cdot n_{cell} \quad (2.42)$$

where  $M_{N_2}$  the molecular weight of nitrogen, and  $r_{O_2,in}$  is oxygen volume fraction  $\cong 0.21$ . The molar mass of nitrogen is  $28 \times 10^{-3} \text{ kg mole}^{-1}$ . The mass flow rate of inlet air can be calculated as (Barbir, 2005):

$$\dot{m}_{air,in} = \frac{\lambda_{O_2}}{r_{O_2,in}} \frac{M_{air}}{4F} i \cdot A_{cell} \cdot n_{cell} \quad (2.43)$$

And the air flow rate at the exit is then simply a sum of oxygen and nitrogen flow rates (Barbir, 2005):

$$\dot{m}_{air,out} = \left[ (\lambda_{O_2} - 1) M_{O_2} + \lambda_{O_2} \frac{1 - r_{O_2,in}}{r_{O_2,in}} M_{N_2} \right] \frac{i \cdot A_{cell} \cdot n_{cell}}{4F} \quad (2.44)$$

The mass flow rate of water in the cathode exhaust is equal to the mass flow rate of water injected to humidify the air before it enters to cathode side, plus water generated in the cell and plus the net water transport across the membrane. The net water transport across the membrane is the difference between electro osmotic drag and water back diffusion. The outlet water mass flow rate becomes:

$$\dot{m}_{H_2O,ca,out} = \dot{m}_{H_2O,ca,in} + \dot{m}_{H_2O,gen} + \dot{m}_{osm,mem} - \dot{m}_{diff,mem} \quad (2.45)$$

where  $\dot{m}_{H_2O,ca,out}$  is the mass flow rate of water leaving the cathode,  $\dot{m}_{H_2O,ca,in}$  is the mass flow rate of water vapor entering the cathode, and  $\dot{m}_{H_2O,gen}$  is the mass flow rate of vapor generated in fuel cell reaction. The mass flow rate of water vapor entering the cathode consists of the mass flow rate of water injected to fully humidify the air and the amount of water vapor in the air inlet to the compressor. The mass flow rate of water injected to fully humidify the air will be explained at the humidifier model. The mass flow rate of water vapor in the air inlet to the compressor can be calculated as (Barbir, 2005):

$$\dot{m}_{H_2O \text{ in air in}} = \frac{\lambda_{O_2}}{r_{O_2,in}} \frac{M_{H_2O}}{4F} \frac{\phi_{amb} * P_{sat}(T_{amb})}{p_{atm} - \phi_{amb} * P_{sat}(T_{amb})} i \cdot A_{cell} \cdot n_{cell} \quad (2.46)$$

where  $M_{H_2O}$  is the molecular weight of water,  $\phi_{amb}$  is the relative humidity in the ambient,  $P_{sat}(T_{amb})$  is the the water vapor saturated pressure at ambient temperature, and  $p_{amb}$  is the ambient pressure. The mass flow rate of water generated from the fuel cell reaction can be calculated by the following equation (Mench, 2008):

$$\dot{m}_{H_2O,gen} = M_{H_2O} \cdot \frac{i \cdot A_{cell} \cdot n_{cell}}{4F} \quad (2.47)$$

Water at cathode exhaust may be present as liquid water with water vapor depending on the air flow rate, stoichiometry, and temperature and pressure at the outlet. The water vapor content at the cathode outlet is the smaller of the total water flux (Barbir, 2005):

$$\dot{m}_{H_2O,ca,out,v} = \min \left[ \frac{\lambda_{O_2} - r_{O_2,in}}{r_{O_2,in}} \frac{M_{H_2O}}{4F} \frac{P_{sat}(T_{stack})}{p_{ca} - \Delta P_{ca} - P_{sat}(T_{stack})} i \cdot A_{cell} \cdot n_{cell}, \dot{m}_{H_2O \text{ in air out}} \right] \quad (2.48)$$

where  $\Delta P_{ca}$  is the difference in pressure between the inlet and outlet on the cathode side. The amount of liquid water is the difference between the total water present at the exhaust of cathode and water vapor content at the cathode outlet (Barbir, 2005):

$$\dot{m}_{H_2O,ca,out,liq} = \dot{m}_{H_2O,ca,out} - \dot{m}_{H_2O,ca,out,v} \quad (2.49)$$

The mass flow rate of water liquid transfer across fuel cell membrane will be explained at the next section and the amount of water injected to fully humidify the air will be explained at the humidifier model.

### 2.1.4 Membrane Hydration Model

Transport of water content inside the membrane of fuel cell takes place by the electro-osmotic drag and the back-diffusion of water. Electro-osmotic drag means the transport of water molecules from the anode to the cathode by the hydrogen protons flowing through the membrane. Back diffusion occurs in the PEM fuel cell due to gradient of water concentration across the membrane. The concentration of water on the cathode side is higher than that on the anode side which causes diffusion of water from the cathode to the anode side. Figure 2.7 illustrates mass flow rates in the membrane flow model.

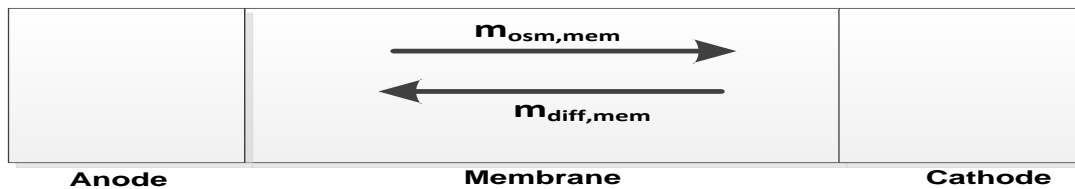


Figure 2.7. Mass flow in the membrane flow model

The mass flow rate of water content on the membrane can be described as (Ahn , 2011):

$$\dot{m}_{H_2O,mem} = \dot{m}_{osm,mem} - \dot{m}_{diff,mem} \quad (2.50)$$

where  $\dot{m}_{\text{osm,mem}}$  is the mass flow rate of water transfer to the membrane by electro osmotic drag force, and  $\dot{m}_{\text{diff,me}}$  is the mass flow rate of water transfer to the membrane by back diffusion.

The amount of water drag is proportional to the current density (I). The flux of water by electro-osmotic drag is calculated by the following equation (Mench, 2008):

$$\dot{m}_{\text{osm,mem}} = MW_{\text{H}_2\text{O}} \cdot n_d \cdot \frac{i \cdot A_{\text{cell}} \cdot n_{\text{cell}}}{F} \quad (2.51)$$

where  $n_d$  is the electro-osmotic drag coefficient in units of water molecules per proton. The electro- osmotic drag coefficient,  $n_d$ , can be calculated from the membrane water content,  $\lambda_m$  (Mench, 2008):

$$n_d = 0.0029\lambda_m^2 + 0.05 \lambda_m - 3.4 \times 10^{-19} \quad (2.52)$$

The water content in the membrane,  $\lambda_m$ , defined as the ratio of water molecules to the number of sulfonic acid groups within the ionomer, is calculated from the water activities  $a_w$  (Mench, 2008).

$$\lambda_m = 0.043 + 17.8a_w - 39.85 a_w^2 + 36.0a_w^3 \quad (2.53)$$

The water activity,  $a_w$ , needed to solve for  $\lambda_m$  is defined as (Mench, 2008):

$$a_w = \frac{y_v P}{P_{\text{sat}}(T)} = \text{RH} \quad (2.54)$$

where P is the pressure of anode or cathode. The amount of water concentration across the membrane that is caused by back diffusion is calculated by the following equation (Mench, 2008):

$$\dot{m}_{\text{diff,mem}} = - W_{\text{H}_2\text{O}} \cdot A_{\text{cell}} \cdot D_w \cdot \frac{C_w^m}{t_m} \quad (2.55)$$

In this thesis, the amount of water transfer by back diffusion assumed equal to 0.9 of water transfer by electro osmotic drag.

### 2.1.5 Heat Transfer Model

The energy released in the electrochemical reaction must be taken away from the stack to maintain it at the constant the desired temperature. The thermodynamic steady state energy balance of the fuel cell is given as:

$$\sum \dot{Q}_{i,in} = \sum \dot{Q}_{i,out} + W_{el} + \dot{Q}_{cool} + \dot{Q}_{env} \quad (2.56)$$

where  $\dot{Q}_{i,in}$  is the rate of energy entering with the reactant gases,  $\dot{Q}_{i,out}$  is the rate of energy leaving with the unused reactant gases,  $W_{el}$  is the electrical power generated,  $\dot{Q}_{cool}$  is the rate of heat carried from the fuel cell to the coolant, and  $\dot{Q}_{env}$  the rate of heat dissipated by the exposed stack surface to the environment. Figure 2.8 illustrates mass and energy flow of the fuel cell stack.



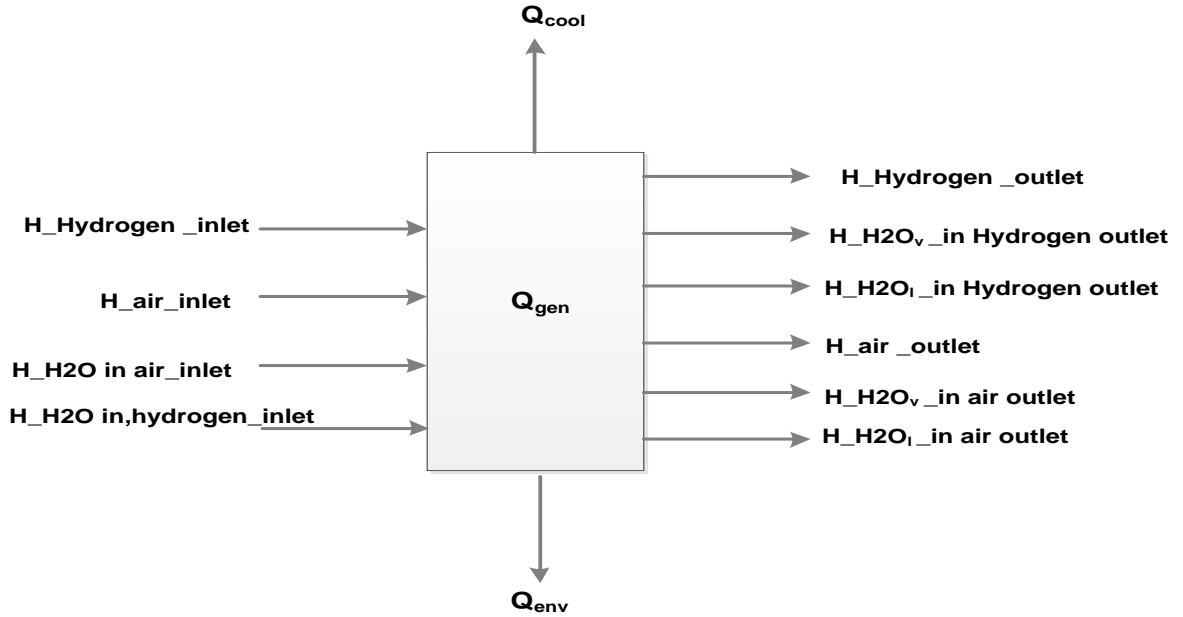


Figure 2.8. Energy balance of the fuel cell Stack

The inlet and outlet energy flow rates by reactant flows entering the fuel cell can be calculated from the following equations:

$$\dot{Q}_{in} = \sum \dot{m}_{i,in} \cdot C_{p_i} \cdot (T_{in} - T_{ref}) \quad (2.57)$$

$$\dot{Q}_{out} = \sum \dot{m}_{i,out} \cdot C_{p_i} \cdot (T_{stack} - T_{ref}) \quad (2.58)$$

where  $\dot{m}_{i,in}$  ,  $\dot{m}_{i,out}$  are the mass flow rates of gas in the inlet and outlet of fuel cell,  $\text{kg s}^{-1}$  ;  $C_{p_i}$  is the constant pressure specific heat,  $\text{J} \cdot \text{g}^{-1}\text{K}^{-1}$ ; and  $T_{in}$  is the inlet temperature of the reactants, K. The enthalpy of water vapor can be calculated as:

$$H = \dot{m}_{\text{H}_2\text{O}(g)} (C_{p,\text{H}_2\text{O}(g)} \cdot (T - T_{ref}) + H_{fg}^0) \quad (2.59)$$

where  $H_{fg}^0$  is the enthalpy of evaporation which is equal to  $2500 \text{ J g}^{-1}$  at  $0^\circ\text{C}$ . The enthalpy of liquid water can be calculated as:

$$H = \dot{m}_{\text{H}_2\text{O}(l)} \cdot C_{p,\text{H}_2\text{O}(l)} \cdot (T - T_{\text{ref}}) \quad (2.60)$$

If the gas has a higher heating value, that is, it combustible, its enthalpy is then:

$$H = \dot{m} (C_p \cdot (T - T_{\text{ref}}) + H_{\text{HHV}}^0) \quad (2.61)$$

where  $H_{\text{HHV}}^0$  is the higher heating value of that gas (J/g) at 0 °C. The heating values are reported at 25 °C. Therefore, the higher heating value may need to be calculated at the chosen temperature. For hydrogen it is (Barbir, 2005):

$$H_{\text{HHV}}^0 = H_{\text{HHV}}^{25} - \left[ C_{p,\text{H}_2} + \frac{1}{2} \frac{M_{\text{O}_2}}{M_{\text{H}_2}} C_{p,\text{O}_2} - \frac{M_{\text{H}_2\text{O}}}{M_{\text{H}_2}} C_{p,\text{H}_2\text{O}(l)} \right] \cdot 25 \quad (2.62)$$

where  $H_{\text{HHV}}^{25}$  is the higher heating value of that hydrogen (J g<sup>-1</sup>) at 25 °C. The generated electrical power output is given by the following equation:

$$W_{\text{elc}} = i \cdot A_{\text{cell}} \cdot v_{\text{cell}} \cdot n_{\text{cell}} \quad (2.63)$$

where  $I$  is the cell current;  $v_{\text{cell}}$  is the voltage of the cell; and  $n_{\text{cell}}$  is the number of cells in the stack. The rate of heat absorbed by the cooling fluid and carried out of the fuel cell stack can be calculated from the following equation:

$$\dot{Q}_{\text{cool}} = \dot{m}_{\text{cool}} \cdot C_{p,w} (T_{\text{stack}} - T_{\text{cool}}) \quad (2.64)$$

where  $\dot{m}_{\text{cool}}$  is the mass flow rate of the coolant water ;  $C_{p,w}$  is the specific heat of water at constant pressure; and  $T_{\text{cool}}$  is the temperature of water which enters the fuel cell, K .

The rate of heat is dissipated by the exposed stack surface to the environment can be calculated from the following equation (Yangjun et al, 2003):

$$\dot{Q}_{env} = \dot{Q}_{conv} + \dot{Q}_{rad} \quad (2.65)$$

$$\dot{Q}_{env} = (h \cdot A)_{air} \cdot (T_{stack} - T_{amb}) + \sigma \cdot \epsilon_{stack} \cdot A \cdot (T_{stack}^4 - T_{amb}^4) \quad (2.66)$$

where  $\dot{Q}_{conv}$  is the heat loss due to convection;  $\dot{Q}_{rad}$  is the heat loss due to radiation;  $h_{air}$  is the convective heat transfer coefficient of air,  $W \cdot m^{-2} \cdot K^{-1}$  A is the stack exposed surface area,  $m^2$ ;  $\sigma$  is Stefan-Boltzmann constant,  $5.67 \times 10^{-8} W \cdot m^{-2} \cdot K^{-4}$ ; and  $\epsilon_{stack}$  is the emissivity of stack surface taken to be equal to 0.75 .

## 2.2 Fuel Cell System Model

In this section, the fuel cell system model is presented. The fuel cell system components include: a compressor to bring the reactant air to the required pressure, humidifier to ensure an adequate hydration level of the membrane, a cooling system (consisting of a water pump and radiator fan) to maintain the required operating temperature, and an air cooling condenser to recover liquid water from the exhaust air and provides any additional liquid water that is needed by the system.

### 2-2-1 Compressor Model

The primary objective of the use of the compressor in fuel cells is to increase the pressure of the air before it enters into the stack in order to improve the reaction rate and increase the specific power. The thermodynamic behavior of an air compressor consists of temperature rise of a gas as its compressed and the required compressor power. The compression process is assumed to be reversible and adiabatic, i.e.; isentropic, and the gas is an ideal gas. The inputs to the compressor module are the atmospheric pressure and ambient temperature, and the voltage input to the compressor from the fuel cell stack. Power required simply the change in enthalpy of the gas:

$$P = \dot{m}_a \cdot C_p [T_{a,out} - T_{amb}] \quad (2.67)$$

where  $\dot{m}_a$  is the mass flow rate of air compressed, and  $C_p$  is the constant pressure specific heat of air. The mass flow rate of air used is calculated as:

$$\dot{m}_a = \frac{M_a \cdot \lambda \cdot P}{0.21 \cdot 4 \cdot F \cdot v_{cell}} \quad (2.68)$$

where  $\lambda$  is stoichiometric ratio of air,  $M_a$  is the molecular weight of air,  $P$  is the total power output from fuel cell, and  $v_{cell}$  is the cell voltage.

The temperature of the air leaving the compressor is calculated from the following equation:

$$T_{a,out} = T_{amb} + \frac{T_{amb}}{\eta_{comp}} \left[ \left( \frac{p_2}{p_1} \right)^{\frac{\gamma-1}{\gamma}} - 1 \right] \quad (2.69)$$

where  $\eta_{comp}$  is the isentropic efficiency of compressor,  $\gamma$  is the ratio of the specific heat capacities of the gas,  $\gamma = \frac{C_p}{C_v} = 1.4$  : and  $C_v$  is the constant volume specific heat.

The isentropic efficiencies of a compressor is defined as the ratio between the actual performance of a device and the performance that would be achieved under idealized conditions for the same inlet state and the same exit pressure. If we substitute the value of  $T_{a,out}$  from equation (2.74), the power needed for adiabatic compression of air is:

$$P_{comp} = \dot{m}_a \cdot C_p \cdot \frac{T_1}{\eta_{comp}} \left[ \left( \frac{p_2}{p_1} \right)^{\frac{\gamma-1}{\gamma}} - 1 \right] \quad (2.70)$$

### 2.2.2 Humidifier Model

Air flow from the intercooler is humidified before entering the stack by injecting water into the air stream in the humidifier, also the hydrogen flow from the heater is humidified before it enters the fuel cell to prevent drying of the membrane near the

cell inlet. The temperature of flow is assumed to be constant . The water injected is assumed to be in the liquid form at ambient temperature. The humidity ratio is defined as the rate of moisture mass flow per dry mass flow:

$$\omega = \frac{\dot{m}_v}{\dot{m}_{dry}} = \frac{M_w}{M_{H_2}} \frac{P_{H_2O,sat}}{P_{H_2}} \quad (2.71)$$

where  $\dot{m}_{dry}$  is the dry mixture includes everything except the water vapor, and  $\dot{m}_v$  is the mass flow of water vapor. If the dry mixture is hydrogen, the molecular mass of hydrogen = 2.02 kg kmole<sup>-1</sup> and the molecular mass of water = 18 kg kmole<sup>-1</sup>, the humidity ratio in a pure hydrogen humidified stream defined as:

$$\omega = \frac{18}{2} \frac{P_{H_2O,sat}}{P_{H_2}} = 8.91 \frac{P_{H_2O,sat}}{P_{H_2}} \quad (2.72)$$

where  $P_{H_2O,sat}$  is the saturated pressure of water vapor (partial pressure) at stack temperature, and  $P_{H_2}$  is the partial pressure of hydrogen. The amount of injected water to fully humidify the hydrogen is calculated as:

$$\dot{m}_{inj,w} = 8.91 \frac{P_{H_2O,sat}}{P_{H_2}} \cdot \dot{m}_{H_2,in} \quad (2.73)$$

where  $\dot{m}_{H_2,in}$  is the rate of hydrogen entering the anode. Also the molecular mass of air is 28.85 kg kmole<sup>-1</sup> and the humidity ratio defined as:

$$\omega = \frac{18}{28.85} \frac{P_{H_2O,sat}}{P_{H_2}} = 0.622 \frac{P_{H_2O,sat}}{P_{H_2}} \quad (2.74)$$

The amount of injected water to humidify the air is calculated as:

$$\omega = 0.622 \frac{P_{H_2O,sat}}{P_{air}} \dot{m}_{air,in} \quad (2.75)$$

### 2.2.3 Radiator Model

The main function of radiator is to dissipate waste heat from the coolant to the environment by forced convection. It is used to keep a constant cell operating temperature of the fuel cell. The radiator model covers the steady-state heat transfer between the air and the coolant as a function of ambient temperature, air mass flow, coolant flow and coolant inlet temperature. The heat transfer equation for the radiator may be expressed as:

$$\dot{Q}_{\text{radiator}} = \dot{m}_{\text{air}} \cdot C_{P_{\text{air}}} (T_{\text{rad,out}} - T_{\text{amb}}) \quad (2.76)$$

where  $T_{\text{rad,out}}$ ,  $T_{\text{amb}}$  are the inlet and output temperatures of the air flow stream. The energy balance for the radiator may be written as:

$$\dot{Q} = \dot{m}_{\text{air}} \cdot C_{P_{\text{air}}} (T_{\text{rad,out}} - T_{\text{amb}}) = \dot{m}_{\text{cool}} \cdot C_{P,w} (T_{\text{stack}} - T_{\text{cool}}) \quad (2.77)$$

The mass flow rate of air is calculated by the following equation:

$$\dot{m}_{\text{air}} = V \cdot \rho \cdot A_{\text{rad}} \quad (2.78)$$

where  $V$  is the average velocity of air,  $\rho$  is the air density.  $A_{\text{rad}}$  is the frontal area of the radiator which is assumed to be  $0.25\text{m}^2$ . It is assumed that the air velocity equals half the value of the vehicle speed in this thesis. The temperature at the exit of radiator can be expressed as:

$$T_{\text{rad,out}} = T_{\text{amb}} + \frac{\dot{m}_{\text{cool}} \cdot C_{P,w} (T_{\text{stack}} - T_{\text{cool}})}{\dot{m}_{\text{air}} \cdot C_{P_{\text{air}}}} \quad (2.79)$$

The total surface area of radiator can be calculated from the following equation:

$$A_{\text{eff}} = \frac{\dot{Q}_{\text{radiator}}}{U \cdot \Delta T_{\text{LM}}} \quad (2.80)$$

where  $A_{\text{eff}}$  is the effective area of radiator,  $\dot{Q}_{\text{radiator}}$  is the rate of heat transfer,  $U$  is mean overall heat transfer coefficient, and  $\Delta T_{\text{LM}}$  is the log-mean temperature difference. For air cooled heat exchanger a value of overall heat transfer coefficient ( $U$ ) ranges from 300-450 W/m<sup>2</sup>K. We assume it to be equal to 350 W/ m<sup>2</sup>K. The log-mean temperature difference for a compact heat exchanger can be calculated as:

$$\Delta T_{\text{LM}} = \frac{(T_{\text{stack}} - T_{\text{amb}}) - (T_{\text{cool}} - T_{\text{rad,out}})}{\ln((T_{\text{stack}} - T_{\text{amb}}) / (T_{\text{cool}} - T_{\text{rad,out}}))} \quad (2.81)$$

The electric power for the fan can be calculated as:

$$P_{\text{fan}} = dp \cdot q \quad (2.82)$$

where  $P_{\text{fan}}$  is electric power consumption for the fan (W),  $dp$  is total pressure increase in the fan (Pa), and  $q$  is the air volume flow delivered by the fan (m<sup>3</sup>/s)

#### 2.2.4 Pump Model

The pumps are used in this model to recirculate water through the system from the heat exchanger to the fuel cell stack. The corresponding mass and energy balances are given by:

$$\dot{m}_{\text{coolant,in,pump}} = \dot{m}_{\text{coolant,out,pump}} \quad (2.83)$$

$$P_{\text{pump}} = \frac{\dot{m}}{\rho} \cdot dp. \quad (2.84)$$

where  $\dot{m}_{\text{coolant,in,pump}}$  is the mass flow rate entering the pump,  $\dot{m}_{\text{coolant,out,pump}}$  is the mass flow rate exiting the pump,  $P_{\text{pump}}$  is the pump power consumption,  $dp$  is total pressure increase in the pump (Pa), and  $\rho$  is the density of water.

#### 2.2.5 Net System Power and System Thermal Efficiency

The efficiency of the fuel cell power system is the relation between the net electric power output and the total rate of fuel energy entering the fuel cell;

$$\eta_{\text{sys}} = \frac{P_{\text{out}}}{P_{\text{in}}} \quad (2.85)$$

where output electrical energy  $P_{\text{out}}$  is:

$$P_{\text{out}} = P_e - P_{\text{aux}} \quad (2.86)$$

where the gross output power,  $P_e$  was calculated in Eq. 2.19 and the parasitic loads by all auxiliary system equipment,  $P_{\text{aux}}$ , is the sum of all parasitic loads, commonly

$$P_{\text{aux}} = P_{\text{comp}} + P_{\text{pump}} + P_{\text{fan}} + P_{\text{heater}} \quad (2.87)$$

where  $P_{\text{comp}}$  is the power of compressor,  $P_{\text{pump}}$  is the power of hydrogen recirculation and cooling circuit pumps,  $P_{\text{fan}}$  is the power of cooling circuit fan, and  $P_{\text{heater}}$  is the electrical power of heater.  $P_{\text{in}}$  is the rate of chemical energy entering with the incoming fuel,

$$P_{\text{in}} = \dot{m}_{\text{H}_2, \text{in}} \cdot \text{HHV}_{\text{H}_2} \quad (2.88)$$

### 2.3 Vehicle Model

The power required to drive a vehicle on a level road at a steady speed is founded upon a parametric description of the well-known road load equation (Heywood., 1988):

$$P_{\text{road}} = (F_{\text{aero}} + F_{\text{roll}} + F_{\text{accel}} + F_{\text{grade}})V \quad (2.89.a)$$

$$= \left( \frac{1}{2} \rho_{\text{air}} C_d A_{\text{frontal}} v^2 + C_{\text{RR}} m_{\text{veh}} g + m_{\text{veh}} a + m_{\text{veh}} g Z \right) V \quad (2.89.b)$$

where  $P_{\text{road}}$  is the road load power (w),  $V$  is the vehicle speed (m/s),  $a$  is the vehicle acceleration ( $\text{m/s}^2$ ),  $\rho_{\text{air}}$  is the ambient air density ( $\sim 1.2 \text{kg/m}^3$ ),  $C_d$  is the aerodynamic drag coefficient,  $A_{\text{frontal}}$  is the frontal area of vehicle ( $\text{m}^2$ ),  $C_{\text{RR}}$  is the rolling resistance



coefficient,  $m_{veh}$  is the total vehicle mass (kg),  $g$  is the gravitational acceleration ( $9.81\text{m/s}^2$ ),  $Z$  is the road gradient (%).

The road load equation consists of four components as shown in Equation 2.89.a. These components are the aerodynamic drag of the vehicle, the rolling resistance which arises from the friction of the tires, power for vehicle acceleration, and energy storage in the vehicle inertia. It can be assumed that the terms  $P_{accel}$  and  $P_{grade}$  in equation 2.89.a equal to zero at steady state and zero elevation, the road load equation becomes:

$$P_{road} = \left( \frac{1}{2} \rho_{air} C_d A_{frontal} v^2 + C_{RR} m_{veh} g \right) V \quad (2.90)$$

## 2.4 Summary

This chapter presented the fundamental equations of thermodynamics, chemical reactions, and flow charts necessary for the PEM fuel cell system model. The flow of hydrogen and air through the system was modeled using steady-state mass and energy balance equations and the model of auxiliary components and vehicle model was integrated into the overall PEM fuel cell system model. Chapter 3 presents the solution methodology.

## CHAPTER 3

### SOLUTION METHODOLOGY

This chapter presents the development of a thermodynamic zero dimensional model for the simulation and analysis of an automotive PEMFC system model. The mathematical model was developed using the MATLAB program, and output data are exported and analyzed in Excel. For this research, a model was implemented by using fundamental equations of thermodynamics, chemical reactions, and electrochemistry. The model proposed in this study consists of two main parts; the PEMFC stack model and the system model with various components. The system model includes all necessary system components such as compressor, heat exchangers, humidifier, pumps and the fuel cell stack which are linked together with mass and energy streams.

The vehicle speed and the efficiency of the system are dependent on the PEM fuel cell work output which in turn depends on various model input parameters as shown in Figure 3-2. Flow chart of an automotive PEMFC system model is given in Figure 3.1. Iteration procedure is used to calculate the power of fuel cell by the following steps:

- 1- Input the vehicle speed and calculate the propulsion power required to drive the vehicle.
- 2- Start with initial value of current density and calculate the fuel cell power.
- 3- Depending on the fuel cell power, the auxiliary power of the components (compressor power, fan power, pump power, and heater power) can be calculated.
- 4- The total power needed from the fuel cell is equal to the sum of the propulsion vehicle power and auxiliary components power. If the fuel cell power is lower than the total power, the current density is increased and the algorithm returns to step 2, repeating the process until the fuel cell power is equal to the total power.

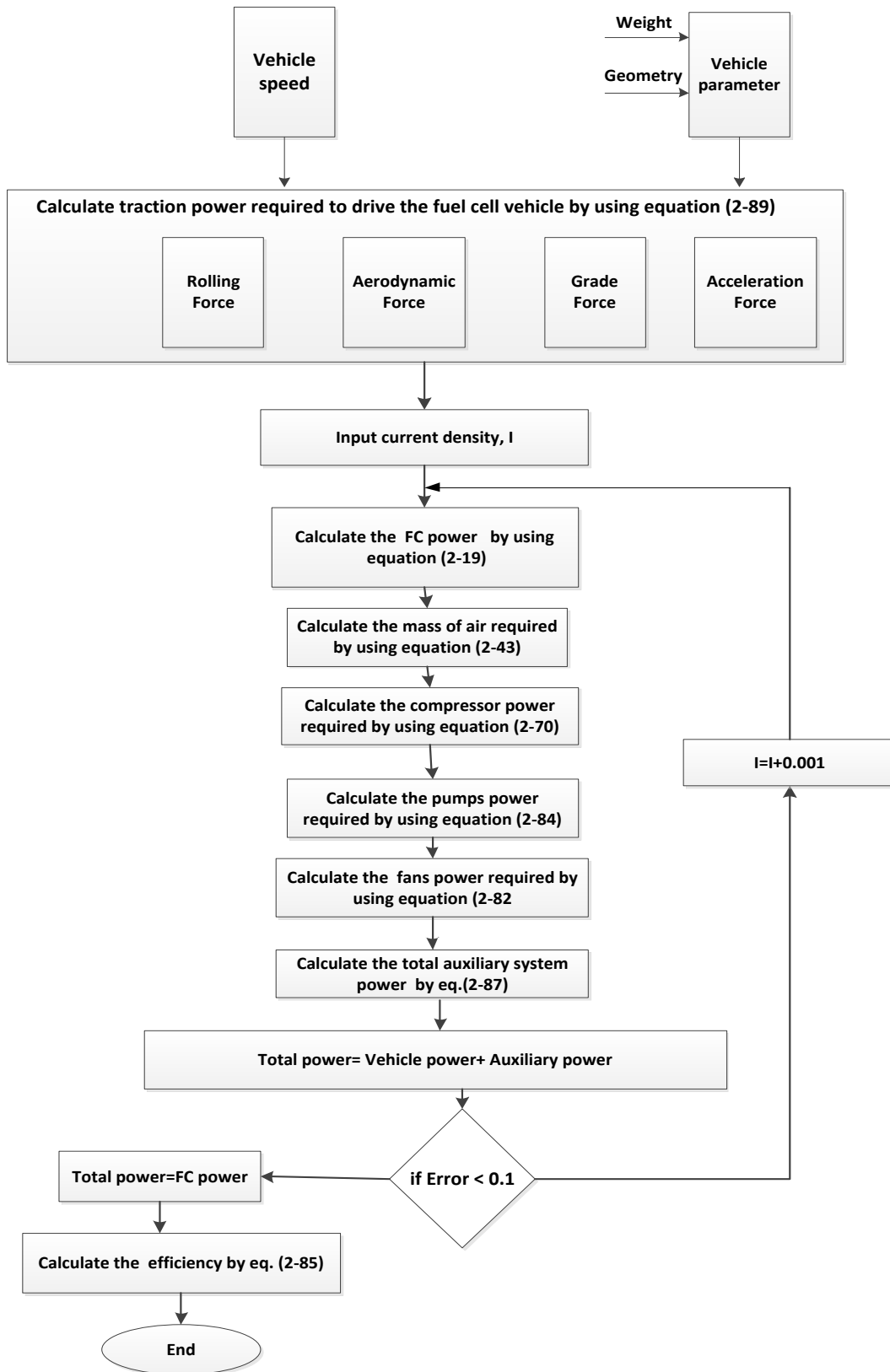


Figure 3.1. Flow Chart of the Automotive PEM Fuel Cell System

### 3-1 PEM fuel cell Stack Model Integration in MATLAB

The fuel cell stack model is composed of four sub models which are the stack voltage, the cathode flow, the anode flow, and the membrane models. The stack voltage is the difference between the open circuit voltage and over-potentials that include the ohmic losses in the membrane, the activation losses in the catalyst on the cathode and anode sides, and the concentration losses. The open circuit voltage of the fuel cell is calculated from the energy balance between electrical energy and chemical energy in the reactants. The anode flow model describe the hydrogen partial pressure and anode flow humidity by using conservation of mass and the characteristic properties of the fluids, separately considering the mass flow rates of hydrogen, and water on the anode side. The cathode mass flow model represents the air flow behavior inside the cathode of the fuel cell stack. The model describe the flow of air and reaction products through the cathode using conservation of mass, separately considering the mass flow rates of oxygen, nitrogen, and water on the cathode side. The membrane hydration model calculates the mass flow rate of water across the membrane which is functions of stack current and relative humidity of the flow inside the anode and cathode flow channels. The general assumptions made for the fuel cell stack model are as follows:

- All gases in the model obey the ideal gas law.
- Fuel flow rate is fixed, and consists of pure H<sub>2</sub>.
- Composition of air is 21% O<sub>2</sub> and 79% N<sub>2</sub>.
- The temperatures at the anode and cathode sides in the fuel cell stack are equal to the fuel cell stack temperature (uniform temperature).
- The product water generated at the cathode side is assumed to be in the liquid phase.
- The environmental state is at standard temperature and pressure conditions, i.e., 298 K and 1 atm.
- The pressure drop in the fuel cell is 0.15 atm (Gurski, 2002).
- Cathode and anode pressures are equal to each other.

Based on the above assumptions, the model needs several input parameters to specify the operating condition of the PEMFC stack.

For the stand-alone execution of the PEMFC stack model, the flow rates of the fuel and air, the operating temperature and pressure, and the relative humidity of the PEMFC must be specified. When the stack model is executed within system model, the flow rates of air and fuel entering PEMFC is calculated in MATLAB based on the required power output from PEMFC model. It is also important to input several thermodynamics, electrochemical parameters and constants needed to complete the calculations of the PEMFC model. All the input parameters are listed in Table 3-1.

**Table 3.1.**The Fuel Cell Stack Parameters

<b>Parameter</b>	<b>Value</b>	<b>Unit</b>	<b>Reference</b>
Thickness of gas diffusion layer	0.0254	cm	Gurau et al., (1998)
Thickness of catalyst layer	0.00287	cm	Gurau et al., (1998)
Membrane thickness	0.023	cm	Gurau et al., (1998)
Anode exchange current density	0.6	A.cm <sup>-2</sup>	Berning et al.,(2002)
Cathode exchange current density	4.4× 10 <sup>-7</sup>	A.cm <sup>-2</sup>	Berning et al., (2002)
Anodic transfer coefficient	0.5	-	Siegel et al., (2004)
Cathodic transfer coefficient	0.55	-	Siegel et al., (2004)
Ionomer equivalent of anode catalyst layer	0.55	-	-
Ionomer equivalent of cathode catalyst layer	0.4	-	-
Expansion constant for concentration polarization	0.05	V	-
Electrode porosity	0.6	-	Guvelioglu et al., (2005)
Membrane ionic conductivity	0.1	-	Meyers et al., (2002)
H <sub>2</sub> diffusion coefficient at reference state	0.0376	-	Hu et al., (2004)
O <sub>2</sub> diffusion coefficient at reference state	0.0522	-	Hu et al., (2004)

The inputs to the PEMFC models also need several constants during the calculation of results, and these are listed in Table 3.2.

**Table 3.2.** PEMFC Model Constants

<b>Parameter</b>	<b>Value</b>	<b>Unit</b>
Faraday constant, $F$	96485	C
Universal gas constant, $R$	8.3146	J. mol <sup>-1</sup> . K <sup>-1</sup>
Reference temperature, $T_{ref}$	298.15	K
Reference pressure, $P_{ref}$	101.325	atm

The PEMFC model outputs are calculated by using MATLAB, and these are listed in Table 3-3.

**Table 3.3.** PEMFC Model Outputs

<b>Parameter</b>	<b>Unit</b>
Nernst voltage, $E_{Nernst}$ (Eq.2-16)	V
Cell potential $v_{cell}$ , (Eq.2-17)	V
Power output of the fuel cell stack, $P$ (Eq.2-19)	W
Overall activation losses, $v_{act}$ (Eq.2-20)	V
Overall ohmic losses, $v_{Ohmic}$ (Eq.2-22)	V
Overall concentration losses, $v_{con}$ (Eq.2-25)	V
Water generated from the fuel cell reaction, $\dot{m}_{H_2O,gen}$ (Eq.2-47)	g. sec <sup>-1</sup>

An algorithm of the fuel cell stack calculation can be seen in Figure 3.1. The primary inputs into the cell model are the operating current density, the anode and cathode operating conditions and the cell temperature. The model outputs are the cell voltage, work and heat output from stack, and the PEMFC exhaust composition.

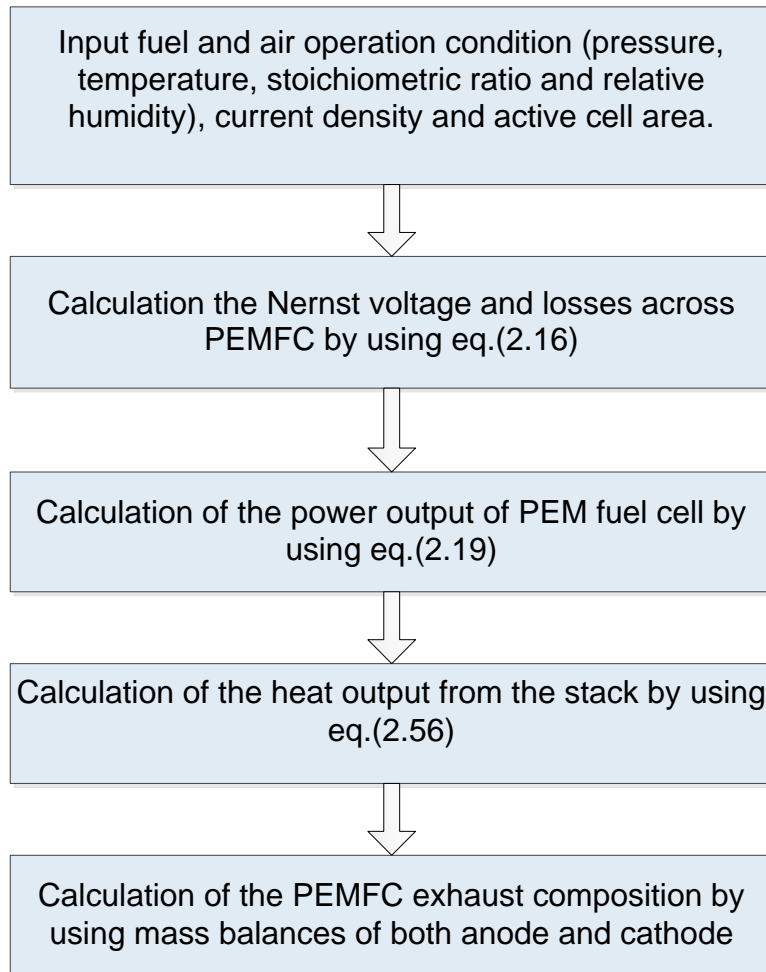


Figure 3.2. PEM fuel cell model overview

### 3-2 Automotive PEM fuel cell System Integration in MATLAB

In this section an automotive PEMFC system is simulated by using MATLAB program. To operate the PEM fuel cell system at the required condition, thermodynamic models for the compressor, pumps, humidifier, and heat exchanger are needed. These components are described in Chapter 2. An automotive PEM fuel cell system operating parameters is presented in this section. The corresponding vehicle parameters used in the analysis of an automotive PEMFC system model are presented in Table 3.4 and the thermal system characteristics which are used in steady state model calculation are shown in Table 3.5.

**Table 3.4.** TOYOTA Vehicle Specifications

Parameter	Value	Unit
Vehicle weight	1880	Kg
Frontal area	2.67	m <sup>2</sup>
Aerodynamic drag coefficient	0.65	-
Rolling resistance coefficient	0.012	-

**Table 3.5.** Thermal System Characteristics

Parameter	Value	Unit
Heat transfer coefficient	5.4	W. m <sup>-2</sup> . K <sup>-1</sup>
Overall heat transfer coefficient	150	W. m <sup>-2</sup> . K <sup>-1</sup>
Emissivity of stack surface	0.75	-
Stefan Boltzman constant	5.7 × 10 <sup>-8</sup>	W. m <sup>-2</sup> . K <sup>-4</sup>
Constant pressure specific heat of water	4182	J. Kg <sup>-1</sup> . K <sup>-1</sup>
Constant pressure specific heat of air	1008	J. Kg <sup>-1</sup> . K <sup>-1</sup>

The PEM fuel cell system model outputs are calculated by using MATLAB, and these are summarized in Table 3.6.

**Table 3.6.** PEM Fuel Cell System Model Outputs

Parameter	Unit
Net power output, $P_{out}$ (Eq.2-86)	kW
System efficiency, $\eta_{sys}$ (Eq.2-85)	-
Thermal efficiency, $\eta_{ther}$ (Eq.2-27)	-
Mass flow rate of air entering to the system, $\dot{m}_{air,in}$ (Eq.2-43)	g. sec <sup>-1</sup>
Compressor power, $P_{comp}$ (Eq.2-70)	kW
Pump power, $P_{pump}$ (Eq.2-84)	kW
Fan power, $P_{Fan}$ (Eq.2-82)	kW
Mass flow rate of hydrogen consumption, $\dot{m}_{H_2,reacted}$ (Eq.2-31)	g. sec <sup>-1</sup>
Radiator load (Eq.2-76)	kW



## CHAPTER 4

### RESULTS AND DISCUSSIONS

In this chapter, first, the analysis of PEMFC stack model is studied in order to obtain the stack gross power and cell voltage (also known as the polarization curve) Then, the analysis of the system power output of a selected PEMFC system will be carried out by focusing on fuel consumption, system efficiency, water management, and heat management at steady state operation.

#### 4.1 Analysis of PEM Fuel Cell Model

The polarization curve (voltage-current relationships) is the most general indicator of fuel cell performance. It shows the voltage output  $V_{\text{cell}}$  of a fuel cell for a given current density  $I$  ( $\text{A}/\text{cm}^2$ ). Voltage-current relationship plays an important role in determining the power output and stack efficiency, and overall system efficiency.

Figure 4.1 shows a typical polarization curve that represents the performance of a fuel cell for an operating pressure of 3 atm and illustrates the different cell losses as a function of current density. The current density is defined as the current in the external circuit per unit cell area. The fuel cell stack parameters are used in the calculation of polarization curve are given in the Table 3.1. It can be seen from Figure 4.1 that the irreversible losses increase as more current is drawn from the fuel cell. The voltage corresponding to zero current case is known as the open circuit voltage. As the current (or the load) increases irreversible losses occur. These irreversible losses are classified as activation polarization, ohmic polarization and concentration polarization. The words “loss” and “polarization” are used interchangeably in fuel cell literature. The polarization curve can be divided into three distinct zones based on the dominance of respective polarization effects. The activation zone (low current densities) is the rapid initial fall in voltage at low current densities. It occurs due to the energy required to initiate the reactions and it is directly related to the nature of the

electrochemical reaction. Ohmic losses are the linear portion of the voltage-current density curve (middle current densities). In this zone the voltage drop is proportional to the current density. The ohmic loss comes from the resistance of the materials to the flow of electrons and protons. The last zone in Figure 4.1 is the concentration polarization zone (high current densities). It is associated with a steep slope and high current densities. It occurs due to mass transport limitations.

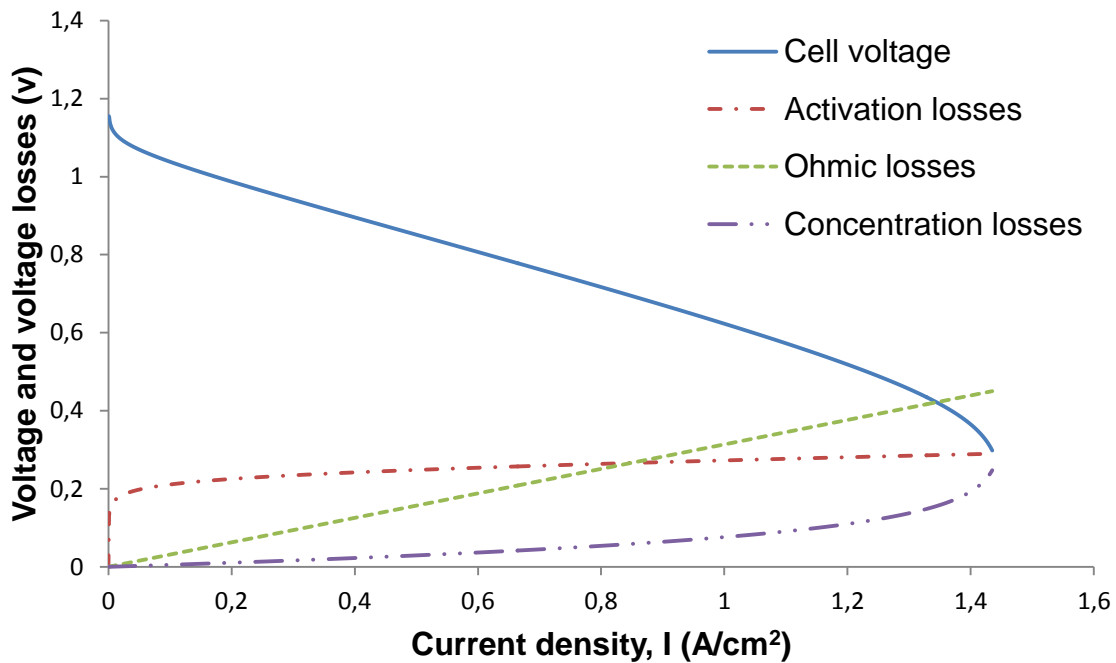


Figure 4.1. Fuel cell voltage and voltage losses as a function of cell's current density for operating pressure of 3 atm

Fuel cell's voltage output as a function of current density at two different operating pressures is shown in Figure 4.2. This simulation was performed in the MATLAB using fuel cell's standard operating conditions; fuel cell operating temperature of 353.15K, membrane humidity of 100%, fuel and air stoichiometric flow ratios are 1.5 and 2, respectively, and reactants partial pressures are 1.5 and 3 atmosphere. It can see from this figure that an increase of fuel cell's operating pressure will cause an increase in cell's output voltage which is typical in fuel cell literature. It is also observed from this figure that the limiting regions of the current density are obtained at 1.184 A/cm<sup>2</sup> and 1.453 A/cm<sup>2</sup> for 1.5 atm and 3 atm operation pressure,

respectively. At the limiting current density, the concentration at the surface falls to zero, a further increase in current is impossible.

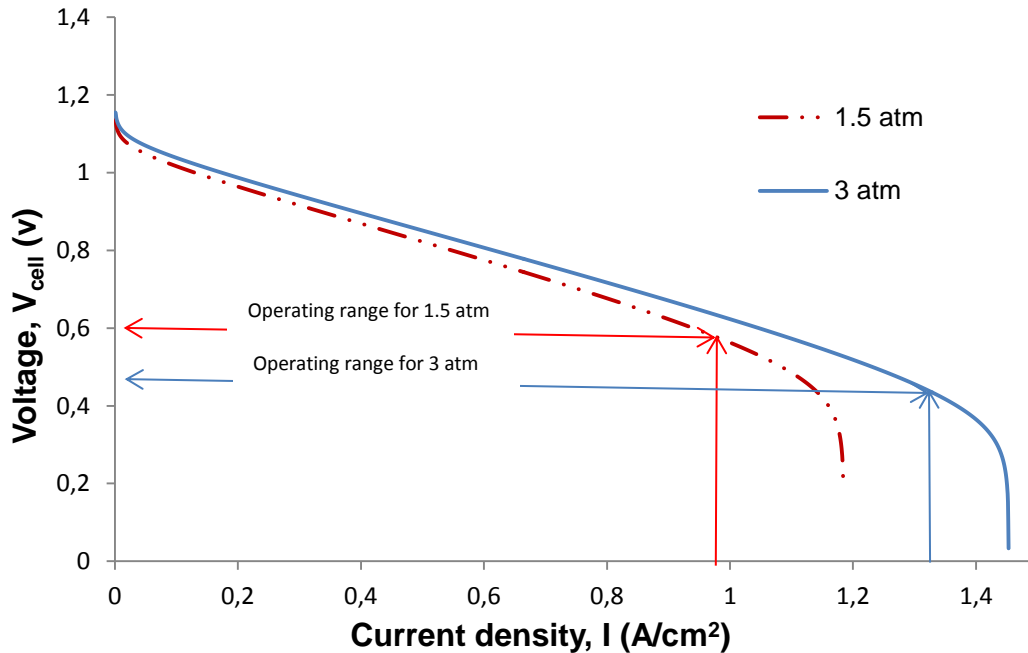


Figure 4.2. Fuel cell output voltages as a function of cell's current density for operating pressures of 1.5 and 3 atm.

It should be noted that the current (or current density) depends on the amount of fuel consumed (each mole of fuel produces  $n$  electrons based on Faraday's law). Therefore, for the same amount of fuel, a higher voltage indicates a higher power output and a higher thermal efficiency. It can be concluded that voltage can also be interpreted as the thermal efficiency.

The power density of the fuel cell as a function of current density at two different pressures is shown in Figure 4.3. The power density as a performance parameter is a direct indicator of the size of the fuel cell for a given power. It also seen from Figure 4.3 that an increase in fuel cell's operating pressure causes an increase in power density especially at higher current densities. A large increase in the net output power can be observed, with a maximum of 0.629W for higher operating pressure and with a maximum of 0.564W for lower operating pressure, corresponding to a significant

increase of 12.5%. It is also seen from the figure that the fuel cell power density increases with increasing current density, reaches a maximum, and then falls as the current density further increases. It should be noted that for a given pressure, the voltage output of a fuel cell (hence the thermal efficiency) steadily decreases with current density whereas the power density shows a non-monotonic behavior. Therefore, the question of choosing a suitable current density often arises in the design process of fuel cell systems. From the literature, it can be inferred that fuel cells are designed to operate at the maximum power density (Vielstich et al., 2009). Therefore, in this thesis, the fuel cell system is designed to supply the required maximum power at a current density corresponding to the maximum power density as outlined below.

The automotive fuel cell system is typical of those found in automotive applications and is similar to the system found in Toyota Motor Corporation FC vehicle. The maximum power of the fuel cell is assumed to be 90 kW. The active cell area is chosen as  $625 \text{ cm}^2$  ( $25 \text{ cm} \times 25 \text{ cm}$ ). For 3 atm pressure, it is required that the fuel cell delivers 90 kW of maximum power at a current density corresponding to the peak power density (in Figure 4.3 it is  $0.63 \text{ W/cm}^2$  at  $1.13 \text{ A/cm}^2$ ). At this point, the fuel cell delivers around 0.43 V as can be seen from Figure 4.2. For a cell area of  $625 \text{ cm}^2$ , 230 cells are needed to produce the required maximum power of 90 kW. Therefore, the number of cells for the fuel cell system is set as 230. If the fuel cell is required to produce less power than 90 kW (based on vehicle operating conditions), the current density (hence the amount of fuel) is reduced. The operating range for this pressure is shown in Figure 4.2. If the same fuel cell (230 cells with  $625 \text{ cm}^2$  active cell area) is operated at a lower pressure of 1.5 atm, at its peak power density point as seen in Figure 4.3 ( $0.56 \text{ W/cm}^2$  at  $0.967 \text{ A/cm}^2$ ), the fuel cell will deliver less power (around 81 kW). Again, if less power is required at 1.5 atm, the current density is reduced as seen in Figure 4.2. Overall, the fuel cell will deliver a maximum power of 90 kW at 3 atm and 81 kW at 1.5 atm, respectively.

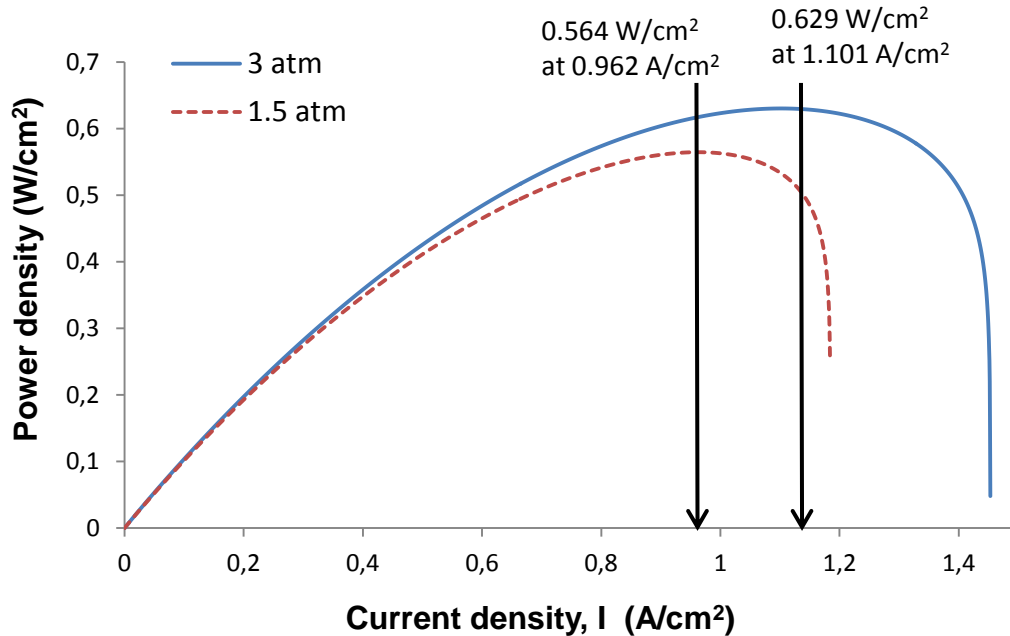


Figure 4.3. The power density of fuel cell as a function of cell's current density for different pressures.

## 4-2 Analysis of an Automotive PEM Fuel Cell System Model

### 4.2.1 Power Output

A PEM fuel cell system requires the use of components such as compressor, pumps, fans and heaters that require power input. As a result, the auxiliary power consumed by these devices must be subtracted from the overall gross power generated by the fuel cell stack to calculate the total power required to drive the vehicle. The power generated by the fuel cell stack can be determined from the voltage, current density and the number of cells. The vehicle speed can be calculated from the road load equation which is discussed in the Section 2.3.

Figure 4.4 shows the required power output as a function of vehicle speed for two different operating pressures. We can see from this figure that the PEMFC system model can be operated at low or high pressure. Slightly higher power output from stack is obtained at 3 atm operating pressure but the net system power must be

checked by calculating auxiliary power requirements for other components such as air-supply and cooling systems.

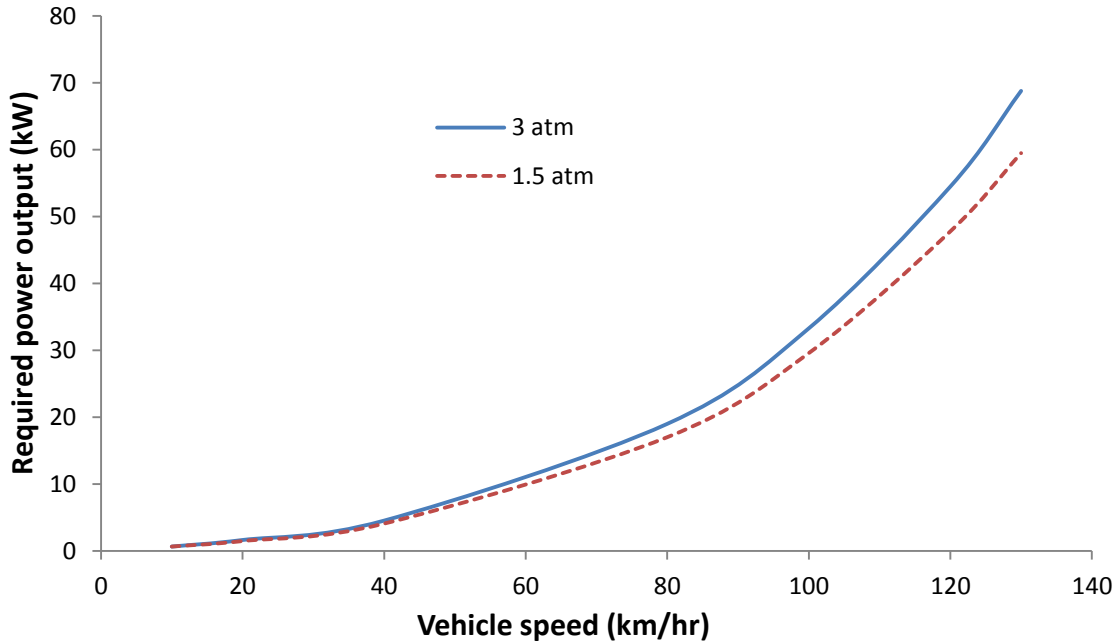


Figure 4.4. Required power output as a function of vehicle speed for two different operating pressures.

Figure 4.5 shows the vehicle power as a function of vehicle speed. It is clear from the figure that when the speed of the vehicle increases, the vehicle power increases too.

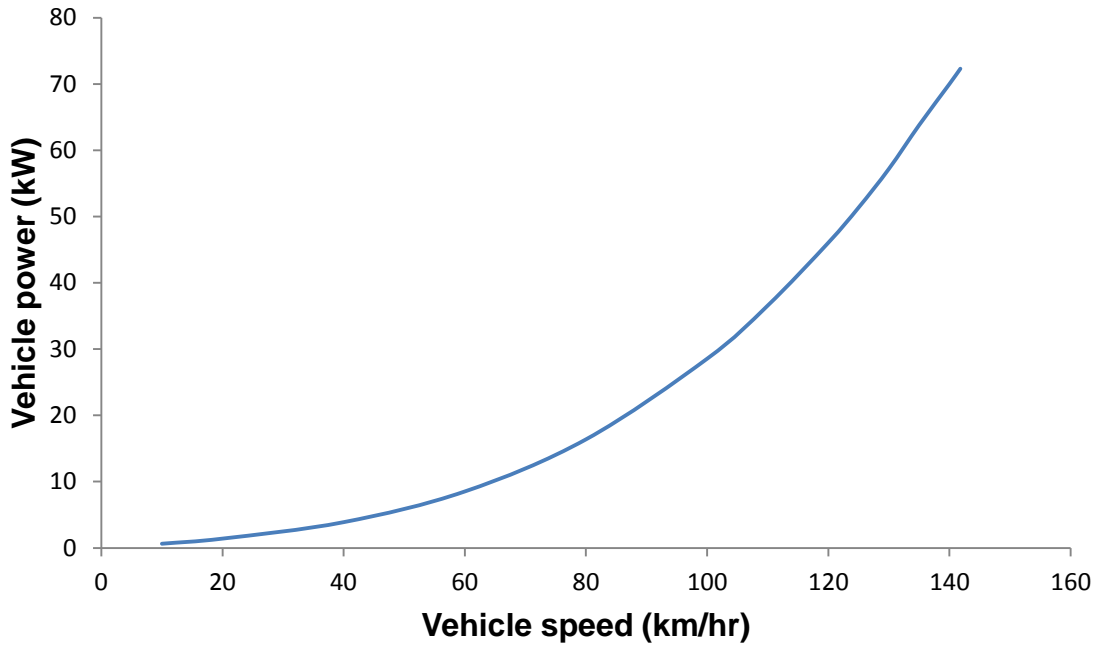


Figure 4.5. Propulsion power required as a function of vehicle speed

Figure 4.6 shows the auxiliary power requirement as a function of vehicle speed at two different operating pressures. We can see from this figure that an increase of system operating pressure causes a slight increase in the power needed for auxiliary components. If the system operates at 3 atm operating pressure, a relatively large portion of the total power output from PEM fuel cell is used to operate air compressor, while an electrical heater demands the highest portion of the auxiliary power at 1.5 atm operating pressure as will be discussed below.

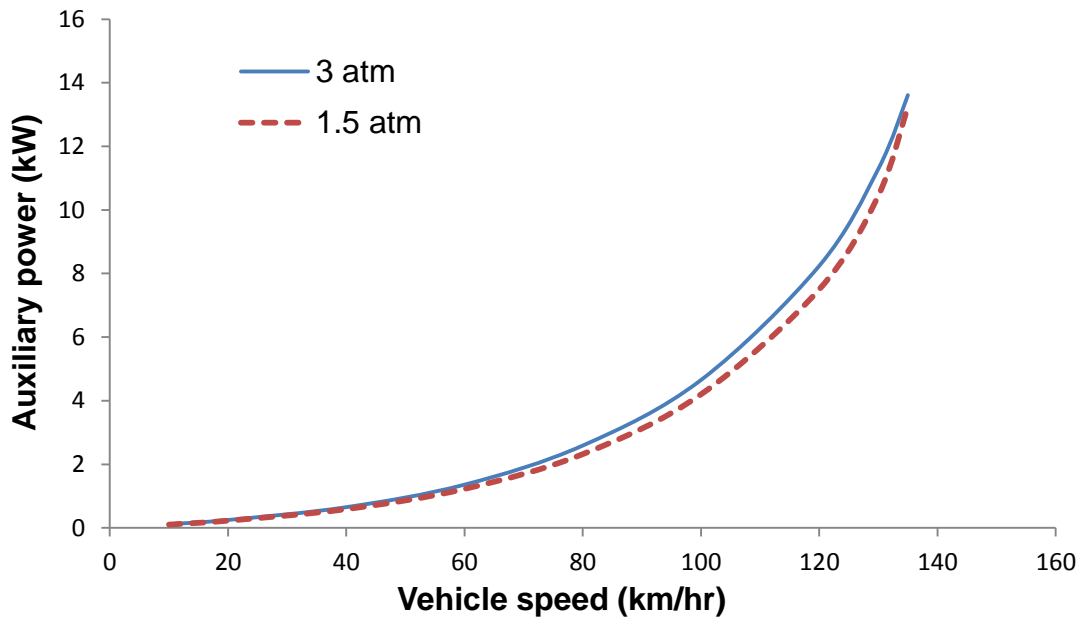


Figure 4.6. Auxiliary powers as a function of vehicle speed for two different operating pressures.

Figure 4.7 shows the breakout of the auxiliary power as a function of vehicle speed at 3 atm operating pressure. The auxiliary components include a compressor, electrical heater, coolant pump, injection pump, radiator fan, and an intercooler fan. It is possible to see from this figure that the electrical power consumed by compressor is growing faster than the rate of electrical power consumed by other auxiliary components. It is also noted that the compressed air would need to be cooled before entry into a humidifier by using an intercooler. It is presented that the temperature of the incoming air to the humidifier is decreased in an air cooler (Hosseini et al. 2012).



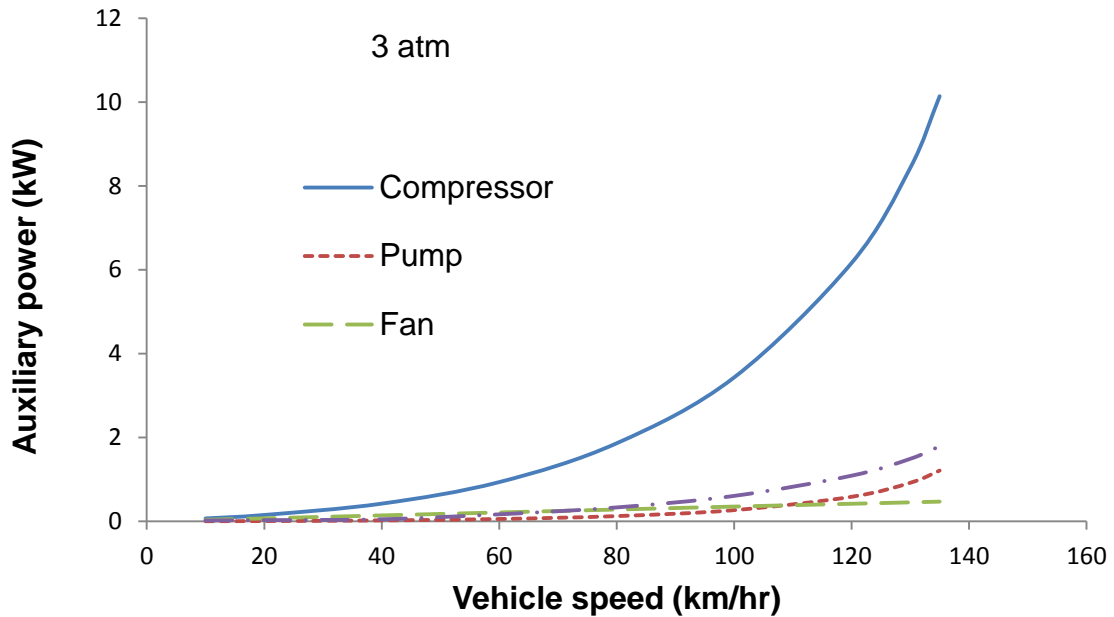


Figure 4.7. Auxiliary powers as a function of vehicle speed for 3 atm operating pressure.

Figure 4.8 shows the auxiliary power as a function of vehicle speed at 1.5 atm operating pressure. In low operation pressure, the outside air from the compressor would need to be heated before entering the humidifier. Therefore, the waste heat at the exhaust needs to be heated and then it will be used to heat the hydrogen and air to the required temperature. It is seen from the figure that the electric energy required by the heater constitutes the largest portion of auxiliary power requirement of the system.

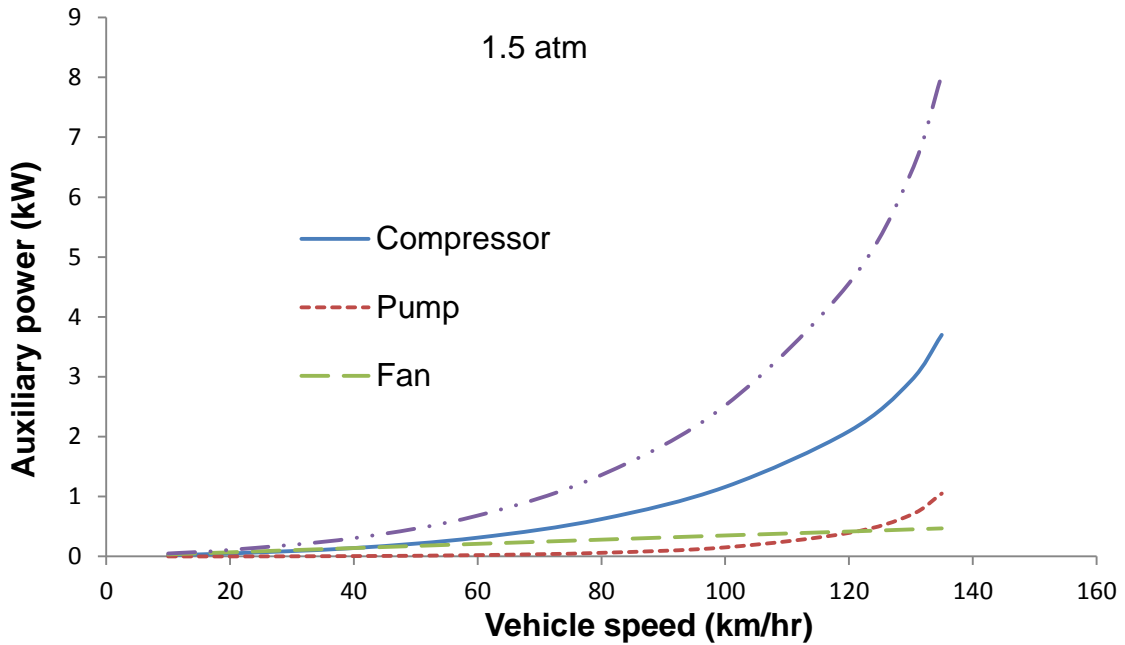


Figure 4.8. Auxiliary powers as a function of vehicle speed for 1.5 atm operating pressure.

#### 4.2.2 Fuel Consumption

The electrical power produced by a fuel cell is directly proportional to the amount of fuel consumed because each mole of fuel provides specific moles of electrons. Figure 4.9 shows the hydrogen consumption as a function of vehicle speed at two different operating pressures. It is clear from this figure that when the speed of the vehicle increases, it needs a larger amount of energy, accordingly more amount of fuel is consumed.

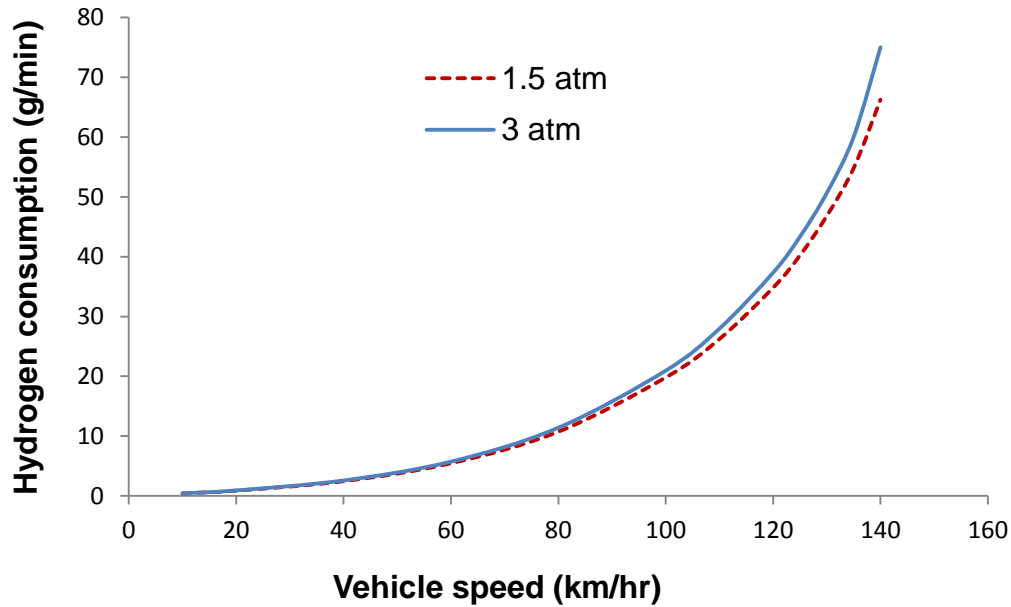


Figure 4.9. Hydrogen consumption as a function of vehicle speed for two different operating pressures.

#### 4.2.3 Fuel Cell Thermal Efficiency, and System Thermal Efficiency

Figure 4.10 shows the efficiency curves as a function of vehicle speed at two different operating pressures. The curves in this figure show the fuel cell thermal efficiency, and the system thermal efficiency. As can be seen, increasing the system pressure from 1.5 to 3 atm is beneficial for the fuel cell thermal efficiency while it has a negligible effect on the system efficiency.

The fuel cell thermal efficiency curves present the relation between the electricity produced and the maximum available work for vehicle propulsion. It is viewed from the curves that the fuel cell thermal efficiency decreases with increasing the vehicle speed due to the increase of fuel consumption by the vehicle. It is also seen that an increase in the operation pressure increases the fuel thermal efficiency due to the increase in the power output from the fuel cell at high pressures.

In system thermal efficiency curves, it can be seen that the increasing in vehicle speed from 10 km/hr to 140 km/hr decreases the system thermal efficiency significantly. This is mainly due to the electrical power consumed by compressor and other auxiliary components which have been deducted from the power generated from stack. By entering proper operating parameters, the model generated in this study could do system optimization, and select the best working condition for the system. In comparison with the values in the literature, the value for the system thermal efficiency decreases from 38% to 22% for 3 atm operating pressure, 2.5 air stoichiometry ratio, and 1.1 fuel stoichiometric ratio (Wishart et al. 2006). Similarly, in this thesis the system thermal efficiency decreases from 38.2% to 25% at the same range of current density for 3 atm operating pressure, 2.0 air stoichiometry ratio, and 1.5 fuel stoichiometry ratio.

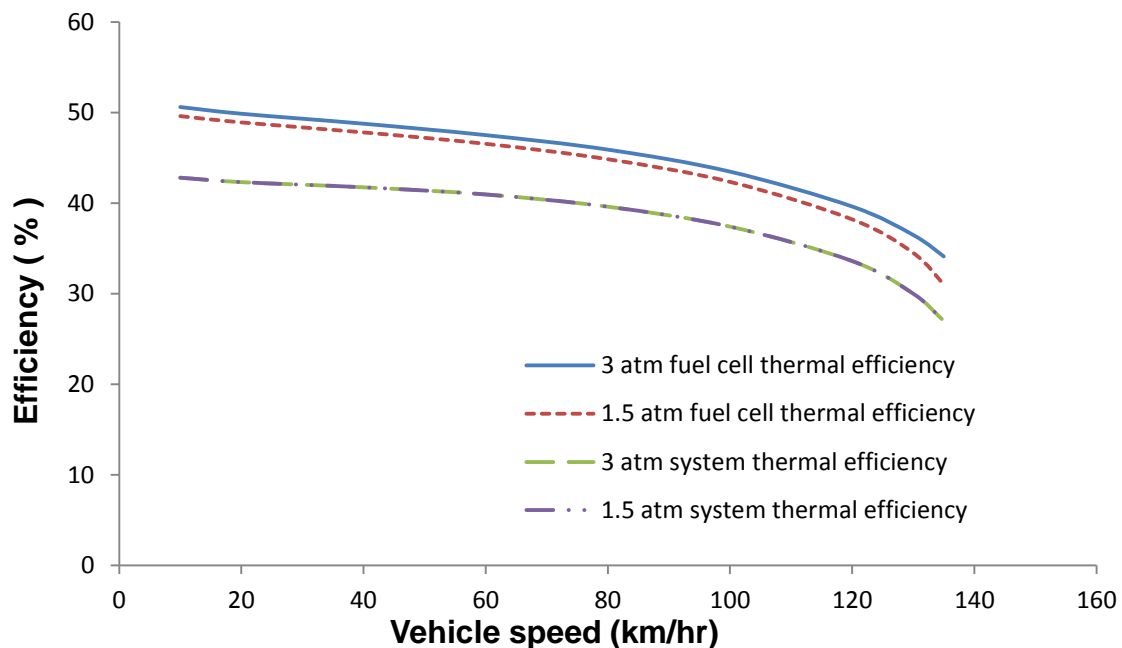


Figure 4.10. Efficiencies as a function of vehicle speed at two different pressures

#### 4.2.4 Water Management

On the water balance of PEMFC system, the amount of water entering the system in ambient air, plus water injected to humidify gases, plus water generated inside the

cathode due to electrochemical reaction must be larger than or equal to the amount of water leaving the system with exhaust air and hydrogen. Water at the exhaust may be in liquid or gaseous state. The state of water depends on the operating conditions of fuel cell (air stoichiometric ratio and operation pressure and temperature). Liquid water is easily separated from the gaseous stream in condenser. Figure 4.13 shows the amount of water (liquid and vapor) at the exit of stack and injected water required for humidification process as a function of vehicle speed for 3 atm pressure. It is viewed from the result that the average value of water at the exit of fuel cell stack consists of 60% liquid water and 40% of water vapor. At high pressures the vapor pressure of water is high thus the boiling point of water increases. Therefore, the amount of liquid water increases with increasing operation pressure. It is also viewed from the figure that the liquid water at the exit of fuel cell is greater than the injected water and it is enough to humidify the reactants before entering to the fuel cell without using a condenser

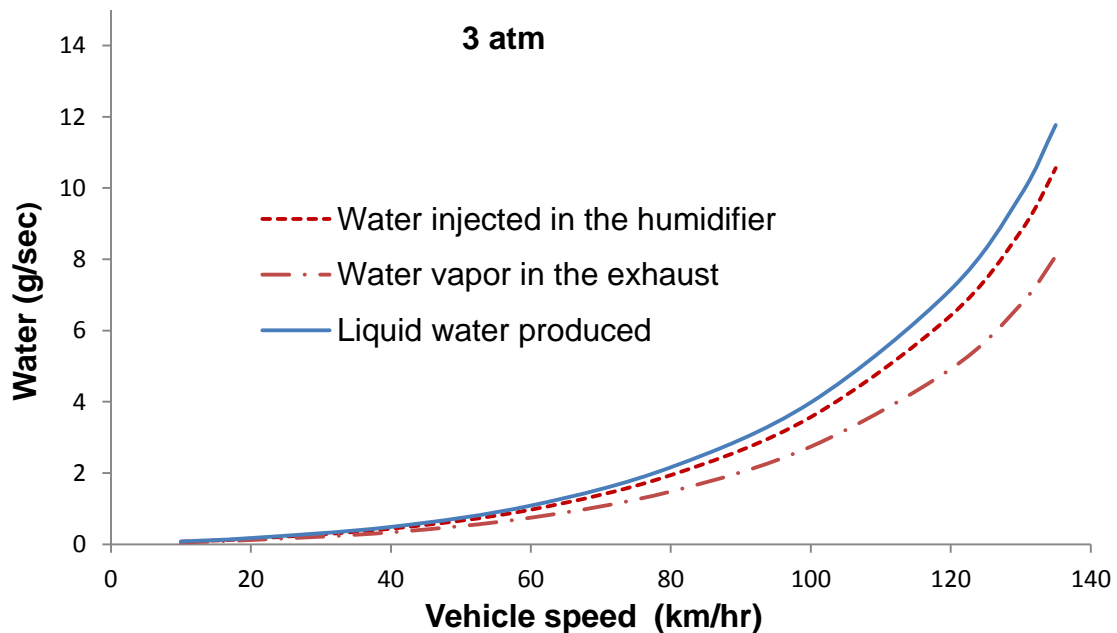


Figure 4.11. The amount of water at the exit of stack and injected water required for humidification process as a function of vehicle speed for 3 atm operating pressure.

Figure 4.12 shows the amount of water (liquid and vapor) at the exit of stack and injected water required for humidification process as a function of vehicle speed for 1.5 atm pressure. It can be inferred from the figure that the average value of water at the exit of fuel cell stack consists of 32% liquid water and 68% of water vapor. Also the amount of liquid water at the exit of fuel cell is lower than the injected water and therefore not sufficient to humidify the reactants before entering to the fuel cell. It is clear that lower operating pressures necessitates large amount of water recovery in the condenser which results in a very high parasitic load for condenser fan. Bao et al. (2006) studied the effect of different pressures on a fuel cell system and found out that when the system operated at low pressures, a condenser would be needed.

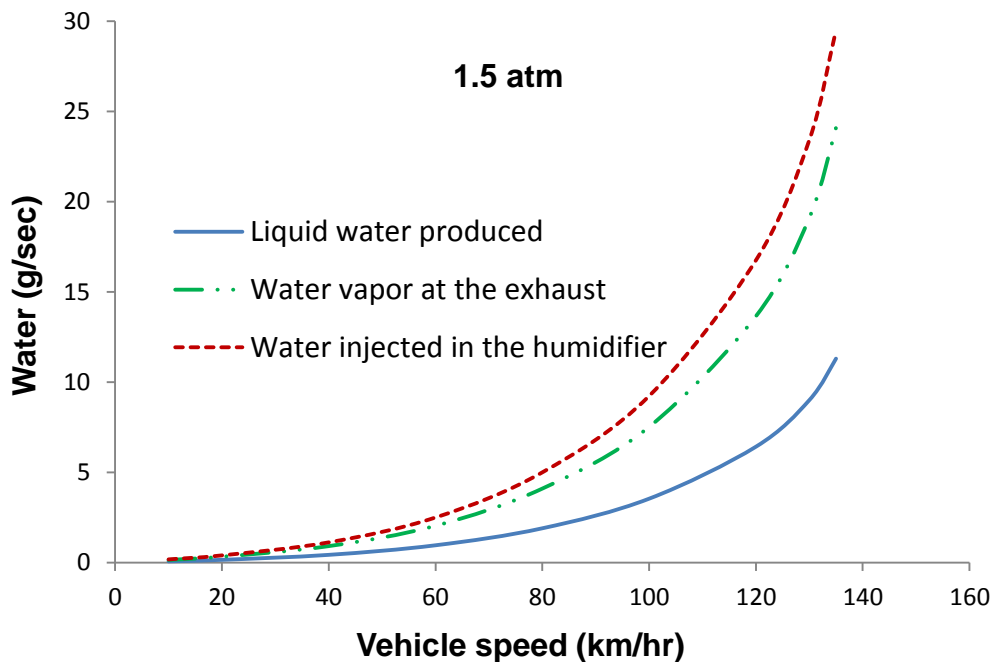


Figure 4.12. The amount of water at the exit of stack and injected water required for humidification process as a function of vehicle's speed for 1.5 atm operation pressure.

Figure 4.13 shows the water needed for humidification processes as a function of vehicle speed for two different operating pressures. It can be seen from the figure that that an increase in system operating pressure causes a decrease in water needed for humidification processes because the mole fraction of water vapor at the

exhaust decreases with increasing the operating pressure. Therefore it can be concluded that the water management forms a problem in systems that operate at low pressures since they need a large amount of water for humidification and hence a large humidifier.

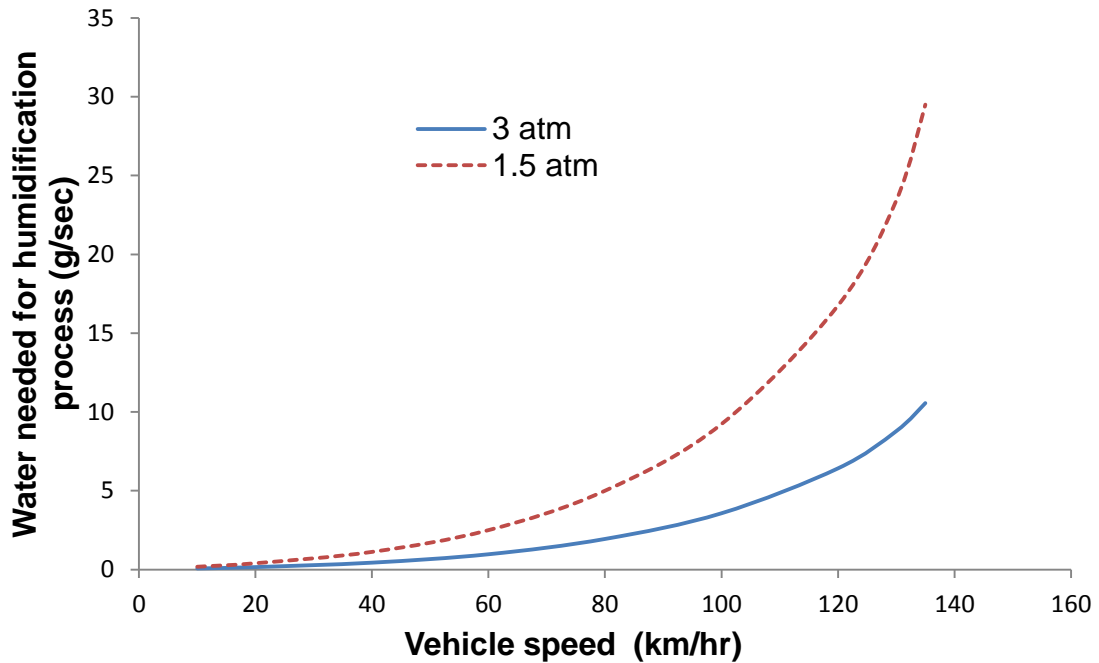


Figure 4.13. The water needed for humidification process as a function of vehicle speed for two different operating pressures.

The air stoichiometry ratio and the operation pressure are two important operating parameters in the water management of PEM fuel cell. Figure 4.14 shows the amount of water at the exit of cathode and injected water required for humidification process at constant vehicle speed at 120 km/hr with a variable air stoichiometric ratio and two different operation pressures. It is seen that the decrease of air stoichiometry at higher operating pressures improves the water management of system because the water at the exit of cathode is enough to humidify the reactant gases and there is no need to a condenser in the system. However, the amount of liquid water at the exhaust of cathode is not enough to humidify the reactants for lower operating pressure at any air stoichiometric ratio.

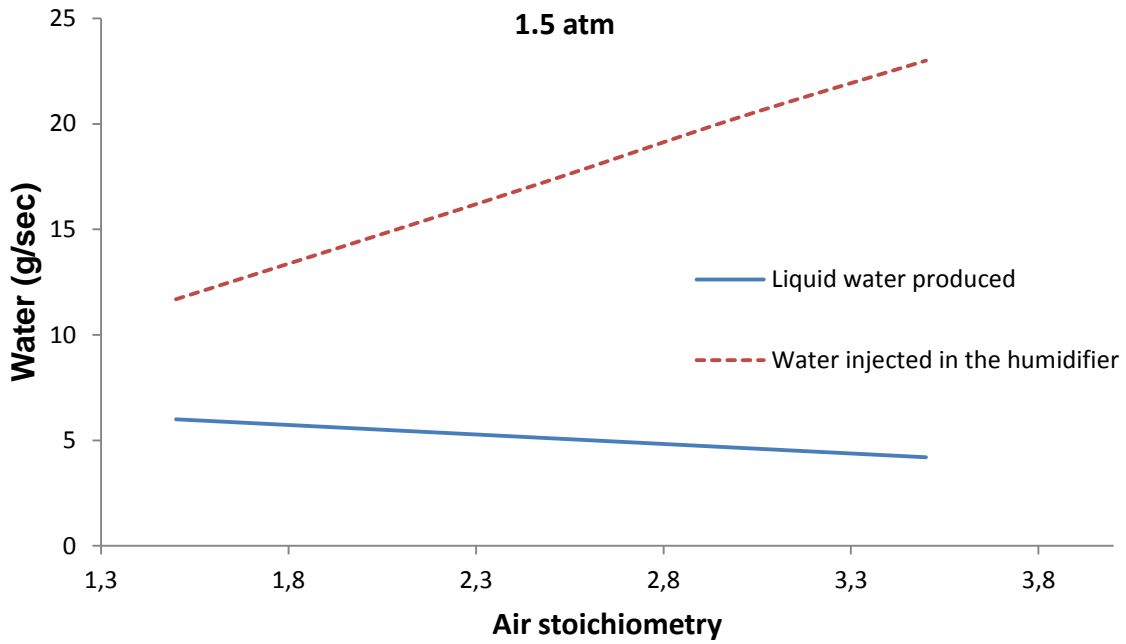
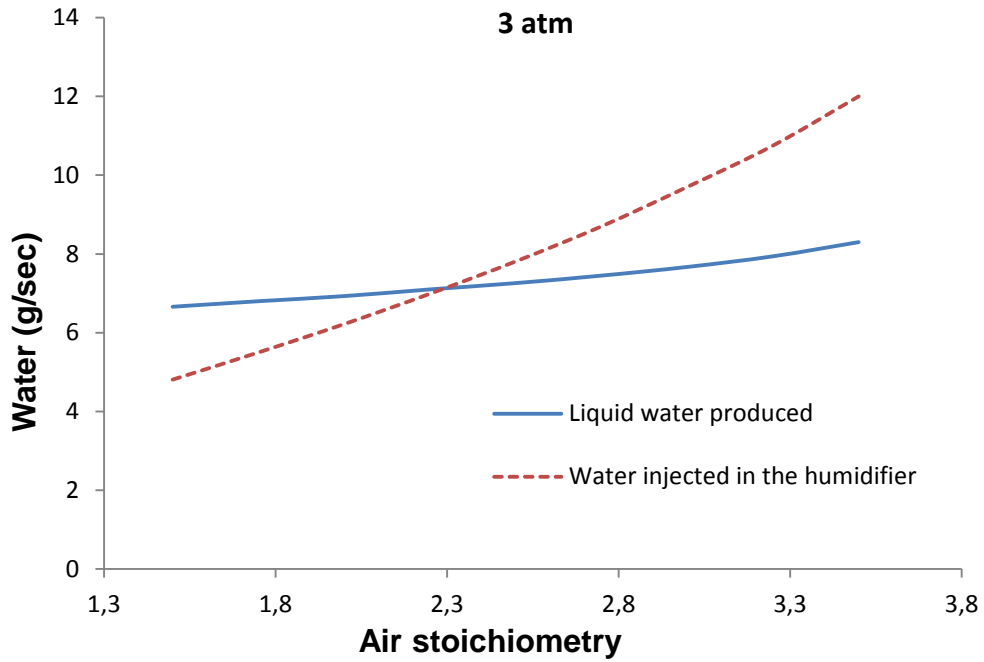


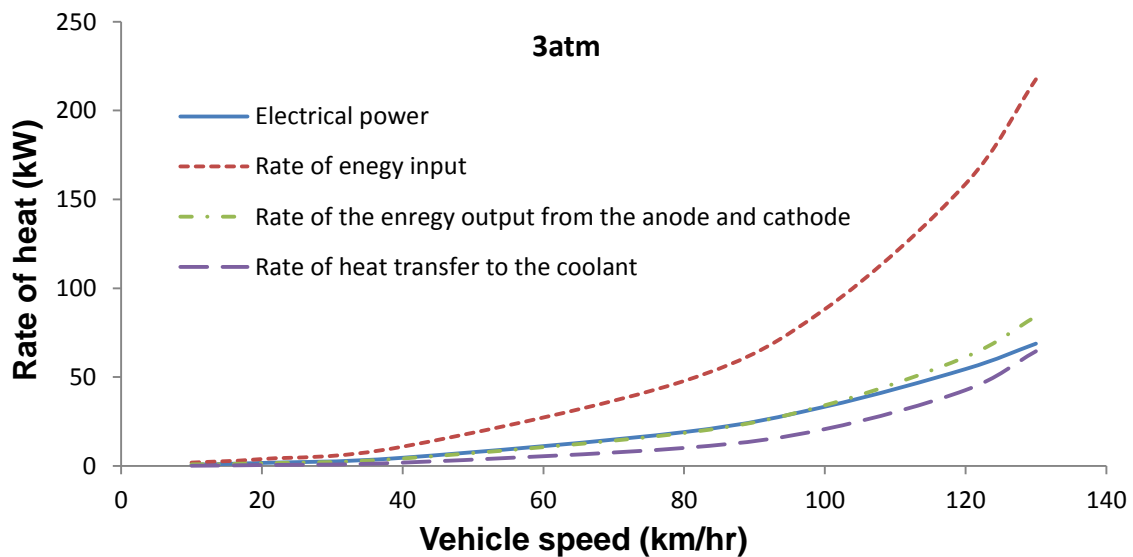
Figure 4.14. The amount of liquid water at the exit of cathode and injected water required for humidification process at constant vehicle speed at 120 km/hr with variable air stoichiometric ratio at two different operating pressures.



### 4.2.5 Thermal Management

Thermal management is one of the most important aspects in the development of fuel cell stack system because the heat is generated in large quantities through an electrochemical reaction in a PEM fuel cell. If the rate of heat generated is too high, the fuel cell stack more overheats and the membrane may lead to dehydration. Low temperatures decrease the rate of the chemical reaction, reduce efficiency, and may lead to water condensation and flooding of electrodes.

As mentioned above, proper thermal management is necessary in order to maintain the desired temperatures inside the cells which are essential for the performance and durability of a fuel cell, and to keep the stack from heating up of the fuel cell stack system. Heat balance of fuel cell stack as a function of vehicle speed for two different operating pressures shows in Figure 4.15. The sum of electrical power generated, the rate of energy leaving with the unused reactant gases, and the rate of heat removal from the fuel cell must be equal to the rate of energy entering with the reactant gases.



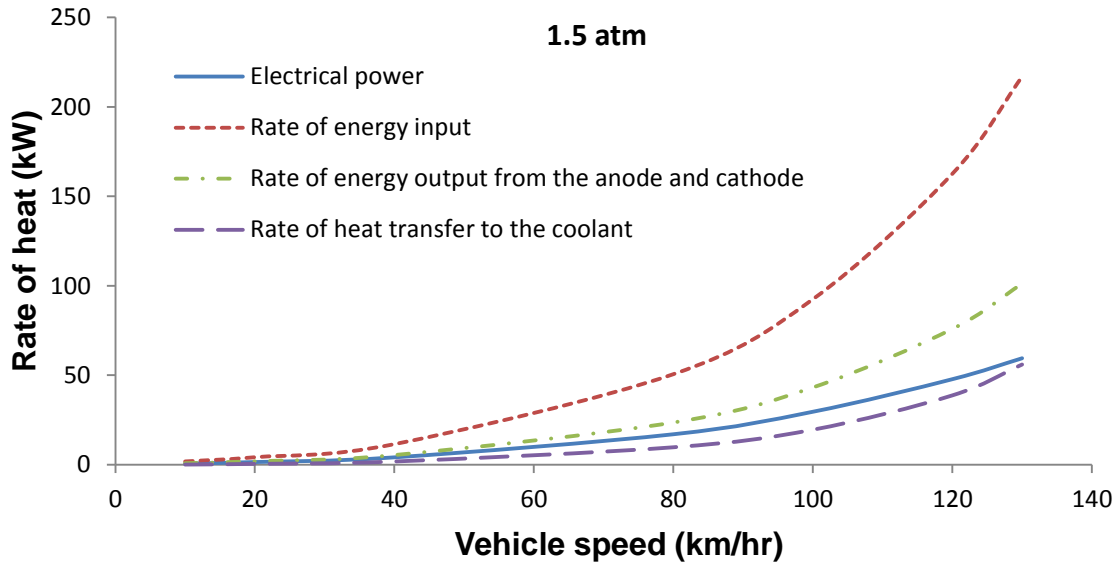


Figure 4.15. Heat balance of fuel cell stack as a function of vehicle speed for two different operating pressures.

Figure 4.16 shows the heat rejected in the radiator as a function of vehicle speed for different pressures. It is seen from the figure that the heat generated in the fuel cell stack at high operating pressure greater than it at low operation pressure. It is clear that higher operating pressures necessities a large amount of heat rejected in the radiator which results in a very high parasitic load for radiator fan.

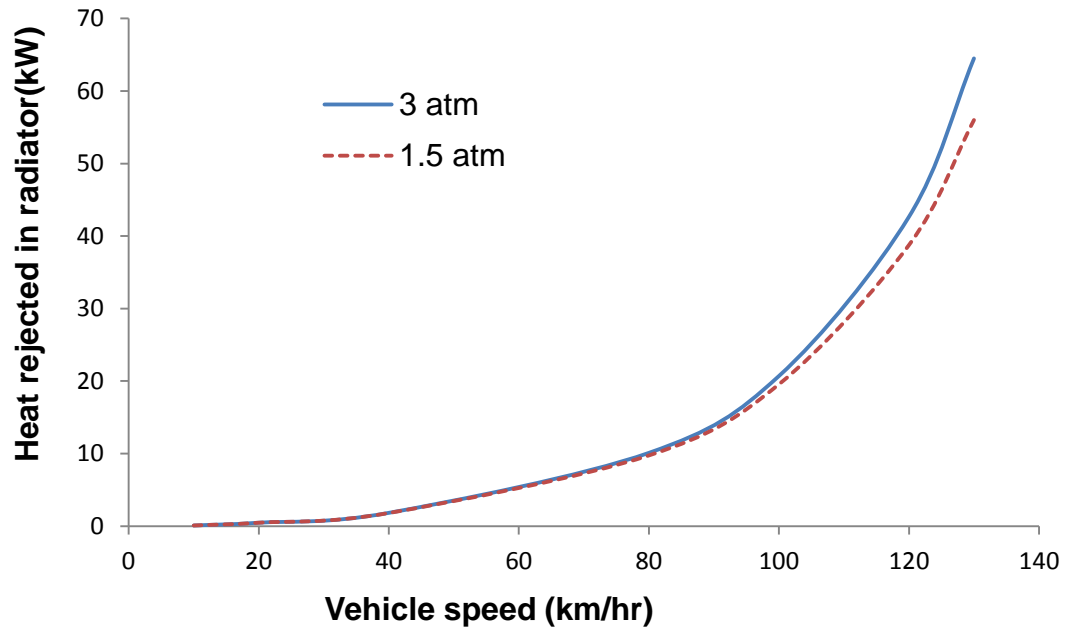


Figure 4.16. Heat rejected in radiator as a function of vehicle speed for two different operating pressures.

The size of the heat exchanger (radiator) depends on the amount of heat to be removed from the fuel cell stack and is also affected by the operation pressure. Figure 4.17 shows that the required heat exchanger area as a function of vehicle speeds at two different operation pressures. It is seen that as the vehicle speed increases the power needed from fuel cell stack also increases, and the effective area of the radiator is increased in order to dissipate all of the waste heat to the surroundings. It means that the radiator size is the key factor to influence the system thermal performance.

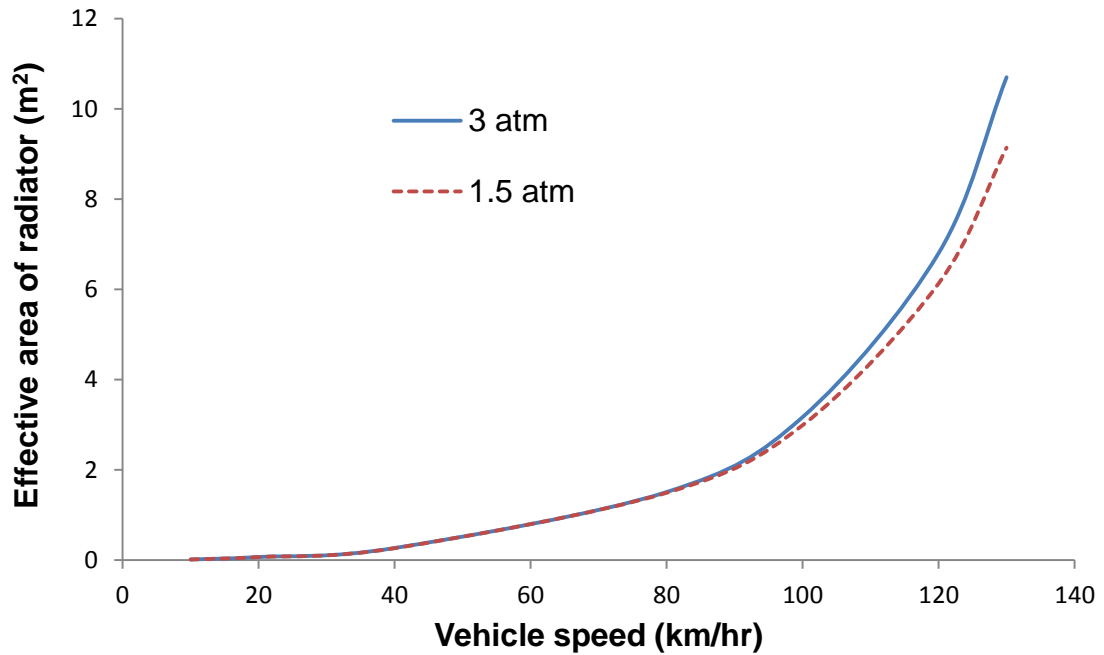


Figure 4.17. Required heat exchanger areas as a function of vehicle speed at two different operation pressures.

Figure 4.18 shows the effect of vehicle speed on the amount of coolant flow rate at different pressures. It is clear from the figure that if the vehicle speed increases, the power needed from fuel cell stack also increases, and the amount of coolant flow rate must be increased to match the rising waste heat output.

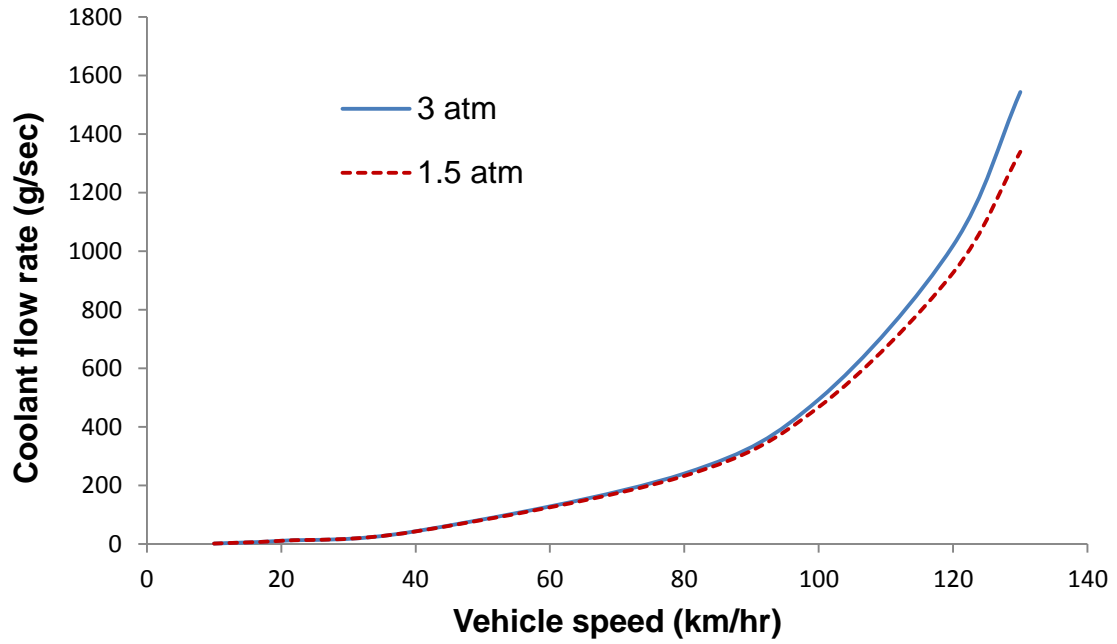


Figure 4.18. The amount of coolant flow rate as a function of vehicle speed for different pressures.

## CHAPTER 5

### CONCLUSIONS AND RECOMMENDATIONS FOR FUTURE WORK

In this study, a steady state thermodynamic model for an automotive PEM fuel cell system model was developed in MATLAB. The model consists of a PEM fuel cell model and models for all necessary auxiliary components such as compressor, pumps, fan, heaters and humidifiers. For the PEM fuel cell stack model standard Nernst voltage was calculated at the given operating conditions and activation, ohmic and concentration losses were modeled using the available theoretical and empirical approaches in the literature. All auxiliary components are modeled using 0-D steady-state mass and energy balance equations. The system model was used to determine the effects of various operating parameters such as vehicle speed, and operating pressure on the size of the system components, heat and water formation, fuel consumption and efficiency. The PEM fuel cell stack was designed to consist of 230 cells with a maximum power of 90 kW at 3 atm operating pressure. The different system configurations had to be adopted for two different operating pressures tested in this thesis 1.5 atm and 3 atm to have adequate thermal and water management. If the system operates at high pressure (3 atm), air cooler is needed to cool down the air that exits from compressor where it has been compressed to high pressures. However, if the system operates at low pressure (1.5 atm), air heater is needed to raise the air temperature to the desired value where it exits from compressor. In addition, the amount of water at the exit of fuel cell stack is not sufficient to humidify the reactants. Thus, a condenser is attached to the system to condense the water vapor in the cathode exhaust stream so that liquid water requirement of the system is met.

The thesis presented has attempted to integrate component models for an automotive PEM fuel cell system that includes a fuel cell stack, air supply system, hydrogen supply system and a thermal circuit. The integration presents a variety of possibilities to study design parameters of a fuel cell system, particularly to consider a realistic

characteristic of the fuel cell system along with a thermal and water management as well as balance of plant. Several conclusions were drawn from these analyses:

- Increasing the operating pressure of the system increases the fuel cell thermal efficiency but has no effect on the system thermal efficiency.
- The system pressure has a significant positive impact on the power density and water balance characteristics of the fuel cell.
- Increasing the vehicle speed has a negative impact on the system efficiency and stack efficiency.
- The auxiliary components are necessary to operate the PEM fuel cell system but decrease the system efficiency.
- Decreasing air stoichiometry at high operating pressure improves the water management system.
- High operation pressure improves water management, since at higher pressures less water is needed to reach the same relative humidity levels. However, the high pressure systems use a high percentage of the fuel cell output power in order to operate the compressor and that causes some loss in system efficiency.
- Water management is one of the problems in systems that operate at low pressure because they need a large amount of water for humidification processes and the sizes of the humidifier and the condenser increase. However, this parasitic power requirement increases due to fan condenser.
- As the operating pressure increases, the size of the radiator increases.

### **Recommendations for Future Work**

Several improvements can be made to the PEM fuel cell system model by the following:

- The existing model can investigate the effects of stack geometry and fuel cell material properties on the system performance.

- The model can further be developed to include the transient analysis.
- The improved model can be used to simulate the vehicle performance in the realistic driving cycles.



## REFERENCES

- [1] Ahn, J.W. Control and Analysis of Air, Water, and Thermal Systems for a Polymer Electrolyte Membrane Fuel Cell , Phd Thesis, Auburn University, **(2011)**.
- [2] Amirinejad, M., Rowshanzamir, S., Eikani, M., Effects of operating parameters on performance of a proton exchange membrane fuel cell, *Journal Of Power Sources*,161 , 872–875, **2006**.
- [3] Badrinarayanan, P., PEM Fuel Cell Water And Thermal Management: A Methodology to Understand Water and Thermal Management in an Automotive Fuel Cell System, Master Thesis, University Of California, **2001**.
- [4] Barbir, F. PEM Fuel Cell Theory and Practice, Elsevier, USA, ebook, 2005.
- [5] Bao, C, Ouyang, M., Yi., B., Analysis of the water and thermal management in proton exchange membrane fuel cell systems, *International Journal of Hydrogen Energy*, 31, 1040-1057, **2006**.
- [6] Berning, T., Lu, D.M., Djilalj, N., Three-dimensional computational analysis of transport phenomena in a PEM fuel cell, *Journal Of Power Sources*, 106, 284-294, **2002**.
- [7] Canut, J.M.L., Abouatallah, R.M., and Harrington, D.A. Detection of membrane drying, fuel cell flooding, and anode catalyst poisoning on PEMFC stacks by electrochemical impedance spectroscopy. *Journal Of Electrochem. Sources*, 153, A857-A864,**2006**.
- [8] Dai, W., Wang, H., Yuan, H.Z., Martin, J., Yang, D., Qiao, J., Ma, J., A review on water balance in the membrane electrode assembly of proton exchange membrane fuel cells. *International Journal Of Hydrogen Energy*, Volume 34, Issue 23, December, 9461-9478, **2009**.
- [9] Freire, T.J.P., and Gonzalez, E.R. Effect of membrane characteristics and humidification conditions on the impedance response of polymer electrolyte fuel cells, *Journal Of Electrochemical.*, vol. 503, pp. 57-68, **2001**.

- [10] Gurau, V., Liu, H., Kakac, S., Two-dimensional model for proton exchange membrane fuel cells, *Journal of Power Sources*, 44, 2410–2422, **1998**.
- [11] Gurski, S.D., Cold-start effects on performance and efficiency for vehicle fuel cell systems, Master Thesis, Faculty of Virginia Polytechnic Institute and State University, **2002**.
- [12] Guvelioglu, G., and Stenger, H., Flow rate and humidification effects on a PEM fuel cell performance and operation, *Journal of Power Sources* 163, 882–891, **2007**.
- [13] Guvelioglu, GH, and Stenger, HG. Computational fluid dynamics modeling of polymerelectrolyte membrane fuel cells, *Journal of Power Sources* 147 95–106, **2005**.
- [14] Hermann, A., Chaudhuri, T., and Spagnol, P. Bipolar plates for PEM fuel cells: review, *International Journal Of Hydrogen Energy*, 30, 1297 – 1302, **2005**.
- [15] Heywood, J.B., *Internal Combustion Engine Fundamentals*, ebook, **1987**.
- [16] Hosseini, M., Shamekhi, AH., Yazdani, A., Modeling and Simulation of a PEM Fuel Cell (PEMFC) Used in Vehicles, *SAE World Congress*, **2012**.
- [17] Hosseinzadeh, E., Rokni, M., Rabbani, A., Mortensen, H., Thermal and water management of low temperature Proton Exchange Membrane Fuel Cell in fork-lift truck power system, *Journal of Applied Energy* ,104, 434–444, **2013**.
- [18] Hu, G., Fan, J., Chen. S., Liu. Y. Cen, K. Q Three-dimensional| numerical analysis of proton exchange membrane -cells (PEMFCs) with conventional and interdigitated flow fields. *Journal of Power Sources*, 136, 1-9, **2004**.
- [19] Ji, M. & Wei, Z., A Review of Water Management in Polymer Electrolyte Membrane Fuel Cells, *Energies*, vol. 2, no. 4, pp. 1057-1073, **2009**.
- [20] Jiao, K., and Li, X., Water transport in polymer electrolyte membrane fuel cells, *Progress in Energy and Combustion Science* 37, 221-291, **2011**.

- [21] Kandlikar, S., and Lu, Z., Thermal management issues in a PEMFC stack – A brief review of current status, *Applied Thermal Engineering*, 29 ,1276–1280, **2009**.
- [22] Larminie, J., and Dicks, A. Fuel Cell Systems Explained, 2nd Ed., John Wiley & Sons, New York.,**2003**.
- [23] Li, H., Tang, Y., Wang, Z., Shi, Z., Wu, S., Song, S., Zhang, J., Fatih, K., Zhang, J., Wang, J., Liu, Z., Abouatallah, R., Mazza, A., A review of water flooding issues in the proton exchange membrane fuel cell, *Journal Of Power Sources*, 178, 103–117,**2008**.
- [24] Maxoulis, CN., Tsinoglou, DN., Koltsakis, GC., Modeling of automotive fuel cell operation in driving cycles, *Energy Conversion and Management*, 45 , 559–573, **2004**.
- [25] Mench, M. Fuel Cell Engines., John Wiley & Sons LTD, **2008**.
- [26] Mert, S.O., Dincer, I., and Ozcelik, Z., Performance investigation of a transportation PEM fuel cell system, *International Journal Of Hydrogen Energy* ,37, 622-633, **2012**.
- [27] Meyers, J., and Maynard, H. Design considerations for miniaturized PEM fuel cells, *Journal of Power Sources*, 109, 76–88, **2002**.
- [28] Moore, R.M., Hauer, K.H., Friedman, D., Cunningham, J., Badrinarayanan, P., Ramaswamy, PS., Eggert, A., A dynamic simulation tool for hydrogen fuel cell vehicles, *Journal of Power Sources*, vol.141, no.2,272-285, **2005**.
- [29] O’Hayre, R., Cha, S.W., Colella, W., and Prinz, F.B., Fuel Cell Fundamentals. New York: John Wiley and Sons , **2006**.
- [30] Peng, J., and Lee, S.J., Numerical Simulation of Proton Exchange Membrane Fuel Cells at High Operating Temperature, *Journal of Power Sources*, Vol. 162, 1182 – 1191, **2006**.

- [31] Schmittinger, W., and Vahidi, A., A review of the main parameters influencing long-term performance and durability of PEM fuel cells, *Journal Of Power Sources*, 180, 1-14, **2008**.
- [32] Siegel, N.P., Ellis, M.W., Nelson, D.J., Spakovsky, M.R., A two-dimensional computational model of a PEMFC with liquid water transport, *Journal of Power Sources* 128 ,173–184, **2004**.
- [33] Spiegel, C. PEM Fuel Cell Modeling and Simulation Using MATLAB, Elsevier Inc. All rights reserved, USA, ebook, **2008**.
- [34] U.S. Department of Energy. Types of Fuel Cells. Available:[http://www1.eere.energy.gov/hydrogenandfuelcells/fuelcells/fc\\_types.html](http://www1.eere.energy.gov/hydrogenandfuelcells/fuelcells/fc_types.html), **2011, 3 August**.
- [35] Vielstich, W., Yokokawa, H., and Gasteiger., HA., Handbook of fuel cells: fundamentals technology and applications. Advances in electrocatalysis, materials, diagnostics and durability, John Wiley & Sons, **2009**.
- [36] Wishart, Z. Dong., and Secanell M., optimization of a PEM fuel cell system based on empirical data and generalized electrochemical semi-empirical model, *Journal of Power Sources* ,161, 1041–1055, **2006**.
- [37] Yan, W.M., Chen, F., Yi Wu, H., Soong, C-Y., Chu, H-S. Analysis of thermal and water management with temperature- dependent diffusion effects in membrane of proton exchange membrane fuel cells, *Journal Of Power Sources*, 129, 127–137, **2004**.
- [38] Yan, W-M., Chen, F., Yi Wu, H., Soong, C-Y., Chu, H-S., Analysis of thermal and water management with temperature- dependent diffusion effects in membrane of proton exchange membrane fuel cells, *Journal of Power Sources*, 129. 127–137, **2004**.
- [39] Yu, S., and Jung, D., Thermal management strategy for a proton exchange membrane fuel cell system with a large active cell area, *Journal Of Renewable Energy*, 33, 2540– 2548, **2008**.

- [40] Yuan, W., Tang, Y., Pan, M., Li, Z., Tang, B. Model prediction of effects of operating parameters on proton exchange membrane fuel cell performance, *Journal Of Renewable Energy*, 35 , 656–666, **2010**.
- [41] Zaffou, R., Kunz, H. & Fenton, J.M., Temperature-Driven Water Transport in Polymer Electrolyte Fuel Cells, *ECS Transactions*, vol. 3, no. 1, pp. 909-913, **2006**.
- [42] Zawodzinski T.A., Derouin C., Radzinski S., Sherman R.J., Smith V.T., Springer T.E., and Gottesfeld S., Water uptake by and transport through Nafion 117 membranes, *Journal Of The Electrochemical Society*, 140(4), 1041–1047, **1993**.
- [43] Zhang, J., PEM Fuel Cell Electro catalysts and Catalyst Layers Fundamentals and Applications, Institute for Fuel Cell Innovation, National Research Council of Canada, ebook, **2008**.

## APPENDIX

### MATLAB CODE

```
%Vehicle design
v_vehicle = Variable;    %Vehicle speed m/sec
m=1880;    %Vehicle weight
Drag_coefficient=0.65;    %Aerodynamic drag coefficient
Frontal_area=2.68;    %Frontal area of vehicle, m2
Rolling_Resistance_Coefficient= 0.012;    %Rolling Resistance Coefficient
Air_Density=1.2;    %Air Density, Kg/ m3
g=9.81;    % gravitational constant
P_vehicle=(0.5*Air_Density*Drag_coefficient*Frontal_area* v_vehicle
^2+m*g*Rolling_Resistance_Coefficient)* v_vehicle;    % vehicle power,
W
er=0.15;
i_cell = 0.001;    % Initial current density of cell, A/cm2
while er>0.11
i_cell = i_cell +0.00001;
%Polarization curve
SR_anode=1.5;    %Fuel stoichiometric flow ratio
SR_cathode=2;    %Air stoichiometric flow ratio
P_a= 303.975/2;    %Pressure of anode, kpa
P_c= 303.975/2;    %Pressure of cathode, kpa
P_comp_out= 1.5;    %Pressure outlet from compressor atm
P_hydrogen= 1.5;    %Hydrogen pressure, atm
T_fc=353;    %Cell temperature, K
R=8.314;    %Universal gas constant
n_anode=2;    %Number of electron transfer through anode
n_cathode=4;    %Number of electron transfer through cathode
F=96485;    %Faraday constant, C.mol-1
T_Ref=298.15;    %Reference temperature, K
P_Ref=101.325;    %Reference pressure, kpa
```

$L_{GDL}=0.0254;$  %Thickness of gas diffusion layer, cm  
 $L_{CL}=0.00287;$  %Thickness of catalyst layer, cm  
 $L_M=0.023;$  % Membrane thickness, cm  
 $i_{o\_anode}=0.6;$  %Anode exchange current density, A/cm<sup>2</sup>  
 $i_{o\_cathode}=4.4*10.^{-7};$  %Cathode exchange current density, A/cm<sup>2</sup>  
 $lonomer\_anode=0.4;$  %lonomer equivalent of anode catalyst layer  
 $lonomer\_cathode=0.3;$  %lonomer equivalent of cathode catalyst layer  
 $Beta= 0.05;$  % Exp. Constant for Concentration Polarization,  $\beta$   
 $porosity= 0.6;$  % Electrode porosity  
 $RH=1;$  %Relative humidity (both anode and cathode) RH,  
 (%)  
 $Delta\_M= 0.1;$  % Membrane ionic conductivity , S/cm  
 $diffusion\_H2\_REF= 0.0376;$  %H<sub>2</sub> diffusion coefficient at reference state, cm<sup>2</sup>  
 sec<sup>-1</sup>  
 $diffusion\_O2\_REF= 0.0522;$  %O<sub>2</sub> diffusion coefficient at reference state, cm<sup>2</sup>  
 sec<sup>-1</sup>  
 $P\_sat= (-2846.4+411.24*(T\_fc-273.15)-10.554*(T\_fc-273.15).^2+0.16636*(T\_fc-$   
 $273.15).^3)*10.^{-3};$  %Saturation pressure @353  
 %Molar fraction of hydrogen  
 $y\_H2=1-(RH*P\_sat./P\_a);$   
 $y\_H2used= y\_H2./SR\_anode;$   
 %Molar fraction of oxygen  
 $y\_O2=(1-(RH*P\_sat./P\_c))*0.21;$   
 $y\_O2used=y\_O2/SR\_cathode;$   
 %Concentration of hydrogen and oxygen  
 $C\_H2=y\_H2used*P\_a./(R*T\_fc);$  %Concentration of hydrogen, Kmol.m<sup>-3</sup>  
 $C\_O2=y\_O2used*P\_c./(R*T\_fc);$  %Concentration of oxygen, Kmol.m<sup>-3</sup>  
 %Effective diffusivity of hydrogen and oxygen  
 $D\_H2eff=porosity.^{(1.5)}*diffusion\_H2\_REF*(T\_fc./T\_Ref).^{(1.5)}*(P\_Ref./P\_a);$   
 %Effective diffusivity of hydrogen, cm<sup>2</sup> s<sup>(-1)</sup>

```

D_O2eff=porosity.^(1.5)*diffusion_O2_REF*(T_fc./T_Ref).^(1.5)* (P_Ref./P_c);
%Effective diffusivity of oxygen, cm^2 s^(-1)
%Limiting current density
IL_anode=n_anode*F*D_H2eff*C_H2*(10).^(-3)./L_GDL; %Limiting current density
of anode, A.cm-2
IL_cathode=n_cathode*F*D_O2eff*C_O2*(10).^(-3)./L_GDL; % Limiting current
density of cathode, A.cm-2
%Open circuit voltage
E_o= 1.229 - 0.85* (10).^(-3) * (T_fc - 298.15) + 4.3085*(10).^(-5)* T_fc
*(log(y_H2used*P_a)+0.5*log(y_O2used*P_c)); % Nernst potential
%Activation losses
Act_anode = R*T_fc./(F*n_anode)*( i_cell./io_anode);
Act_cathode = R*T_fc./(F*n_cathode*(1-0.55))*log(i_cell./io_cathode);
Act_loss=Act_anode+ Act_cathode;
%Ohmic losses
ohmic = i_cell
*((L_CL./(2*Ionomer_anode*Delta_M))+L_M/Delta_M)+(L_CL./(2*Ionomer_cathode*
Delta_M));
%Concentration losses
Conc_anode=- Beta*log(1-( i_cell /IL_anode));
Conc_cathode = -Beta*log(1-( i_cell /IL_cathode));
conc_loss=- Beta*log(1-( i_cell /IL_anode))+Beta*log(1-( i_cell /IL_cathode));
v_cell =E_o - Act_anode - Act_cathode - ohmic - Conc_anode - Conc_cathode;
A_cell= 625; %Area of cell, 25cm*25cm
n_cell= 230; %Number of cell
P_fc = v_cell* i_cell* A_cell* n_cell;
M_air=28.97; %Molecular weight of air
M_H2=2.0158; %Molecular weight of hydrogen
M_O2=31.999; %Molecular weight of oxygen
M_N2=28.013; %Molecular weight of nitrogen
M_H2O=18.02; %Molecular weight of water vapor

```



```

r_O2=0.21; %Molar fraction of oxygen
m_air_in=SR_cathode./ r_O2* M_air./(4* F) * P_fc./ v_cell; % Mass of air required,
g.sec-1
m_hydrogen_in=SR_anode * M_H2./(2* F)* P_fc./ v_cell ; % Mass of hydrogen
entering to the fuel cell, g.sec-1
m_air_out=((SR_cathode-1)* M_O2+(1- r_O2)./ r_O2* M_N2) * (P_fc./ v_cell)./(4* F);
% Mass of unused air, g.sec-1
m_hydrogen_out=(SR_anode-1) * M_H2./(2* F)* P_fc./ v_cell ; % Mass of unused
hydrogen, g.sec-1
m_H2_consumption= m_hydrogen_in- m_hydrogen_out;
%%% Compression process of air
T_amb= 25; %Ambient temperature
RH_amb=0.4; %Ambient relative humidity
T_comp_in= T_amb; %Compressor inlet temperature
RH_comp_in= RH_amb; % Compressor inlet relative humidity
P1_sat = (-2846.4+411.24* T_comp_in -10.554* T_comp_in.^2+0.16636*
T_comp_in.^3)*10.^-5; %Saturation pressure @25C
>> Pv1_comp= RH_comp_in*P1_sat; %pressure of water vapor at inlet of
compressor
>> P_comp_in=1; %Pressure of cathode electrode atm
>> w_comp_in= 0.622*(Pv1_comp./(P_comp_in-Pv1_comp)); %Water content at
the inlet of compressor
%%%%%%%% Mass balance of compressor
w_comp_out= w_comp_in; %Water content at the outlet of compressor
eff_comp=0.8; %Efficiency of compressor
T_comp_out=((T_comp_in+273)+( T_comp_in
+273)./eff_comp*((P_comp_out./P_comp_in).^0.4./1.4)-1))-273; %Compressor
outlet temperature
Pv2_comp=w_comp_out*P_comp_out./(w_comp_out+0.622); %pressure of water
vapor at outlet of compressor

```

```

P2_sat= (-2846.4+411.24*T_comp_out-10.554* T_comp_out.^2+0.16636*
T_comp_out.^3)*10.^-5;          %Saturation pressure @162C
RH_comp_out=Pv2_comp./P2_sat;    % Compressor outlet relative humidity
Cp_air =1.005;                   %Specific heat at constant pressure of air
h_g0=2500;   %Enthalpy of saturated vapor@ 0C Kj/Kg
h_compressor_in= Cp_air * T_comp_in +w_comp_in*(h_g0+1.82* T_comp_in);
h_compressor_out= Cp_air * T_comp_out +w_comp_out*(h_g0+1.82* T_comp_out);
%%% Energy balance of compressor
eff_comp=0.8;
P_compressor= m_air_in*( h_compressor_out- h_compressor_in)/eff_comp;
%%%% Humidification process of air
w_hum_in= w_comp_out;           %Water content at the inlet of humidifier Kg water/Kg
air
T_hum_out=80;                   % Humidifier outlet temperature
RH_hum_out=1;                   %Humidifier inlet relative humidity
RH_inlet_c = RH_hum_out;        %Cathode inlet relative humidity
T_water_injected=25;           %Temperature of water injected to humidifier
h_fg=2442;                       %Enthalpy of evaporative water@ 25C KJ/Kg
h_g2= 2643;                       %Enthalpy of saturated vapor@ 80C KJ/Kg
P3_sat= (-2846.4+411.24*T_hum_out-10.554* T_hum_out.^2+0.16636*
T_hum_out.^3)*10.^-5;          %Saturation pressure @25C
w_hum_out= 0.622*(P3_sat./(P_comp_out-P3_sat));    %Water content at the
outlet of humidifier
%%%%Mass balance of humidifier
m_injected_air =m_air_in*(w_hum_out- w_hum_in);    %Mass flow rate of liquid
water required to humidify air
%h= Cp_air *T+w*h_g           % Enthalpy of gas vapor mixture
%h_g=h_g@0C+1.82*T           % Enthalpy of saturated vapor
h_g0=2501.3;                 %Enthalpy of saturated vapor@ 0C Kj/Kg
h_hum_out = Cp_air *T_hum_out+w_hum_out*h_g2;      %Enthalpy at outlet of
humidifier

```

```

h_evaporation= (w_hum_out-w_hum_in)*h_fg;
%h_hum_in= Cp_air *Tin_hum+w_hum_in*(h_g0+1.82*T_hum_in) %Enthalpy at
inlet of humidifie
%%%%%%%% Energy balance of humidifier
% h_hum-in+ h_evaporation =h_hum_out
T_hum_in=(h_hum_out- h_evaporation -w_hum_in*h_g0)./( Cp_air +w_hum_in*1.82);
% humidifier inlet temperature
W_hum_inlet=( Cp_air *(T_hum_out-T_hum_in)+w_hum_out*(h_g2-
h_fg))./((h_g0+1.82*T_hum_in)-h_fg);
P5_sat= (-2846.4+411.24*T_hum_in-
10.554*T_hum_in.^2+0.16636*T_hum_in.^3)*10.^-5; %Saturation pressure @162C
p_v=w_hum_in*P_comp_out./( w_hum_in+0.622);
RH_heater_out=p_v./P5_sat*100;
h_hum_in= Cp_air *T_hum_in+w_hum_in*(h_g0+1.84*T_hum_in); %Enthalpy at
inlet of humidifier
%%%%%%%% Cooling process of air
T_heater_air_in= T_comp_out;
T_heater_air_out= T_hum_in;
w_heater_air_in =w_comp_out;
%%%%%%%% Mass balance of electrical heater of air
w_heater_air_out= w_heater_air_in;
h_heater_air_inlet= Cp_air * T_heater_air_in + w_heater_air_in*(h_g0+1.82*
T_heater_air_in); %Enthalpy at inlet of heater air
h_heater_air_outlet = Cp_air * T_heater_air_out + w_heater_air_out*(h_g0+1.82*
T_heater_air_out); %Enthalpy at outlet of heater air
%%%%%%%% Energy balance of electrical heater of air
Q_heating_air= (m_air_in*( h_heater_air_outlet - h_heater_air_inlet));
%%%%%%%% Humidification of hydrogen
T_hum_out=80; % humidifier outlet temperature
RH_hum_out=1; %humidifier inlet relative humidity
RH_inlet_a= RH_hum_out; %Anode inlet relative humidity

```

```

h_fg=2442;           %Enthalpy of evaporative water@ 25C Kj/Kg
h_g2= 2643;         %Enthalpy of saturated vapour@ 80C Kj/Kg
w_hum_in2= 0;       %Water content at the inlet of humidifier, Kg water/Kg air
P3_sat= (-2846.4+411.24*T_hum_out-10.554* T_hum_out.^2+0.16636*
T_hum_out.^3)*10.^-5; %Saturation pressure @25C
w_hum_out2= 9*(P3_sat./(P_hydrogen-P3_sat)); %Water content at the outlet of
humidifier
m_injected_hydrogen= m_hydrogen_in*( w_hum_out2- w_hum_in2); %Mass flow
rate of liquid water required to humidify hydrogen
%h=Cp_H2*T+w*h_g; % Enthalpy of gas vapor mixture
Cp_H2=14.31; %Specific heat at constant pressure of hydrogen
h_hum_out2= Cp_H2*T_hum_out+w_hum_out2*h_g2; %Enthalpy at outlet of
humidifier
h_evap=(w_hum_out2-w_hum_in2)*h_fg;
%h_hum_in= Cp_H2*T_hum_in2 % Enthalpy at inlet of humidifier
% h_hum_in+ h_evap =h_hum_out %Energy balance of humidifier
T_hum_in2=(h_hum_out2- h_evap)./ Cp_H2; % humidifier inlet temperature
w=(Cp_H2*(T_hum_out-T_hum_in2)+w_hum_out2*(h_g2-h_fg));
h_inlet_heater2=Cp_H2*T_amb; %Enthalpy at inlet of heater
h_outlet_heater2=Cp_H2 *T_hum_in2; %Enthalpy at outlet of heater
Q_heating_H2= m_hydrogen_in*( h_outlet_heater2- h_inlet_heater2);
%%%% Mass balance of water transport through the cathode at steady state
P_cathode= P_comp_out; %Pressure of cathode
P_anode= P_hydrogen; %Pressure of anode
Pressure_drop_ca=0.15; % The pressure drop on the cathode side
m_H2O_air_inlet= SR_cathode./ r_O2* M_H2O./(4* F)* RH_comp_in* P1_sat./(
P_comp_in- RH_comp_in* P1_sat)* i_cell* A_cell* n_cell; % The amount of water
vapor in the air inlet
m_H2O_cathode_vapour_outlet= (SR_cathode- r_O2)./ r_O2* M_H2O./(4* F)*
P3_sat./( P_cathode - P3_sat)* i_cell* A_cell* n_cell; % The amount of water vapor
at the cathode outlet

```

```

m_H2O_generated=9.34*10.^-5*P_fc./v_cell;    % Water produced due to
electrochemical reaction
w_activity= (RH_inlet_a + RH_inlet_c)./2;    % Membrane water activity
water_content= 0.043 + 17.8*w_activity-39.85*w_activity.^2+36.0*w_activity.^3; %
Water content in the membrane
EOD_coefficient=0.0029*water_content.^2+0.05*water_content-3.4* 10^(-19);    %
Electro-osmotic drag coefficient
m_H2O_drag=EOD_coefficient*M_H2O./F*i_cell*A_cell*n_cell;    % Water transfer
due to electro osmotc drag phenomena
m_H2O_diff=0.92*EOD_coefficient*M_H2O./F*i_cell*A_cell*n_cell;    % Water transfer
due to back diffusion
m_H2O_membrane= m_H2O_drag- m_H2O_diff;    % Water transfer through
membrane
m_H2O_injected_air= m_injected_air; %Mass flow rate of injected water in the air,
g/sec
m_H2O_cathode_outlet= m_H2O_air_inlet + m_H2O_generated+
m_H2O_injected_air +m_H2O_membrane;
m_H2O_cathode_vapour_outlet=min( (SR_cathode- r_O2)./ r_O2* M_H2O./(4* F)*
P3_sat./( P_cathode - Pressure_drop_ca- P3_sat)* i_cell* A_cell* n_cell,
m_H2O_cathode_outlet); % The amount of water vapor at the cathode outlet
if m_H2O_cathode_outlet > m_H2O_cathode_vapour_outlet
m_H2O_cathode_liquid_outlet= m_H2O_cathode_outlet-
m_H2O_cathode_vapour_outlet; %The amount of liquid water at the cathode outlet
end
%%%% Mass balance of water transport through the anode at steady state
P_anode= P_hydrogen;    %Pressure of anode
Pressure_drop_an=0.15;    % The pressure drop on the anode side, atm
m_H2O_injected_hydrogen= m_injected_hydrogen;    %Mass flow rate of injected
water in the anode side, g/sec
m_H2O_anode_outlet= m_H2O_injected_hydrogen -m_H2O_membrane;    %The
amount of water the anode outlet

```

```

m_H2O_anode_vapor_outlet=min( (SR_anode-1) * M_H2O./(2* F)* P3_sat./(
P_anode- Pressure_drop_an - P3_sat)* i_cell* A_cell* n_cell, m_H2O_anode_outlet);
% The amount of water vapor at the anode outlet
if m_H2O_anode_outlet > m_H2O_anode_vapor_outlet
m_H2O_anode_liquid_outlet= m_H2O_anode_outlet- m_H2O_anode_vapor_outlet;
% The amount of liquid water at the anode outlet
else
m_H2O_anode_liquid_outlet=0;
end
m_H2O_liquid= m_H2O_anode_liquid_outlet+ m_H2O_cathode_liquid_outlet;
m_H2O_vapor = m_H2O_anode_vapor_outlet+ m_H2O_cathode_vapour_outlet;
m_H2O_injected= m_H2O_injected_hydrogen+ m_H2O_injected_air;
%%%% Energy balance of PEMFC system at steady state
T_fc_ex=76;      % Temperature of coolant end exhaust gases at exit of fuel cell
stack
T_stack=80;      % Temperature of fuel cell stack
Cp_O2=0.913;      %Specific heat at constant pressure of oxygen
Cp_HO2=4.18;      %Specific heat at constant pressure of water, j/g
Cp_HO2_v=1.85;    %Specific heat at constant pressure of water vapor
H_HHV_25=141900;  %Hydrogen higher heating value at 25C, J/g
H_HHV_0= H_HHV_25-( Cp_H2+(0.5*M_O2./ M_H2)*Cp_O2-( M_H2O./
M_H2)*Cp_HO2)* T_amb;
Q_H2_in= m_hydrogen_in*( Cp_H2* (T_stack -T_amb) + H_HHV_0);    %Heat of
inlet hydrogen, W
Q_air_in= m_air_in *Cp_air*( T_stack -T_amb);    %Heat of inlet air , W
Q_H2O_in_air_inlet= (m_H2O_air_inlet+ m_H2O_injected_air )*( Cp_HO2_v*
(T_stack -T_amb) + h_g0);    % Heat of inlet water vapor
Q_H2O_injected_H2= m_H2O_injected_hydrogen * (Cp_HO2_v* (T_stack -T_amb) +
h_g0);    % heat of injected water to hydrogen
Q_in = Q_H2_in+ Q_air_in+ Q_H2O_in_air_inlet+ Q_H2O_injected_H2; % Total heat
at inlet

```

```

Q_H2_out= m_hydrogen_out*( Cp_H2* (T_fc_ex- T_amb) + H_HHV_0);    %Heat of
outlet hydrogen, W
Q_air_out= m_air_out *Cp_air* (T_fc_ex-25);    %Heat of outlet air, W
Q_H2O_liquid_air_out= m_H2O_cathode_liquid_outlet* Cp_HO2* 0;    % Heat of
outlet liquid water outlet
Q_H2O_vapor_air_out= m_H2O_cathode_vapour_outlet *( Cp_HO2_v* (T_fc_ex-
T_amb) + h_g0);    % Heat of water vapor outlet at air side
Q_H2O_vapor_H2_out= m_H2O_anode_vapor_outlet *( Cp_HO2_v*( T_fc_ex-
T_amb) + h_g0); % Heat of water vapor outlet at hydrogen side
Q_H2O_liquid_H2_out= m_H2O_anode_liquid_outlet* Cp_HO2* 0;    % Heat of outlet
liquid water outlet
Q_out = Q_H2_out+ Q_air_out+ Q_H2O_liquid_air_out+ Q_H2O_vapor_air_out+
Q_H2O_vapor_H2_out+ Q_H2O_liquid_H2_out; % Total heat at outlet
W_el= v_cell* i_cell* A_cell*n_cell;    %Electricity generated
A_surface_fc=0.355;    % Surface area of fuel cell, m^2
h=5.4;    %Heat transfer coefficient, W/m^2K
T_Ref= 273.15;
Q_conv=h* A_surface_fc *( T_stack - T_amb); %Heat losses due to convection, W
S_B = 5.67*10.^(-8);    %Stefan. Boltzman constant,W/m^2 K
e = 0.75;    %Emissivity of stack surface
Q_rad=S_B*e* A_surface_fc*(( T_stack + T_Ref).^4-( T_amb+ T_Ref).^4);    %Heat
losses due to radiation, W
T_cool_rad_out =66;    %Temperature of coolant at exit of radiator
Q_coolant= Q_in- Q_out- W_el- Q_conv- Q_rad;
m_coolant= Q_coolant./ (Cp_HO2*( T_fc_ex- T_cool_rad_out));
%Pump design
dp=750;    % total pressure increase in the pump, Pa
density_water=1000;    % density of water, kg.m^3
P_Pump1= m_coolant* dp/ density_water;    % Power of pump required to circulation
cooling water

```

```

P_Pump2= (m_H2O_injected_air + m_H2O_injected_hydrogen ) * dp/ density_water;
% Power of pump required to circulation injected water
P_Pumps = P_Pump1+ P_Pump2;    %Work required to drive the pumps
%Design of radiator
A_radiator=0.5*0.5;
Air_Flow_rate= Air_Density*0.5*v_vehicle*A_radiator;
T_ex_rad= T_amb+( Q_coolant*10. ^3./( Air_Flow_rate* Cp_air));
dT1= T_fc_ex- T_ex_rad;
dT2= T_cool_rad_out- T_amb;
LMTD=( dT1- dT2)./log(dT1./ dT2);
U=150;    % Overall heat transfer coefficient of air
Effective_area_rad= Q_coolant./(U* LMTD);
%fan radiator design
dp=50;    % total pressure increase in the fan, Pa
P_fans= 2*Air_Flow_rate* dp./ Air_Density;    % Power of fans of radiator and air
cooler
P_heater= Q_heating_H2+ Q_heating_air;
P_AUX= P_compressor + P_Pumps + P_fans+ P_heater;
P_fc_t =P_vehicle+ P_AUX;
system_efficiency = (P_fc- P_AUX)./( m_hydrogen_in *H_HHV_0)*100;
thermal_efficiency = P_fc./( m_hydrogen_in *H_HHV_0)*100;
er= ((P_fc_t- P_fc)./ P_fc_t)*100;
end

```



## CURRICULUM VITA

### Credentials

Name, Surname : ABDULRAZZAK AKROOT  
Place of birth : Dhamar- Yemen.  
Material statues : Married  
E- mail : abdulrazzaqhmd@yahoo.com  
Address : Yemen – Dhamar

### Education

High School : Dhamar Institute of Science, 1995.  
Bsc : Mechanical Engineering, University of Mosul, Iraq, 2000.  
M.S : Mechanical Engineering, Hacettepe University, Turkey, 2014.

### Foreign Language

English  
Turkish

### Work Experience

**Teacher**, January 2001 - August 2004, Department of Refrigeration and Air conditioning Systems, Institute of Technology and Industry, Sana'a- Yemen.

**Engineer**, August 2004 – September 2006, Department of Operation and Maintenance, Local Corporation for Water, Dhamar-Yemen.

**Head**, September 2006 - August 2009, Department of operation and Maintenance, Local Corporation for Water, Dhamar-Yemen.